Physics – Uspekhi **55** (10) 977 – 1007 (2012)

REVIEWS OF TOPICAL PROBLEMS PACS numbers: **05.45. – a**, 05.45.Mt, 33.20.Ea, 33.20.Fb, 33.80.Wz, 42.62.Fi

Intramolecular vibrational redistribution: from high-resolution spectra to real-time dynamics

A A Makarov, A L Malinovsky, E A Ryabov

DOI: 10.3367/UFNe.0182.201210e.1047

Contents

Abstract. Intramolecular vibrational redistribution is a fundamental phenomenon observed in polyatomic molecules when sufficiently excited vibrationally. In this paper, results mostly from the last two decades of research on this subject are summarized, obtained either from infrared spectroscopy with a resolution of as high as 10^{-4} cm^{-1} or, in a different approach, by using various pump-probe schemes with a temporal resolution from dozens of picoseconds to subpicoseconds.

1. Introduction

1.1 Representative example

In early 1990, paper [1] was published, which clearly directed the way to a new field in molecular spectroscopy and initiated a series of high-class investigations performed by several experimental groups. It is convenient to explain the essence of the matter by the example of this paper rather than to consider numerous previous publications which, of course, should be (and will be) mentioned but which contain, however, only fragmentary parts of the problem indicated in the title of this review.

The authors of paper [1] studied, by developing their previous idea [2], the vibrational spectrum of the acetylene H – C bond at the end of chain molecules, of which the simplest, except for acetylene, is propyne (H – C ≡ C – CH$_3$), followed in the sequence by butyne and pentyne.[1] The corresponding $\nu_1 \approx 3333$ cm^{-1} vibrational mode in these molecules is the highest-frequency mode. The studies were performed in a cooled molecular beam, so that the maximum of the distribution over rotational states corresponded to small rotational quantum numbers and, therefore, the absorption spectrum was relatively simple. A number of regularities were observed which characterize in the aggregate the effect called 'intramolecular vibrational redistribution' (IVR) in the literature. We will describe these regularities and discuss their physical meaning.

A A Makarov, A L Malinovsky, E A Ryabov Institute of Spectroscopy, Russian Academy of Sciences,
ul. Fizicheskaya 5, 142190 Troitsk, Moscow, Russian Federation
Tel. +7 (495) 851 08 72, +7 (495) 851 02 31
Fax +7 (495) 851 08 86
E-mail: amakarov@isan.troitsk.ru, almalino@isan.troitsk.ru, ryabov@isan.troitsk.ru

Received 27 October 2011, revised 11 May 2012
Uspekhi Fizicheskikh Nauk **182** (10) 1047 – 1080 (2012)
DOI: 10.3367/UFNr.0182.201210e.1047
Translated by M Sapozhnikov; edited by A Radzig

[1] Strictly speaking, according to the nomenclature of chemical substances, these are 1-butyne and 1-pentyne, where the number 1 indicates the position of the triple C ≡ C bond. Below, we will more often use explicit structural formulas for these molecules but sometimes, for brevity, their simplified notation will also be invited.

The absorption spectrum of a propyne molecule was ascribed to the usual parallel absorption band of a symmetric top molecule [3]. The spectrum consisted of three branches corresponding to the selection rules $\Delta J = -1$ (P branch), $\Delta J = 0$ (Q branch), and $\Delta J = +1$ (R branch) (where J is the total angular momentum) with the additional rule $\Delta K = 0$ (where K is the angular momentum projection onto the symmetry axis of the molecule). The Q branch is extremely narrow, while the P and R branches consist of series of almost equidistant lines separated by a distance of $2B$ in the rigid top approximation (B is the rotational constant relating to the moment of inertia with respect to the axis perpendicular to the molecular symmetry axis). However, already for the next more complex butyne ($H-C\equiv C-CH_2CH_3$) molecule, each of the lines in the P and R branches becomes a multiplet without any strongly dominating line, thus suggesting a strong mixing of the once excited $|v_1 = 1\rangle$ state of the v_1 mode with the composite $|\mathbb{V}\rangle$ states of other lower-frequency modes at the same total energy $E \approx 3333$ cm^{-1}. An example in presented in Fig. 1.

One can see that the multiplet width is considerably smaller than the separation between adjacent J lines. This circumstance significantly simplifies the interpretation of the spectrum, which includes:

(i) the determination of the mean distance between lines in the multiplet, which characterizes the density of states $|\mathbb{V}\rangle$ (so far without their specification);

(ii) the determination of the multiplet width, which characterizes the rate at which the population redistribution from the 'instantly' prepared state $|v_1 = 1\rangle$ (which is, of course, not stationary) over states $|\mathbb{V}\rangle$ would occur; and

(iii) the analysis of the statistics of distances between lines in the multiplet and their intensity statistics, which can give information on the properties of states $|\mathbb{V}\rangle$.

A butyne molecule proved to be a rather convenient subject for studies, because the spectral resolution of $\sim 10^{-4}$ cm^{-1} available in experiments [1] was sufficient for completely resolving each J multiplet. This was not achieved in the case of a more complex pentyne ($H-C\equiv C-CH_2CH_2CH_3$) molecule, whose spectrum, however, was identical as a whole to the spectrum in Fig. 1.

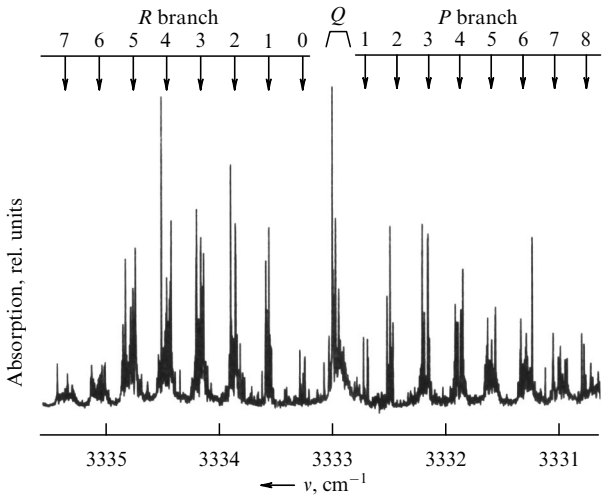

Figure 1. Spectrum of the v_1 band (the H–C acetylene type bond) in the $H-C\equiv C-CH_2CH_3$ molecule in a cold beam. The rotational temperature is 6 K. The processing of the multiplet structure in P and Q branches gives the value 114 ± 30 levels per cm^{-1} for the 'density' of vibrational levels involved in transitions. This value agrees well with the result of calculations. (Taken from Ref. [1].)

The main conclusion of paper [1] for a butyne molecule is that *all* vibrational states in the vicinity of v_1 play the role of $|\mathbb{V}\rangle$. This conclusion is based on a comparison of the experimental density ρ of states $|\mathbb{V}\rangle$ with the vibrational density of states ρ_{vib} calculated from the known vibrational frequencies of the given molecule. At the same time, it was shown that the unresolved spectral structure of a pentyne molecule, for which the density of vibrational states is approximately 25 times higher than that for a butyne molecule, means that the spectrum contains contributions from no fewer than one third (i.e. quite probably, from *all*) vibrational states in the vicinity of v_1.

It was also found that the width of the multiplet weakly depended on J. This means that anharmonic interactions between modes dominate over vibrational–rotational interactions in the mechanism of mixing of the $|v_1 = 1\rangle$ state with $|\mathbb{V}\rangle$ states. In addition, the widths of multiplets for butyne and pentyne molecules are almost the same, which speaks for the v_1 mode primarily interacting with the spatially close environment.

Finally, another important observation concerns the statistics of the separation ΔE between levels in multiplets. Such a statistics is obviously non-Poissonian. (The Poissonian statistics with the distribution function $\mathcal{F}(\Delta E) = \rho \exp(-\rho \Delta E)$ describes the situation where the positions of energy levels are random.) This is much closer to the Wigner statistics with the distribution function

$$\mathcal{F}(\Delta E) = \frac{\pi \rho^2}{2} \Delta E \exp\left[-\frac{\pi \rho^2}{4} (\Delta E)^2\right], \tag{1.1}$$

which demonstrates the mutual repulsion of the interacting levels (in particular, $\mathcal{F}(0) = 0$).

It is also important that the absence of any noticeable multiplet structure in the v_1 spectrum of propyne indicates the likely threshold character of the effect upon increasing the complexity of the molecular structure at fixed vibrational energy.

We see that this example is quite informative. In Section 1.2, we establish the qualitative correspondence between the observed effect and some key definitions of statistical physics and nonlinear dynamics.

1.2 Basic terms

The main qualitative feature of the above-considered example is the involvement of all vibrational states with close energies in mixing, which was emphasized previously. This feature can be called *ergodicity*, similarly to classical systems, where ergodicity means the equiprobable presence of a system (for infinite time) at all points of the phase space hypersurface corresponding to the specified energy.

A stronger property is *stochasticity*, which means in the classical case the exponential divergence of the trajectories of motion of a system in the phase space for an arbitrarily small variation in initial conditions. Although it is this term (or its synonym — chaos) that is most often used in the description of the IVR effect, we should note that the question of *quantum chaos* is a debated topic. It is clear that, instead of a classical point in the phase space, we can deal in the quantum case with a wave packet. However, the point of view dominates [4] that the true criterion of the quantum chaos is the Wigner distribution (1.1) of distances between

adjacent levels, which was mentioned in Section 1.1, although other statistic characteristics are probably more universal [5].

The term *mixing* is often used. This is a rigid mathematical concept whose content is explained in the ergodic theory (see, for example, § 6 in monograph [6]). Mixing provides in a certain sense the sufficient condition for ergodicity. We have also used this term in a clear context because no cluster of transitions in Fig. 1 contains any individual line whose intensity is so large that it can be comparable with the integrated intensity of other lines.

Also, the *integrability* of a dynamical system is usually considered. A Hamiltonian system with N degrees of freedom has N independent integrals of motion, i.e. quantities retaining in time their initial value. Their analogs in the quantum case are quantum numbers. For a molecule with s vibrational degrees of freedom, these are mode occupation numbers v_i. In the absence of coupling between modes, each (harmonic) eigenstate $|h\rangle$ is described by a set of occupation numbers

$$|h\rangle \equiv |v_1\rangle\,|v_2\rangle \ldots |v_s\rangle\,. \tag{1.2}$$

However, the example in Section 1.1 demonstrates the situation in which the mode energies in eigenstates are random and in no way can be close to the integers of the corresponding quanta. In such cases, the system is said to be *nonintegrable*, and A Einstein was the first to note the impossibility of quantization (in particular, according to Sommerfeld's recipe) in the nonintegrable case [7].

By listing all these terms, we assume that they are equivalent for real vibrational Hamiltonians. We will apply the term 'IVR' most often also as 'mixing' but sometimes, having in mind the particular content, we will use other terms as well.

Finally, another term, *vibrational quasicontinuum* is related directly to the spectrum of transitions itself, i.e. to the object similar to J multiplets in the P- and R-branches, which is presented in Fig. 1. Its meaning is clear from the discussion in Section 1.1, namely, IVR leads to the blurring of one line to a band consisting of many lines.

The third part of Introduction is devoted to the history how the concepts of random dynamics crossed with molecular physics. It is extremely important that such a crossing led to the understanding that nature gave researchers a huge number of quantum dynamical systems differing in their complexity, specific features of their bonds, symmetry, etc., which opened up the possibility for comprehensive experimental studies of quantum chaos.

1.3 History of earlier studies

In 1936, L D Landau published a paper, "Toward a theory of monomolecular reactions" [8], in which he clearly described the physical nature of the dissociation of a large polyatomic molecule with the vibrational energy stored in it exceeding the dissociation energy of the weakest chemical bond. According to Ref. [8], the molecule can be treated as a closed equilibrium system, and its dissociation as the result of a statistical fluctuation leading to the concentration of a significant part of the energy in a weak site.

By that time, the elements of the theory, which was later called the RRKM theory (the abbreviation from the surnames of its authors [9–14]), had already existed. This theory proposes a rather simple formula for calculating the probability of the decay of a molecule per unit time, which is based on the only assumption about the rapid (compared to decay) energy exchange between different vibrational modes of the molecule. The mechanism of such an energy exchange is obvious and assumes the presence of the cross three-, four-, and higher-order anharmonic terms in the expansion of the potential energy $U(q_i)$ as a function of dimensionless normal coordinates g_i in a Taylor series near the equilibrium position:

$$U = \frac{1}{2}\sum_{i=1}^{s} v_i\, q_i^2 + \frac{1}{3!}\sum_{ijk} \Phi_{ijk}\, q_i\, q_j\, q_k + \frac{1}{4!}\sum_{ijkl} \Phi_{ijkl}\, q_i\, q_j\, q_k\, q_l + \ldots\,, \tag{1.3}$$

where v_i are the frequencies of normal vibrations, and Φ are anharmonic constants.[2]

The RRKM theory was successfully used for many years [15–19]. Its validity and, hence, the validity of the basic assumption about the relatively rapid mixing of vibrational modes for energies exceeding the dissociation limit of a polyatomic molecule are doubtless. However, with the advent of high-power pulsed infrared (IR) lasers by the early 1970s, the idea of rapid pumping of an individual mode of a molecule was proposed to produce the predominant dissociation of the corresponding (not the weakest) bond or initiate an exotic chemical reaction in a gas mixture [20, 21].

This topic became rather popular and widely discussed in the last quarter of the 20th century in the field of laser photophysics and photochemistry. A process in which an IR laser pulse quasiresonantly excites a vibrational molecular mode was called multiphoton (or multiple-photon[3]) excitation (IR MPE), and dissociation observed at high enough laser pulse energy densities [22–24] was called IR MPD. In most experiments, excitation was performed by 10–1000-ns IR pulses from a CO_2 laser in the wavelength range from 9 to 11 μm.

The results of numerous experimental and theoretical papers are summarized in a number of reviews and monographs [25–35]. These studies were motivated, along with the circumstances mentioned above, by the demonstration of the isotope-selective dissociation of BCl_3 [36] and SF_6 [37] molecules with respect to boron and sulfur isotopes, which was achieved early in the development of this method. This effect (although some other schemes were also used) became the face of a new technique, laser isotope separation [38–40], and later found technological implementation, resulting in the creation of an industrial facility for carbon isotope separation [41]. However, the initial goal — the selective breaking of a molecular bond [42, 43] — still remains a dream due to restrictions imposed by the IVR process.

The understanding of the fundamental role of IVR in the IR MPE process came after the publication of paper [44], where the redistribution of vibrational energy in an isolated polyatomic molecule was treated as a manifestation of dynamic chaos inherent in nonlinear systems with many degrees of freedom. At that time, publications in this field were rather scarce. In fact, a supporting point was the

[2] Hereinafter, we express energy in wavenumbers (i.e. [cm^{-1}]). Therefore, because normal coordinates are dimensionless, v and Φ are also measured in these units.

[3] The term 'multiple-photon' is often used along with the term 'multiphoton' in the literature in English.

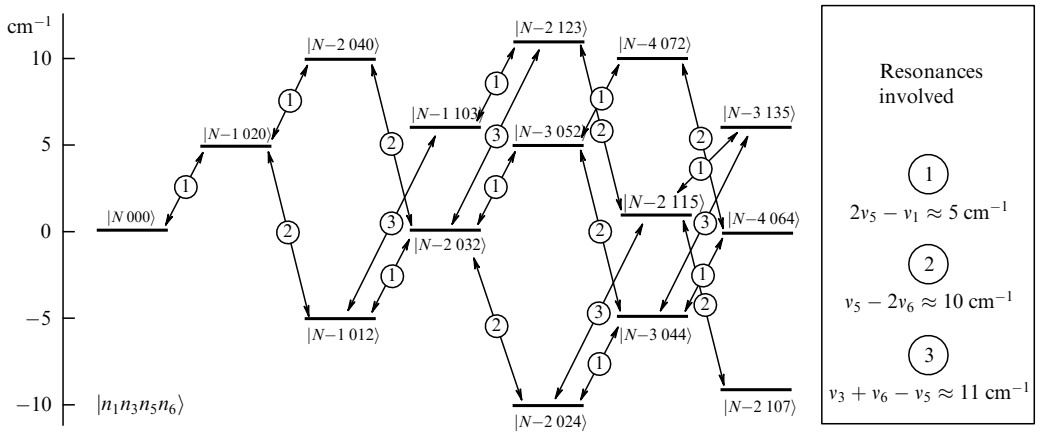

Figure 2. Mixing over a chain of the harmonic states of the CF_3I molecule due to three-frequency anharmonic resonances (fragment of a picture). The initial state was chosen with N quanta in the v_1 mode and zero occupation numbers for other modes.

Chirikov criterion [45] based on analytical estimates and numerical experiments. The Chirikov criterion asserts that the passage from regular motion to stochastic (chaotic) motion occurs during "the overlap of nonlinear resonances."

What does such a statement mean for a polyatomic molecule? In the region of low vibrational energies, the harmonic approximation mainly operates — small harmonic corrections to energies and wave functions are calculated by the perturbation theory. In some cases for individual pairs of closely lying levels, the perturbation theory is inapplicable. The example of the intermode resonance in a CO_2 molecule is well known (the Fermi resonance [46]), where the energy of one quantum of the symmetric vibration v_1 is approximately equal to the energy of two quanta of the deformation vibration v_2. This would be of no significance for the transition spectrum (in the given case, the Raman spectrum relative to which the v_1 mode is active) if anharmonicity was absent: only one strong v_1 band would be observed. However, the anharmonic term in potential energy (1.3), proportional to $q_1q_2^2$, couples the v_1 and $2v_2$ states, and because the corresponding nondiagonal matrix element $U_{v_1 2v_2}$ of the interaction considerably exceeds the distance between the unperturbed levels, both superposition eigenstates, split by $\pm U_{v_1 2v_2}$, are equally strongly manifested in the Raman spectrum.

Examples of the accidental closeness of energy levels, resulting in the deviation of IR and Raman spectra from almost harmonic spectra, are not rare in molecular spectroscopy. This, however, is not yet related to the overlap of resonances. But, as the vibrational energy in the molecule increases, the closeness of the levels becomes no longer accidental, but regular (as illustrated by the diagram of intermode resonances in a CF_3I molecule in Fig. 2). As the vibrational energy increases, the density of states and anharmonic matrix elements also increase. In response to this, the perturbation theory becomes violated at a certain instant of time not simply for individual pairs of levels, but globally. This is called the overlap of resonances, and this effect leading to IVR (in other formulations, to stochastization, chaos, mixing) was explained by the author of paper [44].

We restricted ourselves to the qualitative explanation of the Chirikov criterion. The literature on dynamic chaos is rather voluminous. This topic is related to many fields in physics, in particular, to questions concerning the substantiation of statistical mechanics [47, 48], the theory of vibrations in nonlinear lattices [49–51], the problem of motion stability in celestial mechanics [52–54], accelerator technology [45], nonlinear waves in plasma [55], and so forth. Many of these subjects were considered in monographs, reviews, and general collections; we cite here the most important of them [4, 56–70], which can be often used as introductory textbooks. This list should be supplemented with classical studies [6, 71–74], where the focus is on the mathematical aspects of the problem.

One of the main subjects brought up during the advancement of IR MPE studies was that about the energy beginning from which the mode mixing effect shows its worth. Even before the perception of dynamic-chaos ideas, it became intuitively clear that a quasicontinuum of transitions exists above some vibrational energy because molecules in the field of narrowband laser radiation easily acquire energy despite the anharmonicity of a vibrational mode. The concept of a quasicontinuum appeared as a working hypothesis in one of the first papers [23] and was at once discussed in papers [75–77] devoted to theoretical simulations of the IR MPE process. The problem appeared of how to extract information from the spectrum of optical transitions in the quasicontinuum. On the other hand, this new subject imposed new requirements on experiments.

The work that we described in Section 1.1 marked one of the significant qualitative jumps. We will return to this and similar papers in Section 3 after considering in Section 2 elements of the theory of spectra of transitions in the quasicontinuum.

Somewhat later, with the advent of ultrashort IR laser pulses, the real-time observation of the IVR process became possible in principle. Research in this field became the natural development of methods used earlier for direct or indirect characterization of the vibrational mode distribution produced in the IR MPE process. An example of such a continuity is demonstrated by papers [78] and [79], separated in time by a quarter of a century. The authors entertained the same approach by analyzing the IR MPE products. However, the authors of Ref. [78] excited SF_6 molecules by 100-ns pulses and analyzed the velocity and angular distributions of products, while the authors of Ref. [79] excited CH_2N_2 molecules by 100-fs pulses and performed the time-resolved detection of CH_2 radicals by laser-induced fluorescence.[4] In

[4] Various spectroscopic methods for detecting free radicals produced upon IR MPD are described, for example, in Refs [80, 81] and in Section 5.4.

the first case, the authors concluded that the experiments were in complete agreement with the RRKM theory, while the data obtained in the second case confirmed the nonstatistic nature of dissociation.

However, the main experiments were performed and are being performed by exciting molecules considerably lower than the dissociation limit. The aim of experiments with long pulses was to find the boundary (possibly conditional) where the vibrational motion goes from regular to stochastic motion, while the aim of experiments with short pulses was to observe IVR in real time. A review of corresponding methods and results is presented in Section 4.2.

In Section 5, we briefly discuss a number of issues related to the IVR problem, but lying outside the scope of our review.

2. Spectroscopy of optical transitions in the vibrational quasicontinuum of polyatomic molecules: elements of the theory

2.1 Statistics of ergodic states

Harmonic states (1.2) describe vibrational properties of polyatomic molecules by neglecting anharmonic effects. True vibrational $|g\rangle$ states differ from harmonic $|h\rangle$ states. In general, the $|g\rangle$ states can be formally expanded in the harmonic basis:

$$|g_\alpha\rangle = \sum_\beta c_{\alpha\beta}\,|h_\beta\rangle\,. \tag{2.1}$$

In the region of low vibrational levels, where anharmonicity is reduced to a weak perturbation, [5] the structure of $|g\rangle$ states is close to the structure of harmonic $|h\rangle$ states, i.e. one of the coefficients in expansion (2.1) equals approximately unity, while the other coefficients are small. The density of states and anharmonic interaction increase with increasing energy, which should finally lead to a strong mixing of many neighboring states.

We will assume that the structure of true states for a strongly enough excited polyatomic molecule satisfies the following conditions:

(i) the $|g_\alpha\rangle$ state with energy E_α contains contributions from a great number $\widetilde{N}$ of harmonic states belonging to the energy interval $\delta\widetilde{E} \approx \widetilde{N}/\rho_{E_\alpha}$ (where ρ is the density of states for the corresponding energy);

(ii) contributions from the states lying in the interval $\delta\widetilde{E}$ are statistically random, i.e. correlations between expansion coefficients $c_{\alpha\beta}$ and vibrational quantum numbers in $|h_\beta\rangle$ states are absent; and

(iii) outside the interval $\delta\widetilde{E}$, coefficients $c_{\alpha\beta}$ depend on large scales only on the energy difference $|E_\alpha - E_\beta|$, decreasing in the general case with increasing $E_\alpha - E_\beta$ and remaining statistically random within small energy intervals.

The properties of the states formulated for a strongly enough vibrationally excited molecule are hypothetical: they could be confirmed or refuted based on exact quantum-mechanical calculations involving many harmonic levels and anharmonic constants entering into expansion (1.3) in normal coordinates. Such calculations are more or less systematized only for the simplest quantum systems. Notably, for systems of two coupled oscillators, they, based on the model Hénon–Heiles system [82] and its generalization — the system described by the Toda Hamiltonian [83] — show [84–86] that, indeed, the eigenstates above some critical energy possess property (i), i.e. they have substantially nonzero projections on many states of the harmonic basis (such states are called 'global' in the literature).

Condition (ii) provides the strengthening of condition (i). It is the fulfillment of this condition that contains the concept of 'ergodicity' (see Section 1.2). Formally, the ergodicity of states does not follow from their globality. However, the analysis of numerical calculations performed in review [85] indicates that these two properties of states for real vibrational Hamiltonians are probably inseparable.

But it is most important for us that property (ii) agrees with the experimental results presented as an example in Section 1.1.

2.2 Intramolecular vibrational redistribution (IVR) dynamics of ergodic states

Expansion (2.1) has one simple, but important, consequence. Let a harmonic $|h_\beta\rangle$ state be prepared at the instant $t = 0$. This state is the superposition of true states

$$|h_\beta\rangle = \sum_\alpha \widetilde{c}_{\beta\alpha}|g_\alpha\rangle\,, \tag{2.2}$$

where $\widetilde{c}_{\beta\alpha}$ is a matrix inverse to $c_{\alpha\beta}$ in expansion (2.1). The prepared $|h_\beta\rangle$ state is not stationary. It evolves according to the series expansion [6]

$$\left|h'_\beta(t)\right\rangle = \sum_\alpha \widetilde{c}_{\beta\alpha}\exp\left(-\frac{\mathrm{i}}{\hbar}\,E_\alpha t\right)|g_\alpha\rangle\,,\quad \left|h'_\beta(t=0)\right\rangle \equiv |h_\beta\rangle\,. \tag{2.3}$$

If the expansion contains contributions from many true states (and this is namely assumed for the ergodicity region), then, due to dephasing of different terms, the initial superposition is destroyed with time. The characteristic time τ_{IVR} of this process is determined by the width δE of the energy interval making the main contribution to the expansion: $\tau_{\mathrm{IVR}} \sim \hbar/\delta E$. It should be pointed out, however, that the fraction of the initial state in $|h'_\beta(t)\rangle$ remains, nevertheless, finite. Being time-averaged, this fraction is on the order of $(\rho_{E_\beta}\,\delta E)^{-1}$.

We will apply these considerations to our example in Section 1.1, illustrated in Fig. 1. In this example, the initially prepared harmonic $|v_1 = 1\rangle$ state of a butyne molecule contains one quantum of the highest-frequency mode v_1, while the occupation numbers of the other 23 modes are zero. Consider the situation in a more general form. Following review [87], we will call the initially prepared state 'the zero-order bright state' (ZOBS), assuming that it is the only harmonic state in a comparatively narrow energy region to which the optical transition from the ground state can occur. We will sometimes denote this state for clarity by $|\mathcal{ZOBS}\rangle$, and in formulas, as a rule, by $|\mathcal{Z}_0\rangle$. Other states in this sense are 'dark states'; we will also call them 'bath states' and denote them by $|\mathcal{B}_s\rangle$.

Consider the spectrum of interaction between the $|\mathcal{Z}_0\rangle$ state and $|\mathcal{B}_s\rangle$ states. The shape of this spectrum principally depends on the structure of true bath states. Let us represent

[5] There are exclusions for individual level pairs of a Fermi resonance type (see Section 1.3).

[6] Utilizing customary formulas containing Planck's constant, we remember that, because we express energy in 'spectroscopic' wavenumbers (see footnote 2), Planck's constant $\hbar$ is measured in [$\mathrm{cm^{-1}\,s}$] ($\hbar \approx 5.3\times 10^{-12}$ $\mathrm{cm^{-1}\,s}$).

the vibrational Hamiltonian in the form

$$\widehat{H}_{\rm vib} = \widehat{H}_a(q_a) + \widehat{H}_b(q_b) + \widehat{V}(q_a, q_b) = \widehat{H}_a(q_a) + \widehat{H}_b(q_b) + q_a \widehat{V}^{(1)}(q_b) + q_a^2 \widehat{V}^{(2)}(q_b) + \dots , \qquad (2.4)$$

where we separated the vibrational coordinate q_a responsible for excitation of the $|\mathcal{Z}_0\rangle$ state from other coordinates, and also expanded the interaction operator $\widehat{V}$ of the v_a mode with other modes into a power series in q_a.

Consider first the situation, where the states of the truncated Hamiltonian $\widehat{H}_b$ are harmonic, and assume for simplicity, as in the example demonstrated in Section 1.1, that the v_a mode has the highest frequency. We will also take into account that matrix elements for the coordinate of a harmonic oscillator are nonzero only for transitions with the change $\Delta v = \pm 1$ in the vibrational quantum number, and for the coordinate squared with $\Delta v = 0, \pm 2$. Then, in general, the strongest are interactions of v_a with $v_i + v_j$ and $2v_i$ types of combinations, because they correspond to the lowest terms $q_a q_i q_j$ and $q_a q_i^2$, respectively, in the first term $q_a \widehat{V}^{(1)}(q_b)$ of the expansion of $\widehat{V}$ in formula (2.4). However, two-frequency combinations can be absent in the proximity of the $|\mathcal{Z}_0\rangle$ state. Then, the strongest interactions are those with $v_i + v_j + v_k$ type states, etc.

Notice at once that not all combination states of the same order identically interact with v_a. First, symmetry selection rules exist. Second, the interaction of v_a with some combination states can be considerably suppressed due to the structural features of a molecule. Thus, in our initial example, the sum frequency of one quantum (~ 3000 cm^{-1}) of the valence C–H vibration of the methyl group and one quantum of some low-frequency deformation or torsion vibration can fall into the region of frequency $v_1 \sim 3333$ cm^{-1} of the end H–C vibration. However, it seems that the spatial remoteness of the methyl group makes this interaction weak. In any case, it was assumed in Ref. [1] that the v_1 mode most strongly interacts with the combination $v_{\rm C\equiv C} + 2v_{\rm H-C\equiv C}$ including one quantum of the valence vibration of the triple C ≡ C bond and two quanta of the deformation vibration of the end acetylene group. The corresponding term in expansion (2.4) is $q_1 q_{\rm C\equiv C} q_{\rm H-C\equiv C}^2$.

So far, the cornerstone of our qualitative analysis performed above has been that, in the case of the harmonic structure [7] of the eigenstates of the bath Hamiltonian $\widehat{H}_{\rm b}$, the *strong hierarchy* of interactions $V_s = \langle \mathcal{Z}_0 | \widehat{V} | \mathcal{B}_s \rangle$ exists (Fig. 3a). The hierarchy is destroyed when the eigenstates of $\widehat{H}_b$ are ergodic. Then, the interaction spectrum becomes fundamentally different. Its small-scale fluctuations become random, while large-scale peculiarities either are smoothed (broadened, Fig. 3b) or disappear completely (Fig. 3c). Consider first precisely this case, where we are interested in the dynamics of the population redistribution from the initial $|\mathcal{Z}_0\rangle$ state to the $|\mathcal{B}_s\rangle$ state.

Reference points in the solution to this problem are two exact results, one of which is related to the level decay to a continuous spectrum, and the second to the Bixon–Jortner model [88]. It is often assumed that the solution in the first case is reduced to the exponential decay of the amplitude of the initial state, as for radiative spontaneous decay [89]. In most situations in reality, when we are dealing with a continuous spectrum, this limited knowledge is sufficient. However, we should bear in mind that the exponential decay exactly corresponds only to the situation where the continuous spectrum is infinite and the matrix element of interaction $V(s) = \text{const}$, and also that the problem has an exact solution for *any* function V of the *continuous variable* s [90–93]. This solution demonstrates that the single-exponential decay is a good approximation if the function $V(s)$ weakly varies on the energy scale $\hbar W$, where $W \approx (2\pi/\hbar)\, V^2$ is the initial-state decay rate.[8]

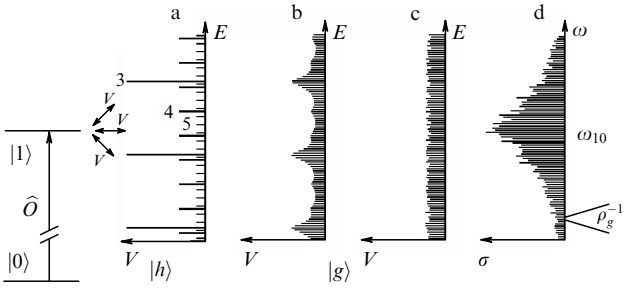

Figure 3. Interaction of the excited state of the v_a ($v_a = 1$) mode with a bath states for a close total vibrational energy. The interaction spectrum is shown for cases where the reservoir states are (a) harmonic, $|h\rangle$, and (b, c) ergodic, $|g\rangle$. Two peculiarities are qualitatively distinguished: the hierarchy of anharmonic interactions of different orders (third, fourth, and fifth), and broadening and partial or complete overlap of resonances. (d) The shape of the optical transition line ($\widehat{O}$ is the transition operator) for the interaction spectrum shown in Fig. 3c: the result of numerical calculations with the normalization of V_{1g} in this example on average to $(5/\sqrt{\pi})\, \rho_g^{-1}$.

The situation is more complicated in the case of a discrete spectrum of $|\mathcal{B}_s\rangle$ states. Equations for the time-dependent amplitudes $z_0(t)$ and $b_s(t)$ of states $|\mathcal{Z}_0\rangle$ and $|\mathcal{B}_s\rangle$, respectively, have the form

$$\frac{{\rm d}z_0(t)}{{\rm d}t} = -\frac{\rm i}{\hbar} \sum_s V_s b_s(t) \exp\left(-\frac{\rm i}{\hbar} E_s t \right),$$
$$\frac{{\rm d}b_s(t)}{{\rm d}t} = -\frac{\rm i}{\hbar} V_s z_0(t) \exp\left(\frac{\rm i}{\hbar} E_s t \right), \qquad (2.5)$$

where E_s is the energy of the $|b_s\rangle$ state measured from the energy of the $|\mathcal{Z}_0\rangle$ state. Here, the exact solution is possible only for several particular cases [88, 91, 94–96], the simplest of them corresponding to the situation where the spectrum of $|\mathcal{B}_s\rangle$ states is equidistant, i.e. $E_s = (s + a)\, \rho^{-1}$, where ρ^{-1} is the distance between adjacent $|\mathcal{B}_s\rangle$ levels (ρ is the density of states), and the matrix element of interaction $V_s \equiv V = \text{const}$ (the Bixon–Jortner model). In this case, the system of equations (2.5) has an analytical solution. For our initial conditions $z_0(0) = 1, b_s(0) = 0$, the solution has a very simple form,[9] $z_0(t) = \exp(-\pi\hbar^{-1} V^2 \rho t)$, in the time interval $0 \leqslant t \leqslant 2\pi\hbar\rho$. However, the decay of the $|\mathcal{Z}_0\rangle$ state is restricted by this time interval. Then, a partial return with oscillations takes place.

[7] It is more accurate to use the term 'quasiharmonic structure' or 'almost harmonic structure', meaning the situation where corrections from anharmonic terms to $\widehat{H}_b$ are small.

[8] Being a function of a continuous variable, the matrix element V is measured in units of [cm$^{-1/2}$].

[9] When $\rho \to \infty$ (assuming that the value of $V^2\rho$ does not change), this solution exactly coincides with the solution for the case of a continuous spectrum.

It seems there is no point in assigning a meaning to the exact behavior of the system, which, except for the population decay rate $W=2\pi\hbar^{-1}V^2\rho$, also depends on the parameter a, the more so as the model simplifies the actual situation. In reality, the positions of $|\mathcal{B}_s\rangle$ levels are arbitrary (only the density of states ρ has a physical meaning). In addition, the matrix element of interaction V_s fluctuates from state to state (only the average value of its square $\langle V_s^2\rangle$ has a physical meaning). However, although the behavior of each system described by equations (2.5) is individual, it is useful to consider general regularities inherent in an *ensemble* of systems. Why does this make sense? We will illustrate the answer to this question by our example discussed in Section 1.1.

If we take an individual J multiplet in the P- or R-branch of the spectrum in Fig. 1, this procedure makes no sense because we obtain sufficient information from the measurement results to describe the dynamics of interest to us. Indeed, the solution for $z_0(t)$ from the system of equations (2.5) can be written in the general form as

$$z_0(t)=\sum_m \left|\tilde{z}_0^{(m)}\right|^2 \exp\left(-\mathrm{i}\,\lambda_m t\right), \tag{2.6}$$

where λ_m are the eigenvalues of the system of algebraic equations

$$\lambda\tilde{z}_0=\sum_s V_s\tilde{b}_s\,,\quad \lambda\tilde{b}_s=\frac{E_s}{\hbar}\,\tilde{b}_s+V_s\tilde{z}_0\,, \tag{2.7}$$

and $\tilde{z}_0^{(m)}$ is the projection $\langle\mathcal{Z}_0|\mathcal{M}\rangle$ of the initial state $|\mathcal{Z}_0\rangle$ onto the mth eigenstate $|\mathcal{M}\rangle$. Notice next that the positions of lines correspond to eigenvalues λ_m, and their relative intensities to quantities $|\tilde{z}_0^{(m)}|^2$. From this and expression (2.6), we find the time-dependent population $\mathcal{P}(t)=|z_0(t)|^2$ of the $|\mathcal{Z}_0\rangle$ state.

Assume, however, that spectral lines cannot be resolved due to a high density of states. Then, we can estimate from the width of the spectrum only the decay rate W, while other specific features of the IVR dynamics, in particular, the average population of the $|\mathcal{Z}_0\rangle$ state at large times, cannot be estimated. This quantity is called the dilution factor σ [97] and is expressed in terms of the solution (2.7) as

$$\sigma=\left\langle|z_0(t)|^2\right\rangle_t=\sum_m\left|\tilde{z}_0^{(m)}\right|^4. \tag{2.8}$$

Why is this quantity important? The answer to this question will be completely clear in Section 4 from a review of experiments on real-time IVR, allowing the measurement of σ. Moving ahead, we distinguish the main circumstance. The dynamics described by system of equations (2.5) involves two competing factors: the decay of the $|\mathcal{Z}_0\rangle$ state with the rate W, and a tendency to the return with the characteristic time specified by the density of states ρ. Obviously, σ will decrease with increasing $\varkappa=\hbar W\rho$. By introducing the statistics of positions of levels E_s and interactions V_s, we can numerically obtain the universal dependence $\sigma(\varkappa)$, which has a meaning if the statistics is physically substantiated.

Based on the results of Dyson and Mehta [98], E Wigner assumed in paper [99] published in 1967 that the spectral properties of complex dynamical systems are described by the eigenvalues of the so-called Gaussian orthogonal ensemble (GOE) of random matrices (see also Refs [100–102]). It was proved that in this case the statistics of distances between adjacent energy levels is described by expression (1.1), which was mentioned above in connection with the results of the experiment described in Section 1.1, and also in Section 1.2 in connection with quantum chaos criteria.

This hypothesis was verified later in nuclear spectroscopy [103–105] for excited electronic molecular states [106–108], atomic Rydberg states [109, 110], and quantum billiards [111], in which particles move stochastically in the classical limit (the Sinai billiard [112]), or their models in the form of microwave resonators [113]. It was definitely concluded that the observations and calculations of the level positions agree well with the Wigner distribution.

The theory and experiment also lead to an unambiguous conclusion about the statistics of eigenvectors of the GOE that the squares of modulo U of their projections on basis states obey the Porter–Thomas distribution [100, 101, 103, 114, 115]:

$$\mathcal{F}(U)=\frac{1}{\sqrt{2\pi\langle U\rangle U}}\exp\left(-\frac{U}{2\langle U\rangle}\right). \tag{2.9}$$

These statistics can be naturally applied to small-scale fluctuations of matrix elements V_s (Fig. 3c). Indeed, let us consider some harmonic state $|h\rangle$ from the states that most strongly (see Fig. 3a) interact with $|\mathcal{Z}_0\rangle$. Due to the mixing of this state with other dark states, the quantity V_s will be proportional to the projection $\langle h|\mathcal{B}_s\rangle$, i.e. its modulo square is distributed according to formula (2.9).

Before discussing the statistical properties of quantities E_s and V_s, we formulated the problem as the description of the averaged dynamics of an ensemble of systems obeying equations (2.5), with E_s and V_s as random parameters. Results obtained in Ref. [116] are presented in Fig. 4. At the initial stage, the evolution of the population $\mathcal{P}$ is virtually independent of the product $\varkappa=\hbar W\rho$ and is completely determined by the quantity $W=2\pi\hbar^{-1}\langle|V_s|^2\rangle\rho$. Oscillations present in the Bixon–Jortner model are suppressed during averaging, although small fluctuations are present. At large times, the population $\mathcal{P}_\varkappa$ tends to the stationary value which decreases with increasing $\varkappa$ (Fig. 5). This stationary value, of course, completely agrees with the quantity σ (2.8) averaged over the ensemble.

The dependences displayed in Fig. 4 are used in interpreting real-time observations of IVR; however, not for some initial state but for a Boltzmann ensemble where numerous vibrational–rotational states are present (see Section 4).

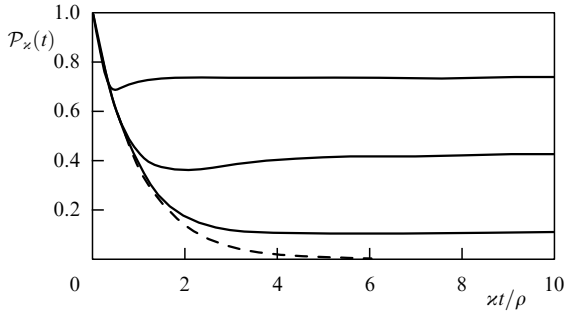

Figure 4. Time dependence of the population of the $|\mathcal{Z}_0\rangle$ state averaged over 10,000 tests. The curves correspond to the parameter $\varkappa=0.05$, 0.50, and 5.00 (from top to bottom). For comparison, the dashed curve shows a pure exponent $\exp(-Wt)\equiv\exp(-\varkappa t/\hbar\rho)$ [116].

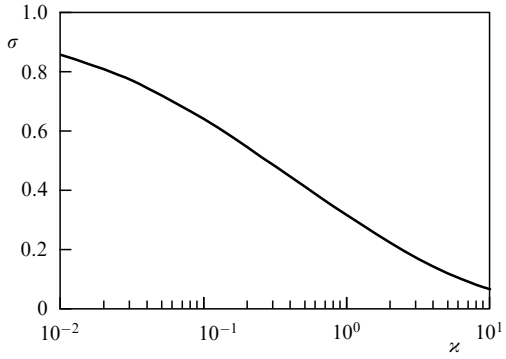

Figure 5. Dependence of the dilution factor (2.8) on the parameter $\varkappa = \hbar W\rho$. Eigenvalue and eigenvector problem (2.7) was solved with random sets of the E_s and V_s values generated according to statistical distributions (1.1) and (2.9), respectively [116].

2.3 Spectra of transitions between ergodic states

The situation where the initial vibrational state is not the ground state, but 'almost harmonic' does not differ from that considered in the previous section. Cardinal complications appear when the spectrum of optical transitions from ergodic states is discussed. Here, we should at once make an important remark that an individual ergodic state is a statistically random (in the sense of Section 2.2) realization of an ensemble of harmonic states with close energies [92, 117].

Hence it follows that, although *each* ergodic state is characterized by its own *individual* spectrum of transitions, the main physical information is contained in the spectrum of transitions from an *ensemble* of close ergodic states, while individual spectra in passing from one state to another reflect only statistical fluctuations. In this connection, it is reasonable to begin with the consideration of the spectrum of transitions from an *ensemble of almost harmonic states*, wherein the IVR effect is absent, but the main anharmonic corrections to transition frequencies are taken into account.

Consider for definiteness upward transitions from the $|g_\alpha\rangle$ state to the $|g_{\alpha'}\rangle$ state near the frequency v_a of one of the modes active with respect to the optical process to which the operator $\widehat{O}$ corresponds. For simplicity, we assume that the v_a mode is nondegenerate. In the harmonic basis, only one upward vibrational transition can occur from each $|h_\beta\rangle$ state to the $|h_\beta^{(+)}\rangle$ state in which the occupation numbers of all modes, except for v_a, are the same as in $|h_\beta\rangle$ (i.e. $v_b^{(\beta_+)} = v_b^{(\beta)}$ for $b \neq a$), while the occupation number of the v_a mode increases by unity: $v_a^{(\beta_+)} = v_a^{(\beta)} + 1$.

Let us now introduce the main harmonic corrections to the energies of the $|h\rangle$ states. Taking them into account, the frequency of the $|h_\beta\rangle \to |h_\beta^{(+)}\rangle$ transition has the form

$$\omega_\beta^{(+)} = v_a + 2x_{aa}v_a + \sum_{b\neq a} x_{ab}v_b\,, \tag{2.10}$$

where x are spectroscopic anharmonic constants, and we restrict our consideration to the transition intensity $I_\beta^{(+)}$ written in the harmonic approximation, thus expressing it in the $|v_a{=}0\rangle \to |v_a{=}1\rangle$ transition intensity units as $I_\beta^{(+)} = v_a^{(\beta)} + 1$. Then, taking the expansion $|g_\alpha\rangle = \sum_\beta c_{\alpha\beta}|h_\beta\rangle$ (2.1) as a starting point, we will see that, if the $|h_\beta^{(+)}\rangle$ states were the *eigenstates*, a paling of lines with frequencies $\omega_\beta^{(+)}$ (2.10) and intensities $|c_{\alpha\beta}|^2(v_a^{(\beta)}+1)$ would be observed.

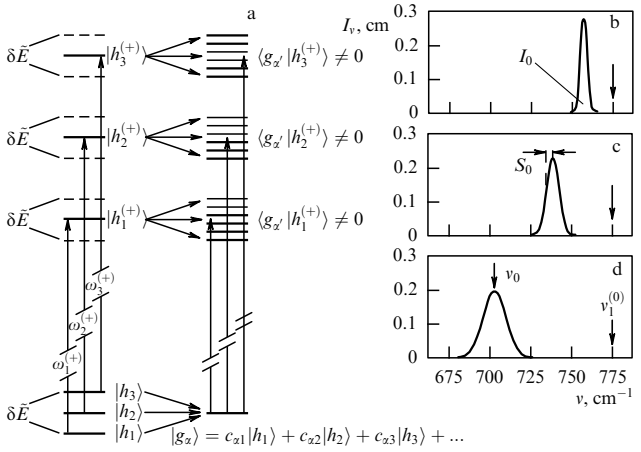

Figure 6. (a) Illustration for the case where the similarity of the spectra of transitions between ergodic $|g\rangle$ states with the spectra of transitions for ensembles of $|h\rangle$ states can be expected. The allowed transitions between $|h\rangle$ states are shown in the left part. The mixing of different $|h\rangle$ states leads to the formation of the $|g_\alpha\rangle$ state in the right part of the diagram. Optical transition can occur from the $|g_\alpha\rangle$ state to the $|g_{\alpha'}\rangle$ state having the nonzero projection onto some of the states $h^{(+)}$. (b–d) Shapes of the inhomogeneous band profile in the quasicontinuum of the SF_6 molecule (Stokes Raman scattering in the v_1 band) calculated for different energies: 7000 (b), 15,000 (c), and 30,000 cm^{-1} (d) [119].

However, this is not the case: the $|g_{\alpha'}\rangle$ eigenstates near the energy $E_\alpha + v_a$, being ergodic, are also the *superpositions* of regular states, and, therefore, an optical transition from the $|g_\alpha\rangle$ state can occur to *any* $|g_{\alpha'}\rangle$ state having the nonzero projection onto *any* $|h_\beta^{(+)}\rangle$ state. The corresponding expression for the nondiagonal matrix element of the operator $\widehat{O}$ takes the form

$$\langle g_\alpha|\widehat{O}|g_{\alpha'}\rangle = \sum_\beta c_{\alpha\beta}^* c_{\alpha'\beta_+}\langle h_\beta|\widehat{O}|h_\beta^{(+)}\rangle\,. \tag{2.11}$$

Nevertheless, the limiting case is realistic [118, 119] when the spectrum of $|g_\alpha\rangle \to |g_{\alpha'}\rangle$ transitions is *similar* to the above-described spectrum consisting of lines with frequencies $\omega_\beta^{(+)}$ and intensities $I_\beta^{(+)}$. This is the situation (Fig. 6a) when the energy interval $\delta\widetilde{E}$ of mixing regular states (see Section 2.1) is much smaller than the dispersion of frequencies $\omega_\beta^{(+)}$. Then, each of the lines is transformed into a 'quasicontinuum' with the width $\delta\widetilde{E}$ and integral intensity $I_\beta^{(+)}$. The resulting spectrum is *inhomogeneous* because its broadening is caused by the difference in the frequencies of transitions from different regular $|h_\beta\rangle$ states contributing to the $|g_\alpha\rangle$ state. The number $\widetilde{N}$ of these states is considerably larger than the number of significant terms in the sum in formula (2.11). Therefore, if we do not take into consideration the small-scale structure, the interference of different terms entering into this sum weakly affects the shape of the spectral envelope.

It is relevant to begin the analysis of transitions between ergodic states, both from the theoretical point of view and for processing experimental results, by constructing inhomogeneously broadened spectra for ensembles of the $|h\rangle$ states. For brevity, we will call these spectra *basis* spectra, and the effect itself *statistical* inhomogeneous broadening (SIB), as distinguished from other rather trivial inhomogeneous effects.

The calculation of the basis spectrum for the specified total vibrational energy of a molecule is rather simple if the vibrational frequencies and spectroscopic anharmonic con-

stants of the molecule are known. An example for an SF_6 molecule [119] is demonstrated in Figs 6b–d. The choice of this molecule for studies was not accidental. It was assumed earlier [120] that the inhomogeneous effect makes a dominant contribution to the ν_3 IR absorption band width in the quasi-continuum of an SF_6 molecule. References to corresponding experimental papers will be given in Section 5.5. Here, we note that numerical experiments [119] performed for different modes of SF_6 and WF_6 molecules led to the following main conclusions:

(i) a spectral histogram for transitions from those states with the given energy subjected to smoothing is approximated well by the Gaussian profile

$$I(\nu) = \frac{I_0}{S_0\sqrt{2\pi}} \exp\left[-\frac{(\nu-\nu_0)^2}{2S_0^2}\right]; \tag{2.12}$$

(ii) the three parameters of Gaussian profile (2.12) (the integral I_0, the position ν_0 of its maximum, and the half-width S_0 at the $1/\sqrt{e}$ level) coincide, respectively, with the average intensity, average frequency, and dispersion of transition frequencies calculated for an ensemble, and

(iii) all three parameters are described well enough by linear dependences in a broad range of the vibrational energy E.

Consider now the question of how and to what extent the IVR effect can change the basis SIB spectrum. Notice at once a rather important feature that the IVR effect can cause both the broadening of the basis spectrum and its narrowing.

The situation here qualitatively corresponds to conclusions of the stochastic Kubo theory of the spectral line shape [121], where, notably, a simple model is used: an oscillator with a friction (decay) whose frequency ω undergoes random modulations with the amplitude $\Delta\omega$ and correlation [10] time τ_c. By analogy with this model, the IVR from the ν_a mode corresponds to friction, the IVR between other ν_b modes corresponds to modulation, $\Delta\omega$ corresponds to the width of the basis SIB spectrum, and the case of dominating SIB corresponds to the fulfilment of the inequality $\Delta\omega\,\tau_c \gg 1$, i.e. the relative rate of the change in the oscillator frequency is small compared to the amplitude of this change. Then, as the decay and modulation rates increase, the spectrum of transitions changes qualitatively in the following way. Decay leads to the broadening of the spectrum, while modulation causes its narrowing. Similarly in our problem: the IVR from the ν_a mode tends to broaden the spectrum, while the IVR between other ν_b modes tends to narrow the spectrum.

The collapse of an inhomogeneously broadened line is called 'dynamic narrowing' or 'motional narrowing' in the recent literature. This term originates from the Dicke collisional narrowing effect — the paradoxical narrowing of the Doppler profile of an atomic transition upon increasing the gas pressure, as predicted by Dicke [122], which can be observed if collisions do not cause population redistribution and dephasing, but only change the velocity of atoms. Later on, a similar effect was considered for the Q branch of a Raman band [123–125], where narrowing occurs due to rotational relaxation.

We can formulate general conditions for the possibility of the collapse of an inhomogeneous line profile [126]. Consider a system of parallel transitions, similar to $|h_\beta\rangle \to |h_\beta^{(+)}\rangle$ in Fig. 6a, with identical nondiagonal matrix elements $\langle h_\beta|\widehat{O}|h_\beta^{(+)}\rangle$ of the operator $\widehat{O}$ responsible for the optical transition. We assume that population redistributions (relaxation transitions) are possible only within a group of the $|h_\beta\rangle$ states and within a group of $|h_\beta^{(+)}\rangle$ states, with the corresponding $\beta \leftrightarrow \beta'$ interactions (or the rates of relaxation transitions) being identical in pairs for the upper and lower groups. It is in this case that line narrowing occurs upon increasing the relaxation rate (population redistribution). Both the Dicke model and the situation with the Q branch in Raman spectra satisfy the required conditions with good accuracy.

In our system of parallel transitions in Fig. 6a, the collapse of the SIB spectrum can, in principle, also occur because general conditions are satisfied. However, unlike previous examples, where the relationship between the inhomogeneous width and the rate of collisional relaxation can be controlled by the gas pressure, here the result is assigned by Nature. The only factor that can change this relationship is the total vibrational energy of a molecule.

General regularities in the analytic form can be analyzed only in a model assumption, which may be called the *thermostat approximation*. This approximation assumes that for the specified total vibrational energy E, each ν_i mode is characterized by its equilibrium energy $\varepsilon_i^{(eq)}$ and its rate γ_i of transition to equilibrium. As for equilibrium properties, they are characterized by a single parameter — the effective temperature T_{eff} — which is formally related to the energy E by the expression

$$E = \sum_i \nu_i \left[\exp\left(\frac{\nu_i}{T_{eff}}\right) - 1\right]^{-1}. \tag{2.13}$$

This gives expressions for equilibrium distribution functions with respect to occupation numbers v_i in ν_i modes:

$$f(v_i) = (1-\xi_i)\,\xi_i^{v_i}, \tag{2.14}$$

and for relaxation rates γ_i of ν_i modes:

$$\gamma_i = (1-\xi_i)\,\Gamma_i, \tag{2.15}$$

where $\xi_i = \exp(-\nu_i/T_{eff})$, and Γ_i is the rate of the $v_i = 1 \to v_i = 0$ relaxation transition in the ν_i mode.

The principal weak points of this approximation are quite obvious. First, it is assumed that modes relax independently. Second, an ensemble of states with a narrow energy distribution (for brevity, a microcanonical ensemble) is described by laws that are valid for a canonical ensemble. Third, the relaxation of modes is assumed to occur by the one-quantum mechanism.[11] However, as for the influence of all the above-mentioned negative factors on optical spectra, there are physical arguments [92, 118, 127–130] confirming that the thermostat approximation is substantiated, at least for high enough vibrational energies.

Using the thermostat approximation, we can analytically calculate the transition spectrum in the ν_a mode [92] with relaxation rates $\gamma_{a,b}$ and spectroscopic anharmonic constants

[10] As a representation revealing the physical sense of the correlation time, a model can be considered in which the oscillator frequency undergoes instant jumps by $\Delta\omega$ on average, the mean time between jumps being τ_c.

[11] In an oscillator–thermostat model, transition rates increase upon increasing the occupation numbers: $\Gamma_{v\to v-1} = v\Gamma$. In addition, the relation between the rates of direct and inverse transitions also obeys the principle of detailed balance: $\Gamma_{v-1\to v} = \xi\Gamma_{v\to v-1}$.

x_{ab} as parameters. We restrict ourselves to the description of limiting cases because only they were used when interpreting the experimental results discussed below.

First, let us determine the conditions under which the SIB spectrum collapses into a homogeneously broadened profile. This requires the fulfilment of the inequalities

$$\gamma_b \gg \frac{x_{ab}}{\hbar(1-\xi_b)} \tag{2.16}$$

for all bath v_b modes. In this case, the optical spectrum is described by a Lorentzian with the central frequency coinciding with the center of gravity of the SIB spectrum, and the full width at half-maximum (FWHM) described by the expression

$$\widetilde{\gamma} \approx \frac{2}{\hbar^2} \sum_b \frac{\xi_b \Delta_b^2}{(1-\xi_b)^2 \gamma_b}\,, \tag{2.17}$$

where $\Delta_b \approx x_{ab}$. The quantity $\widetilde{\gamma}$ is the *purely phase* relaxation rate [131, 132] because IVR from the v_a mode is not involved in its formation. One can see that it decreases as the IVR rate increases.

It should be noted here that both above-considered effects (the inhomogeneous broadening and purely phase relaxation) have, in theory, a common nature, namely, the different interaction of the lower and upper level for the optical transition with the environment. An illustrative example is molecules (atoms) embedded into a solid matrix. Such systems, as a rule, possess a broad inhomogeneous spectrum (see, for example, Ref. [133]) related to different Stark shifts of the lower and upper levels and different positions of atoms with respect to their neighbors. However, the spectrum strongly narrows when the solid phase is melted into liquid. This example also clearly demonstrates the analogy with the Kubo modulation (see above). The modulation in a solid is slow (molecules slowly change their positions), while modulation in liquid occurs rapidly, so that the position of a molecule with respect to its neighbors is efficiently averaged.

Consider now the influence of IVR from the optically active v_a mode on the transition spectrum. In fact, it is described by the oscillator-in-thermostat model. The spectrum of a harmonic oscillator is described by a Lorentzian with the FWHM equal to $\hbar\gamma_a$, where the relaxation rate γ_a is given by formula (2.15).[12] The analytical solution for the resonance profile of an anharmonic oscillator was first obtained in papers [135, 136]. In Refs [92, 132], this solution is represented in a more convenient form corresponding to the notation adopted here. The typical evolution of the spectrum from individual lines at oscillator frequencies for $\gamma_a = 0$ to a Lorentzian with the FWHM equal to $\hbar\gamma_a$ (when the condition $\hbar\gamma_a \gg 2x_{aa}/(1-\xi_a)$, similar to Eqn (2.16), is fulfilled) is depicted in Fig. 7.

The resulting spectrum, taking into account the effects considered above, is found as a convolution of different segments. In limiting cases, we have either the SIB spectrum or the convolution of the SIB spectrum with the γ_a Lorentzian or a Lorentzian with the FWHM equal to $\hbar(\gamma_a + \widetilde{\gamma})$, where $\widetilde{\gamma}$ is given by formula (2.17).

[12] The fact that the width of the spectrum does not increase with temperature but decreases despite the increase in the $v \to v-1$ transition probability proportionally to v is called 'the harmonic oscillator paradox' in the literature (see, for example, Ref. [134] and references cited therein).

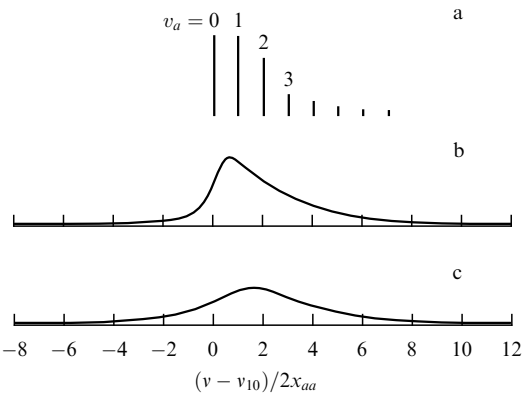

Figure 7. Spectra of upward transitions in an anharmonic molecular mode in the absence of the SIB effect from other modes. The values of the parameters are: $\xi_a = 0.5$; $\gamma_a = 0$ (a); $\gamma_a = x_{aa}/\hbar(1-\xi_a)$ (b); $\gamma_a = 6x_{aa}/\hbar(1-\xi_a)$ (c).

2.4 Where and how the elements of the theory are used below

In this review, we mainly focused on transitions between the lower regular states and upper ergodic states. In that case, information is obtained either from the experimental spectra of the type presented in Fig. 1 (see Section 3) or from experimental results on the IVR dynamics from excited states (see Section 4), which are interpreted by applying dependences like those presented in Fig. 4.

More sophisticated experimental methods mainly concern spectroscopy involving excited electronic states and high overtones. The principles underlying the interpretation of the results here are the same; we, as mentioned at the end of Introduction, will present only a brief discussion in corresponding Sections 5.2–5.4.

As for transitions *between* ergodic states, here we will also restrict ourselves to a brief discussion (see Section 5.5), considering both limiting cases: a Lorentzian with the width caused by IVR, and a spectrum described well by the SIB effect. At the same time, the results of two experiments we consider in more detail. The first focuses on investigations of large molecules, where the thermal population of the initial states of the optical transition is probably such that most of them lie in the region of the vibrational chaos. The shape of the spectrum observed in one of these experiments is probably dominated by SIB, which was reflected in a rather nontrivial way in the picosecond dynamics of the absorption spectrum [137]. This issue is discussed in Section 4.2.3. In the other experiment, that opposite case is probably realized, when IVR between bath modes leads to the narrowing of the SIB spectrum and its transformation into a Lorentzian with width (2.17). This example is related to usual IR absorption spectroscopy, from which we will start the next section.

3. High-resolution IR spectroscopy of cooled molecular beams in IVR studies

3.1 Preliminary remarks

The first seriously motivated attempt to perform the spectroscopy of a quasicontinuum for obtaining information on the IVR rate was reported in paper [138]. The authors studied the absorption spectrum of $(CF_3)_3CH$ molecules in the region of the band corresponding to the high-frequency vibration of the

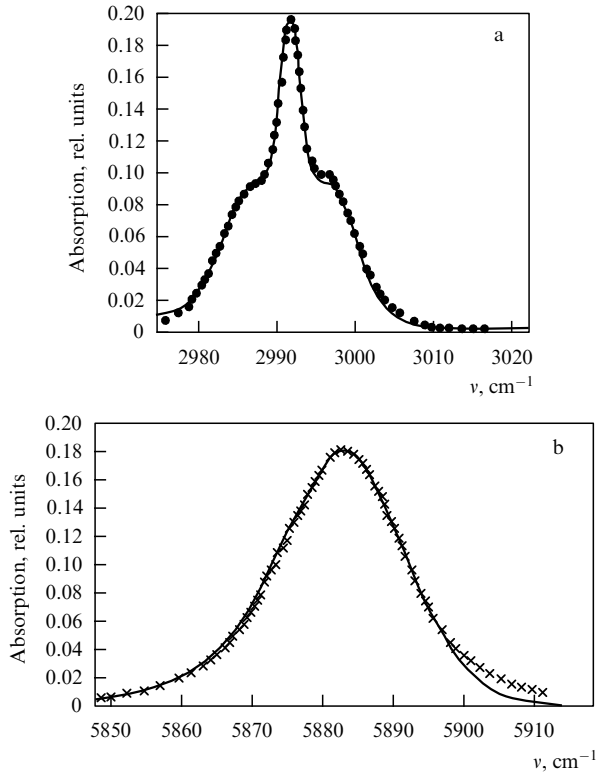

Figure 8. Absorption spectra of the $(CF_3)_3CH$ molecule in the region of the fundamental ν_1 band (a) and the first overtone $2\nu_1$ (b). Experiments (solid curves) are compared with numerical calculations (dots and crosses) including simulations of each rotational component by a Lorentzian with a variable width and taking into account the instrumental functions of the spectrometers used in experiments. (Taken from Ref. [138].)

C–H bond (the $\nu_1 \approx 2991$ cm^{-1} mode) using a spectrometer with a resolution of 0.6–0.8 cm^{-1}, which could not resolve individual vibrational–rotational lines. They observed a continuous band spectrum (Fig. 8a) clearly demonstrating the distortion of the usual *PQR* configuration in which the *Q* branch was much less pronounced than in usual spectra of parallel bands from symmetric tops. Based on this observation, the authors assumed that individual vibrational–rotational lines are broadened due to IVR from the ν_1 mode (in the same sense as in the example in Section 1.1). This spectrum was processed assuming that each vibrational–rotational line is described by a Lorentzian profile with the width γ varied to fit calculations with experimental data. As a result, a linewidth of 3 cm^{-1} was obtained, which gives the IVR rate (according to the authors' assumption) $W \approx 6 \times 10^{11}$ s^{-1}.

The authors of paper [138] also measured the spectrum of the first overtone band of the same vibration. Here, the *Q* branch is not distinguishable at all (Fig. 8b), and the same fitting procedure gave the linewidth of 12 cm^{-1}. The simplest model of the oscillator one-quantum relaxation predicts only a twofold increase in the IVR rate on passing from ν_1 to $2\nu_1$. In this case, we may not assign particular significance to the deviation from the linear law[13] because, due to the strong anharmonicity of the C–H vibration, the structure of the Fermi resonances in the $2\nu_1$ region can strongly differ from that in the ν_1 region.

[13] In particular, the theory predicted a rather irregular dependence of the IVR rate on the occupation number for high-frequency local modes of molecular crystals, for example, in methane [139].

However, subsequent studies of the $(CF_3)_3CH$ molecule revealed that the observed quadratic dependence in not accidental. The same authors, in collaboration with another research team, measured the spectra of higher overtones [140]. In particular, the linewidth of 28 cm^{-1} was obtained for the second overtone ($v = 3$). The authors noted that the absorption band of this 'large' molecule with many low-frequency modes can be inhomogeneously broadened to a great extent at room temperature. However, they failed to explain the evidently quadratic dependence on v observed in experiments and asserted that both IVR from the given mode and the inhomogeneous component should, in principle, give a linear dependence.

The correct interpretation is probably as follows. Assume that the vibrational chaos in $(CF_3)_3CH$ already takes place at the energy (approximately 2000 cm^{-1}) [138]) corresponding to room temperature. Assume also that the IVR rates for bath modes are such that conditions (2.16) are fulfilled for them (for example, $\gamma_b \sim 10^{12}$ s^{-1} and $x_{ab} \sim 1$ cm^{-1}), which lead to the narrowing of the SIB profile and its transformation to a Lorentzian with width (2.17). That being so, it is worth noting that, if we use constants x_{ab} for anharmonic shifts Δ_{ab} in the fundamental band, the step of a frequency progression for overtones is multiplied by v, i.e. quantities vx_{ab} should be used. This yields a quadratic dependence on v observed in experiments [138, 140].

Although the IR absorption spectroscopy is an absolutely classical field with a huge number of publications, the study of $(CF_3)_3CH$ molecules remained unique for some time. This was probably explained by the fact that one-photon excitation energies, even in high-frequency modes, were assumed insufficient for reaching the vibrational chaos region. At that time, however, papers [141, 142] on the spectroscopy of the high overtones of local modes in benzene corresponding to C–H vibrations attracted greater interest.[14] The authors of these papers attempted to link large linewidths with ultrashort IVR times of ~ 100 fs. However, probably being aware of the ambiguity of such an estimate, the authors proposed utilizing the cooled molecular beam technique providing the drastic narrowing of the rotational distribution, which had already been introduced by the time [145, 146] into spectroscopic experiments.

Work in this direction was performed within a few years [147, 148].[15] Indeed, much narrower spectral lines were observed (in particular, the IVR time for the second overtone was estimated as a few picoseconds), which has cast some doubt on the IVR times reported in paper [142] for higher overtone states and on the correctness of accompanying theoretical calculations (see, for example, Refs [150, 151]) pretending to explain them.

We will not consider in detail specific overtone studies,[16] and present key references in Section 5.4. Note here, however, one symbolic coincidence to emphasize how important is a broad and rapid exchange of ideas in the scientific community: above-cited paper [148] was published in the same issue

[14] It is worth noting here an important technical detail: the detection of overtone spectra (beginning from the second overtone) using the optoacoustic effect [143, 144]. A cell with benzene was placed inside the cavity of a cw dye laser. Different dyes and different pump lasers were employed.

[15] The cooled molecular beam technique was applied in combination with selective multilevel saturation spectroscopy [149] in the original version.

[16] Studies using direct high-resolution spectral measurements are considered in Section 3.4.

of the journal as the very first paper [152] in which an attempt was made to reveal qualitative features inherent in IVR in the *fundamental* IR absorption band, rather than in an overtone band, and where the cooled molecular beam technique was also used. In this paper, an appropriate object was found at last. The authors studied the $\nu_{HC} \equiv \nu_1$ acetylene type mode in a butyne ($HC \equiv CCH_2CH_3$) molecule.[17] The attempt was basically successful, although the spectral resolution and the signal-to-noise ratio were still insufficient for conclusions reached in the paper to be correct.

To elucidate this question, we should recall the specific features of the classification of rotational levels (and, consequently, vibrational–rotational IR spectra) of asymmetric top type molecules. Two classification methods are encountered in the literature. The first (see, for example, classic monograph [3]) consists in numbering the $2J+1$ sublevels whereto the value J of the total angular momentum corresponds, by the subscript τ running the values from $-J$ to $+J$ with increasing energy.

The more popular classification method (see, for example, monograph [153]) involves a pair of quantum numbers $\{K_a, K_c\}$ having a clear physical meaning and being assigned to each J sublevel. The subscripts a and c refer to the principal axes of the top with the minimal and maximal inertia moments, respectively. Thus, the subscript a is associated with the maximal rotational constant A, and the subscript c with the minimal rotational constant C ($A > B > C$, where B is an 'average' of the three rotational constants). Then, a topological correspondence of the given sublevel to the level of a prolate symmetric top (when C tends to B) and to the level of an oblate symmetric top (when A tends to B) is established. In each of these cases, the level will be characterized by its quantum number K — the projection of the angular momentum onto the a (K_a)-axis in the first case, and onto the c (K_c)-axis in the second case.

Generally, the interpretation of an IR spectrum is a complicated problem. However, here it is simplified because, first, the butyne molecule is almost a symmetric prolate top, and the ν_{HC} vibration under study occurs with good accuracy along the a-axis. Therefore, the rotational structure of the band is very close to the structure of the parallel band of a symmetric top with the selection rules $\Delta J = 0, \pm 1$ and $\Delta K = 0$, where K_a stands for K in our case, and transitions with $\Delta K_a \neq 0$ are much weaker.

Based on the assignment of spectral lines presented in paper [152], the authors of this paper concluded that the splitting of lines to multiplets, indicating IVR (see Section 1.1), is observed for transitions with $K_a = 0$, but is absent for transitions with $K_a = 1$. This conclusion is illogical because there are no serious grounds to assume that anharmonic interactions of the first excited level of the ν_{HC} mode with bath states ($\mathcal{Z}_0$ and $\mathcal{B}_s$, respectively, in the notation used in Fig. 3) are substantially distinct for different K_a. If, however, vibrational–rotational interactions show their worth, they should be more strongly manifested for states with a larger value of K_a. However, later in paper [1] both the spectral resolution and signal-to-noise ratio were improved. The assignment of the lines was considerably refined, and the authors concluded that no qualitative differences between optical spectra with different K_a were observed. Thus, paper [1] really should be considered as the starting point for subsequent activity in this field.

Later on, most attention was focused on various propyne derivatives. The results of papers devoted to the spectroscopy of the ν_{HC} mode in these molecules are presented in Section 3.3, where the IVR *rates* are mainly discussed. The results of studies of other objects are reviewed in Section 3.5. In Section 3.6, we consider the manifestations of *vibrational–rotational interactions* in IR spectra and the role of these interactions in the IVR itself.

It should be added here that the experiments to measure IR absorption spectra in molecular beams are far from trivial.

[17] To avoid misunderstandings, we introduce the double notation for this mode because in molecular spectroscopy ν_1 traditionally denotes the highest-frequency totally symmetric vibration, and we will encounter below examples of molecules with O–H bonds, or N–H bonds with frequencies in the ranges from 3600 to 3700 cm^{-1}, or from 3350 to 3400 cm^{-1}, respectively.

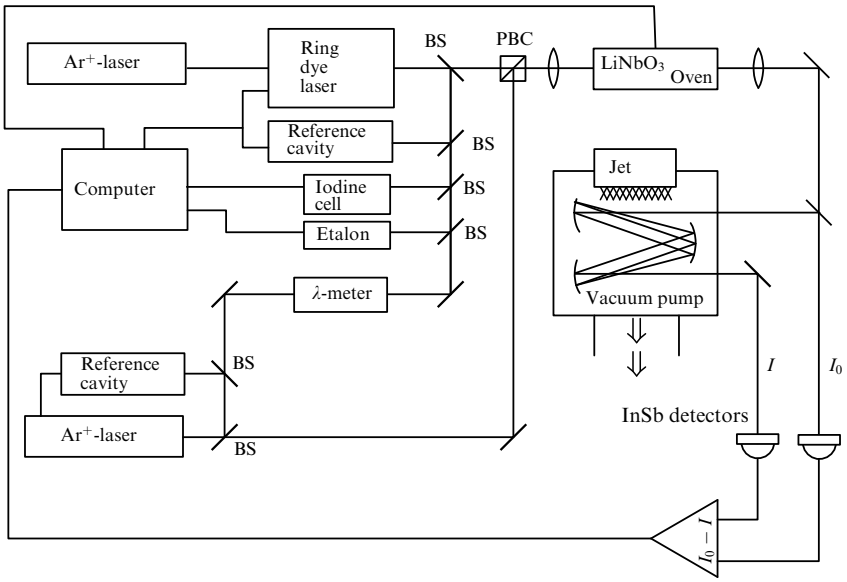

Figure 9. Schematic of a laser spectrometer based on the difference frequency generation and using a nozzle molecular jet. BS — laser beam splitter, PBC (polarization beam combiner) — device for laser beam convergence with orthogonal polarizations. A lithium niobate crystal can be heated to achieve optimal phase-matching conditions. (Taken from Ref. [2].)

The methods applied in these experiments have a number of specific features which are discussed in the next section.

3.2 Experimental technique

The details of the first experiments are most thoroughly described in paper [2] (see the schematic in Fig. 9). Radiation tunable in the 3-μm region was obtained by generating the difference frequency in an $LiNbO_3$ nonlinear crystal from two narrowband cw lasers: an argon laser emitting at a fixed wavelength, and a tunable dye laser. The output power of this radiation source was a few microwatts, and the resulting linewidth was less than 2 MHz (or 1.5×10^{-4} cm^{-1}). Gas was expanded into a vacuum, passing through a 4 cm $\times$ 57 μm slit. The carrier gas was helium (at a pressure of 1000 Torr in a chamber). Translational and rotational temperatures of ~ 4 K were reached due to collisions of the molecules with the carrier gas atoms.

In earlier paper [152], another radiation source based on an F-center laser was used with the linewidth also estimated as 10^{-4} cm^{-1}. The main difference was in the shape of the nozzle, which was supersonic with a diameter of 1 mm. Cooling was somewhat deeper: down to 3 K.

Radiation was detected in both these papers in a standard way by comparing the reference beam intensity with the intensity of the beam propagated through cold gas. The optical length was increased by employing a multipass geometry: approximately 12 passes in papers [1, 2], and 41 passes in paper [152] but, taking the nozzle geometry into account, the total optical path was probably somewhat shorter than in the former case.

In subsequent papers, a collimated (with an aperture) molecular beam was utilized instead of a jet. The advantage is a drastic decrease in the Doppler linewidth upon irradiation of molecules in the transverse direction. Thus, according to estimates [2], the Doppler linewidth achieved due to cooling the translational degree of freedom was only slightly smaller than 10^{-3} cm^{-1}. Therefore, it is easy to recognize that the potential inherent in the laser linewidth cannot be used in full degree. The employment of a collimated beam improves the spectral resolution by almost an order of magnitude, thereby providing the spectroscopy of denser IVR multiplets than these shown in Fig. 1.

However, the application of a beam instead of a jet leads to a considerable decrease in the integrated absorption. For this reason, absorption in experiments with the beam geometry is measured by a different, optothermal method. As a detector, for example, a silicon bolometer at liquid-helium temperature can be utilized, which produces an output signal due to transfer of vibrational excitation to heat in collisions of molecules with the bolometer surface.

The two methods for detecting radiation absorption were compared in detail in paper [154], where a combination of a collimated beam and an optothermal detector was used for the first time to record IVR multiplets. The authors emphasized the necessity of exploiting a laser with the highest possible output power. The study was performed in two spectral ranges: the 3-μm region (ν_{HC} acetylene type vibration), and the 1.5-μm region ($2\nu_{HC}$ overtone). The laser power in the 3-μm region was ~ 20 mW upon pumping an RbCl:Li-F_A crystal by radiation from a commercial Kr^+ laser, while the laser power at 1.5 μm was 150 mW upon pumping thallium color centers in a KCl crystal by radiation from a cw Nd:YAG laser.

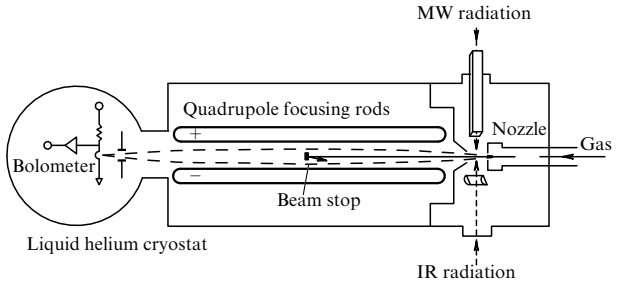

Figure 10. Schematic of an electric-resonance optothermal spectrometer (EROS) operating in both the IR and the microwave (MW) ranges. A screen located in the middle of quadrupole rods reflects molecules initially traveling near the central axis, which increases the contrast of the useful signal. (Taken from Ref. [155].)

Most of the subsequent experiments were performed in this configuration but, beginning from a certain moment, with one important addition. The optothermal detection was employed in combination with a focusing electric field of the quadrupole symmetry (Fig. 10). The field provides the deflection of a molecule, if only it is not a spherical top, either to the axis of the quadrupole device or away from it, depending on the sign of the Stark effect for the given vibrational–rotational state. This experimental setup was called an electric resonance optothermal spectrometer (EROS) [155]. The predominant focusing (defocusing) of the beam component belonging to molecules in which the optical transition is resonant with laser radiation leads to an increase (decrease) of the signal. In both cases, the alternate signal component caused by the radiation modulation is detected.

In some experiments (see, for example, Refs [156, 157]), the method of double MW–IR resonance was additionally applied.[18] This method considerably simplifies the identification of the spectrum in cases where the IVR multiplets belonging to different rotational quantum numbers J overlap.

We should also mention separately papers [161–168] in which various theoretical issues concerning the interpretation of data obtained from high-resolution spectral measurements were considered.

Results obtained in the early 1990s are included in review [169] specially devoted to the topic of this section. These findings are also partially discussed in a thematically broader review [87]. Unfortunately, we cannot recommend later review [170] because it contains many incorrect tabulated data concerning high-resolution spectroscopy.[19]

3.3 Propyne derivatives: IVR rates

3.3.1 Results of measurements. Paper [2] was entirely devoted to studying the propyne ($HC \equiv CCH_3$) molecule. No noticeable mixing of the first excited state of the $\nu_{HC} \equiv \nu_1$ mode with other vibrational states was revealed. This result was confirmed later in paper [171] where the spectrum of transitions from states with projections of the angular

[18] The fundamentals of the double-resonance method are presented, for example, in review [158]. A combination of this method and the EROS technique is considered in Refs [159, 160] (see also Fig. 10).

[19] We report to fans of pseudoscientific figures that the impact factor of the journal in which this review was published was 26.58 (!) as of this writing.

Table 1. IVR times for the first excited state of the ν_{HC} mode of H − C ≡ C − *R* type molecules.

Molecule	IVR time, ps	References
HC ≡ CCH_2OH	400	[174]
HC ≡ CCH_2NH_2	500[1*]	[175]
HC ≡ CCH_2CH_3	269	[169][2*]
trans-HC ≡ $CCH_2CH_2CH_3$	1000	[172][3*]
gauche-HC ≡ $CCH_2CH_2CH_3$	325	[172][3*]
HC ≡ $CCHFCH_3$	133	[172]
HC ≡ CCH_2CH_2F	1480	[172, 176]
HC ≡ CCH_2CH_2Cl	3480	[172, 176]
HC ≡ CCH_2CH_2Br	1990	[172, 176]
HC ≡ $CC(CH_3)_3$	200[4*]	[154]
HC ≡ $CSi(CH_3)_3$	2000	[154]
HC ≡ $CSn(CH_3)_3$	6000	[154]
HC ≡ $CC(CD_3)_3$	40	[178]
HC ≡ $CSi(CD_3)_3$	830[5*]	[169]
HC ≡ $CC(CF_3)_3$	60	[179]
HC ≡ CCH_2OCH_3	300	[172]
HC ≡ $CC(CH_3) = CH_2$	105	[172]
trans-HC ≡ $CCH = CHCH_3$	83	[172]
cis-HC ≡ $CCH = CHCH_3$	183	[172]

[1*] The IVR rate increases with increasing K_a.
[2*] Determined from data in Ref. [1]. In later paper [172], the time 70 ps was reported. Because it was given without any comments, we assume that this is a misprint.
[3*] Considerable refinements compared to the values presented in review [169]: 442 ps for the trans-form, and 241 ps for the gauche-form.
[4*] A different time, 400 ps, was given in previous paper [177].
[5*] Refined value compared to 850 ps presented in Ref. [178].

momentum up to $K = 6$ was studied in detail. The simplest derivatives of propyne are those in which one of the hydrogen atoms of the methyl group is replaced by the halogen atom: HC≡CCH_2F (propargyl fluoride), HC≡CCH_2Cl (propargyl chloride), and HC ≡ CCH_2Br (propargyl bromide). No mixing was observed in these molecules [172], as in propyne.

Among other halogen derivatives, trifluoropropyne (HC ≡ CCF_3) molecules were studied [173], in which the effect for the first excited state of the $\nu_{HC} \equiv \nu_1$ mode was reduced to weak perturbations. However, when the hydrogen atom was replaced by the OH radical (propargyl alcohol) or NH_2 (propargyl amine), the spectrum qualitatively changed in the same way as on passing from propyne to longer chains (butyne, pentyne; see Section 1.1). More complex molecules were also studied. A summary of characteristic IVR times estimated from the Fourier transforms of spectra (see comments on expression (2.5) in Section 2.2) is presented in Table 1.

3.3.2 Mechanisms. A few aspects of the results obtained for IVR rates/times from the ν_{HC} mode have been analyzed in the literature.

(i) It was established (see, for example, papers [1, 169]) that a considerably lower IVR rate than in the systems investigated earlier is probably caused by the spatial position of the H − C bond separated from the molecular core by the specific triple bond of carbon atoms. This raised the question about the nature of the intermediate $|\mathcal{DWS}\rangle$ state[20] coupling the excited level of the ν_{HC} mode with other bath levels. The

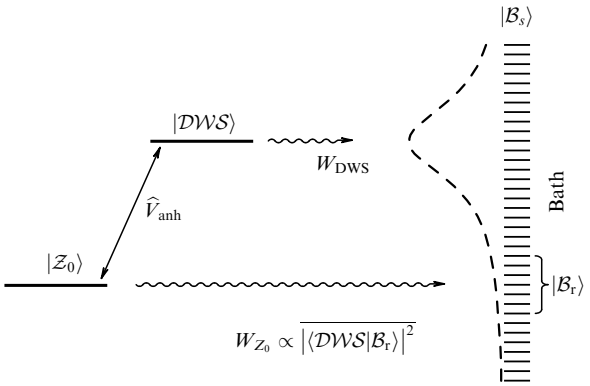

Figure 11. IVR from the ZOBS $|\mathcal{Z}_0\rangle$ state to the bath $|\mathcal{B}_s\rangle$ states when one doorway $|\mathcal{DWS}\rangle$ state dominates. The IVR rate W_{Z_0} is proportional to the mean square of the modulus of the $|\mathcal{DWS}\rangle$ projection on the bath $|\mathcal{B}_r\rangle$ states which are located most closely to the $|\mathcal{Z}_0\rangle$ state. The distribution of $|\langle \mathcal{DWS}|\mathcal{B}_s\rangle|^2$ is described on average by a Lorentzian with a width specified by the rate of IVR from the $|\mathcal{DWS}\rangle$ state, which is schematically shown by the dashed line.

situation was considered in the general form in Section 2.2 and illustrated by the energy level diagram in Fig. 3b. A more specific layout, where one dominating broadened Fermi resonance is shown, is presented in Fig. 11. The authors of paper [1] assumed that the $|\mathcal{DWS}\rangle$ state is a combination of one vibrational quantum of the triple C ≡ C bond (the frequency $\nu_{C\equiv C} \approx 2142$ cm^{-1} for propyne) and two bending vibrational quanta of the H − C ≡ C fragment (the fundamental frequency $\nu_{H-C\equiv C} \approx 633$ cm^{-1} for propyne).

The matrix element $\langle \mathcal{Z}_0|\widehat{V}_{anh}|\mathcal{DWS}\rangle$ of anharmonic interaction between ν_{H-C} and $\nu_{C\equiv C} + 2\nu_{H-C\equiv C}$ was estimated for propyne in Ref. [181] as 7 cm^{-1}. Because the energy difference $E_{DWS} - E_{Z_0}$ between the $|\mathcal{Z}_0\rangle$ and $|\mathcal{DWS}\rangle$ states in this case is much greater than this value, the IVR rate from the $|\mathcal{Z}_0\rangle$ state can be estimated as

$$W_{Z_0} \approx \left(\frac{\langle \mathcal{Z}_0|\widehat{V}_{anh}|\mathcal{DWS}\rangle}{E_{DWS} - E_{Z_0}}\right)^2 W_{DWS}\,, \tag{3.1}$$

where W_{DWS} is the rate of IVR from the $|\mathcal{DWS}\rangle$ state. Note that, even if the matrix element of anharmonic interaction in formula (3.1) is approximately the same for all propyne derivatives, and if the mutual position of two levels is known (which, however, is not always simple to achieve because the combination transition is weak), nevertheless, due to the uncertainty of W_{DWS}, it is difficult to systematize data on IVR rates. It seems that one should attempt to find a regularity in individual fragments of the general picture. Thus, the authors of paper [154] compared the results obtained for a number of molecules and have cast doubt on the hypothesis under consideration,[21] and this hypothesis was not further quantitatively analyzed. Only recent results [116, 182–184] on the real-time observation of IVR in a number of molecules, which are considered in detail is Section 4.2.4, returned this hypothesis to reliable status.

(ii) The discussion of the action produced on the IVR rate by the replacement of the central carbon atom by heavier silicon or tin atoms attracted great interest. The increase in the characteristic IVR time by an order of magnitude on

[20] DWS is the abbreviation of the often used jargon but very descriptive expression 'doorway state'. Another expression, 'key-hole state', is also involved [180].

[21] They literally stated: "We ...believe that ...there is no single state (or small set of states) that act as a doorway for the intramolecular vibrational relaxation [154]."

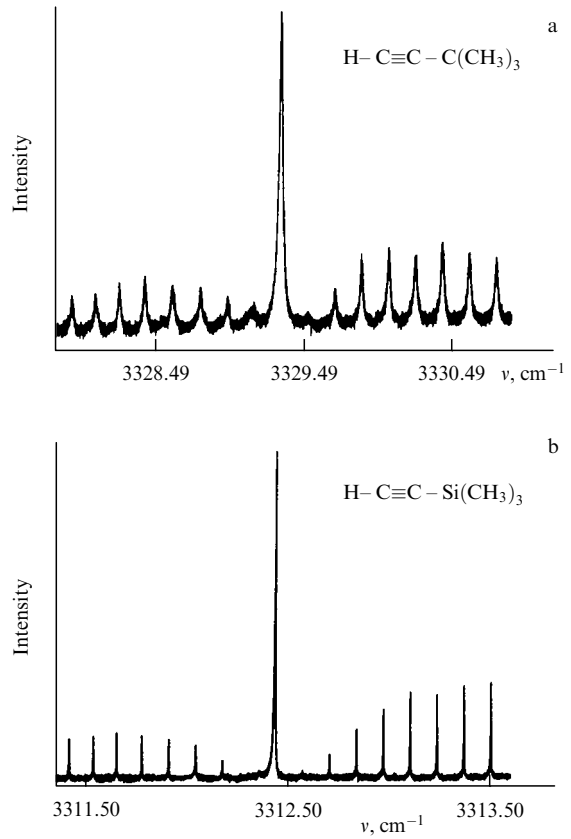

Figure 12. Vibrational–rotational spectra in the fundamental $\nu_1 \equiv \nu_{HC}$ band of $HC \equiv CC(CH_3)_3$ (a) and $HC \equiv CSi(CH_3)_3$ (b) molecules measured by the optothermal method. The spectra have the pronounced *PQR* structure. However, despite a high spectral resolution, the fine structure is not observed due to the huge density of vibrational states in these large molecules. (Taken from Ref. [154].)

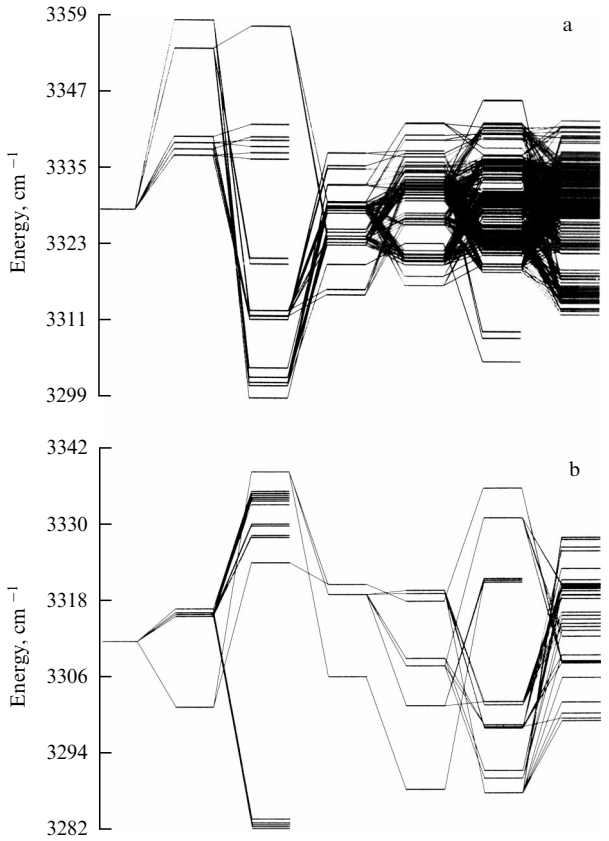

Figure 13. Tier model for $HC \equiv CC(CH_3)_3$ (a) and $HC \equiv CSi(CH_3)_3$ (b) molecules. The initial state at the left corresponds to excitation of one quantum in the $\nu_1 \equiv \nu_{HC}$ mode. Then, the first six links of chains with bonds caused by third- and fourth-order anharmonic interactions are shown. (Taken from Ref. [185]).

passing from $HC \equiv CC(CH_3)_3$ to $HC \equiv CSi(CH_3)_3$ (which is clearly seen from a comparison of the spectra of these two molecules in Fig. 12) and by another three times on passing to $HC \equiv CSn(CH_3)_3$ cannot be explained, as shown in Ref. [154], by the increase in the mass itself. Another hypothesis assumes the increase in the distance from methyl groups to the central atom with increasing mass, which reduces the barrier to internal rotations of these groups. It seems that the most substantiated consideration was arrived at in numerical experiments [185]. The authors simulated IVR as an effect caused by a chain of third- and fourth-order anharmonic interactions subsequently coupling the initial excited state of the $\nu_{HC} \equiv \nu_1$ mode with other states.[22]

The structure of the first tiers for $HC \equiv CC(CH_3)_3$ and $HC \equiv CSi(CH_3)_3$ molecules is shown in Fig. 13. One can see that, despite a considerably higher (by $\sim$ three times [169]) density of states for the molecule with the silicon atom (Fig. 13b), 'the coverage' of states by nearest tiers is greater for the molecule with the central carbon atom (Fig. 13a). The authors [185] concluded that it is this accidental absence of appropriate intermode resonances that leads to a bottleneck at the initial IVR stage, resulting in the low IVR rate.

(iii) The interpretation of a change in the IVR rate upon deuteration of methyl groups is more unambiguous. Both experiment [178] and theory [185] demonstrated about 5–7-fold increase in the IVR rate for the $HC \equiv CC(CD_3)_3$ molecule compared to the $HC \equiv CC(CH_3)_3$ molecule. This is again explained, as in the example (ii), by the increase in the density of intermode resonances, which is caused in this case by the decrease in vibrational frequencies on average.

(iv) The question of the extremely low IVR rate in halogen derivatives of butyne (lines 7–9 in Table 1) and the trans-form of pentyne (line 4 in Table 1) was discussed. The latter case corresponds by definition to a configuration in which hydrogen atoms of two CH_2 groups lie in the same plane, and it was emphasized [189] that the main form of halogen derivatives of butyne is the trans-form, which has the similar 'plane' configuration (the barrier separating it from the gauche-form is approximately 500 cm^{-1}; see also paper [176]). This observation is undoubtedly promising and deserves a detailed interpretation in the future.

3.4 Propyne and its derivatives: spectroscopy of overtones

The study of overtones of the $\nu_{HC} \equiv \nu_1$ mode for molecules in which no signs of IVR have been observed in the fundamental band is of natural interest. The main reason is the possibility of finding the boundary of a passage from regular to stochastic vibrational motion. The first attempt was made in papers [190, 191] where the spectroscopic measurement of the $|2\nu_1\rangle$ state of the propyne ($HC \equiv CCH_3$) molecule was taken by utilizing two-step IR excitation and exploring absorption at the $|\nu_1\rangle \rightarrow |2\nu_1\rangle$ transition.

[22] This approach is called 'the tier model' in the literature (see, for example, Refs [186–188]). This model is qualitatively similar to the mixing mechanism illustrated in Fig. 2.

Table 2. IVR times for the first overtone $|2v_{HC}\rangle$ state of $HC \equiv CX(CY_3)_3$ type molecules.

Molecule	IVR time, ps	References
$HC \equiv CC(CH_3)_3$	110	[154]
$HC \equiv CC(CD_3)_3$	< 40	[178]
$HC \equiv CSi(CH_3)_3$	4000	[154]
$HC \equiv CSi(CD_3)_3$	140	[178]
$HC \equiv CSn(CH_3)_3$	> 1000	[169]
$HC \equiv CC(CF_3)_3$	$< 40^*$	[169]

* A more careful estimate than the time of 5 ps presented in Ref. [179] with a question mark.

Somewhat later, experiments were performed with *direct* excitation of the $|0\rangle \rightarrow |2v_1\rangle$ transition and optothermal detection [192]. Because no signs of IVR from the $|2v_1\rangle$ state were inferred, the second overtone was examined. Here, the two-step $|0\rangle \rightarrow |v_1\rangle \rightarrow |3v_1\rangle$ excitation was applied [193]. The characteristic IVR time from the $|3v_1\rangle$ state was estimated in this paper as 320 ps (see also review [169]). Theoretical simulation performed in work [194] turned out to be in good agreement with experiments.

The first overtone was also studied for yet another $HC \equiv CCF_3$ molecule in which the fundamental transition showed no signs of IVR [173]. The IVR time from the $|2v_1\rangle$ state was estimated as 2 ns.[23]

The first overtones of the $v_{HC} \equiv v_1$ mode have also been studied for a number of $HC \equiv CX(CY_3)_3$ type molecules. We present the corresponding data in Table 2 in the same form as in review [169]. The $|2v_1\rangle$ state in the $HC \equiv CSi(CH_3)_3$ molecule, unlike all other molecules, decays more slowly than the $|v_1\rangle$ state. The model calculation performed in paper [185] did not confirm such a strange behavior. In addition, the calculated IVR time from the $|2v_1\rangle$ state proved to be three times shorter than the experimental time, whereas theoretical calculations and experimental data obtained for other molecules are in much better agreement.

3.5 Other molecules

3.5.1 Results of measurements. We consider here only the results of studies which have clearly demonstrated the presence of IVR based on the observation of the multiplet structure in spectra (as in Fig. 1). The data on IVR times are summarized in Table 3.

3.5.2 Mechanisms. A number of observations were considered, which indicated the diversity of associated effects rather than the generality of IVR characteristics.

(i) A great difference between the IVR rates from C–H vibrations of methyl groups in butyne and pentyne molecules was discussed (second and third lines in Table 3, respectively). It was concluded [196] that a peculiar accelerator of the IVR process in the second case is isomerization, at which the mutual positions of hydrogen atoms in two CH_2 groups change. The authors asserted that the *closeness* to bonds involved in isomerization can accelerate IVR. This idea was further developed in paper [201] for other examples.

Table 3. IVR times for the first excited states of v_{OH} and v_{CH} modes related to methyl groups and groups with the double CC bond.

Molecule	Mode	IVR time, ps	References
$HC \equiv CCH_2OH$	$v_1 \equiv v_{OH}$	60	[174][1*]
$HC \equiv CCH_2CH_3$	$v_{16} \equiv v_{CH}$[2*]	276	[196]
$HC \equiv CCH_2CH_2CH_3$	v_{CH}[2*]	< 40	[1]
$H_2C \equiv CHCH_2CH_3$	v_{CH}[2*]	31	[169][3*]
trans-$H_3CHC = CHCH_3$	v_{CH}[2*]	130	[169][3*]
trans-H_3C-CH_2OH	$v_1 \equiv v_{OH}$	25	[156]
	$v_{14} \equiv v_{CH}$[2*]	59	[197]
cis-$H_2C = CHCH_2F$	v_{HC}[4*]	2000	[198]
gauche-$H_2C = CHCH_2F$	v_{HC}[4*]	90	[198]
H_2FC-CH_2OH	v_{CH}[5*]	275	[157]
$H_2C = C(CH_3)_2$	v_{HC}[4*]	105	[199]
$H_2C = CHOCH_3$	v_{HC}[4*]	660	[200]

[1*] In review [169], the time of 110 ps is presented with a reference to unpublished data.
[2*] Asymmetric CH vibration of the methyl group (with frequency ~ 2990 cm^{-1}).
[3*] In review [169], unpublished data are also cited.
[4*] Asymmetric vibration of the $H_2C =$ group. The frequencies of this CH vibration for four molecules with the double CC bond included in the table lie in the range from 3087 to 3130 cm^{-1}.
[5*] Asymmetric CH vibration of the $CH_2(F)$ group (with frequency ~ 2980 cm^{-1}).

(ii) The spectrum of a methyl vinyl ether molecule (the last line in Table 3) exhibits an additional peak indicating the presence of the $|\mathcal{DWS}\rangle$ state (see Fig. 11 and explanation in the text) which is located very close to the initially excited $|\mathcal{Z}_0\rangle$ state (the energy defect is certainly less than 1 cm^{-1}). However, the authors [200] have failed to find a combination of frequencies of other modes that would play the role of $|\mathcal{DWS}\rangle$.

(iii) The direct measurement of the density of states for the fluorine ethanol molecule (the ninth line in the left column of Table 3) revealed the efficient mixing of two isomeric forms. Moreover, the authors of paper [157] succeeded in determining the isomerization time (approximately 2 ns) from the spectrum, which proved to be much longer than the IVR time.[24]

(iv) The possible reasons for the considerable difference between IVR rates for two isomeric forms of the allyl fluoride molecule were analyzed (seventh and eighth lines in Table 3). The authors of paper [198] explained this by the fact that the frequency of the torsion mode for the *gauche*-configuration is considerably lower than that for the *cis*-form. Therefore, the density of states in the *gauche*-configuration in the vicinity of the excited level under study is much higher. Also, the authors pointed out the absence of isomerization for the given energy.

It is reasonable to supplement Table 3 with one more example from paper [203], where the spectrum of the first overtone of the asymmetric CH vibration of the methyl group

[23] The results obtained for the $HC \equiv CCHO$ molecule are not quite clear. The IVR time from the $|2v_1\rangle$ state was estimated for this molecule as 1250 ps [195]; however, the results of measurements at the fundamental transition are absent. This molecule was not considered in review [169].

[24] The authors noted that the measured time was a few orders of magnitude longer than the isomerization time calculated by the RRKM theory. See also paper [202], where the isomerization time was measured by the MW spectroscopy method in the excited vibrational state.

in the CH_3NO_2 molecule was recorded. The IVR time was estimated as falling from 170 to 300 ps. The authors also reported, albeit without any references, that a comparable value was obtained for IVR from similar overtone states of CH_3SiH_3 and CH_3CD_3 molecules.[25]

3.6 Manifestations of vibrational–rotational interactions

It seems that the most spectacular demonstration of a principally new potential of the method concerns the studies of the vibrational–rotational mixing based on the measurement of the density of transitions, which is possible due to the high spectral resolution. The first paper [180] in this area was based on ethyl alcohol molecules (the $\nu_{14} \equiv \nu_{CH}$ mode). As the rotational quantum number J' in the excited vibrational state increased, the number of lines in multiplets increased from 2 for $J' = 0$ up to 20 for $J' = 4$ (the number of lines was also independent of K'_a). This gave grounds to the authors to assert in the title of their paper that, in this case, the IVR effect is 'assisted' by the rotational degree of freedom. In addition, the authors refined their results in the next paper [197] by improving the spectral resolution: the number of lines increased and their density coincided with the calculated density of *all* vibrational levels multiplied by $(2J' + 1)$ for the given value J'.

A similar result related to the calculation of the number density of lines in multiplets was obtained later in paper [175] for the propargyl alcohol ($HC \equiv CCH_2OH$) molecule, and in paper [174] for the propargyl amine alcohol molecule. A more modest effect of the vibrational–rotational interaction was found in Ref. [192] from analysis of the spectrum of the first overtone of the $\nu_1 \equiv \nu_{HC}$ mode in the propyne ($HC \equiv CCH_3$) molecule. As discussed in Section 3.4, the IVR effect from the $|2\nu_1\rangle$ state is absent in this case; however, perturbations were observed caused by the Coriolis interaction of states with *identical* values of the quantum number K (the so-called z-type Coriolis interaction).[26] A similar observation was made in paper [196] during the analysis of the spectrum of the ν_{16} mode in the butyne molecule.

The role of vibrational–rotational interactions[27] and, as a consequence, of the vibrational–rotational mixing in the IVR process is an extremely interesting and fundamental question. Globally, except for the obvious conservation of the quantum number J, we can talk only about the conservation of the total vibrational–rotational symmetry.[28] As for the quantum number K (K_a), it is quite likely that, because of the enhancement of vibrational–rotational interactions with increasing J, a critical value J_{cr} exists, above which K (K_a) is no longer a 'good quantum number'. Because the spectroscopy of cooled molecular beams deals with small J, in most cases, except for the above-mentioned papers [174, 175, 197], the vibrational–rotational mixing effect may not be observed. We will return to this question in Section 4.3 after a discussion of experimental studies of real-time IVR dynamics.

[25] However, the analysis of the spectrum for $|2\nu_{CH}\rangle$ in the benzene molecule led to an ambiguous conclusion: "the intramolecular vibrational relaxation occurs nonergodically and is characterized by stages taking at least seven different time scales ranging from 100 fs to 2 ns" [204].

[26] The corresponding term in the vibrational–rotational Hamiltonian is proportional to the operator $\hat{J}_z$, i.e. the component of the angular momentum directed along the symmetry axis of the molecule.

[27] The strongest effects are the Coriolis interaction and centrifugal distortion, which rapidly increase in the general case with increasing rotational quantum numbers (see, for example, Refs [205–207]).

[28] The 'breaking' of the symmetry can only be caused by nonadiabatic effects, the mixing of different isomeric modifications, etc.

4. Real-time studies of IVR dynamics

4.1 Review of methods

The main methods and directions of time-resolved spectroscopy were developed back in the 1970s for experiments with liquids (see, for example, papers [208, 209]), where the vibrational excitation of molecules relaxes probably not due to IVR, but due to energy transfer to the environment. The studies of IVR in a pure form are, of course, possible only in gases at comparatively low pressures and assume the use of at least two laser pulses for pumping and probing. The second pulse is delayed with respect to the first pulse by the time interval τ_d, as shown in the top middle part of Fig. 14, and this time can be continuously varied.

Take as a base the situation corresponding to our example from Section 1.1. Excitation is performed at the $|v = 0\rangle \rightarrow |v = 1\rangle$ transition, where v is the occupation number of a high-frequency molecular mode. The upper level of the transition ($|\mathcal{ZOBS}\rangle$ in the terminology of Section 2.2) lies in the energy range where the IVR effect already occurs. Probing can be performed, in principle, by different methods.[29]

(i) The circumstance can be used that high-frequency molecular modes (in particular, involving a light hydrogen atom) are strongly anharmonic, so that the vibrational–rotational $|0\rangle \rightarrow |1\rangle$ and $|1\rangle \rightarrow |2\rangle$ bands are well separated in the spectrum. This allows one to monitor the IVR process by tuning the frequency of a probe laser pulse to the $|1\rangle \rightarrow |2\rangle$ transition, as shown in the top left part of Fig. 14. As the vibrational energy is redistributed to other degrees of freedom, the induced absorption shifts to the blue, because the intermode anharmonicity affecting the $|v=0\rangle \rightarrow |v=1\rangle$ transition frequency is much weaker than the intramode anharmonicity for the same total vibrational energy. The advantage of this method lies in its relative simplicity. The results obtained and their interpretation are discussed in Section 4.2.3.

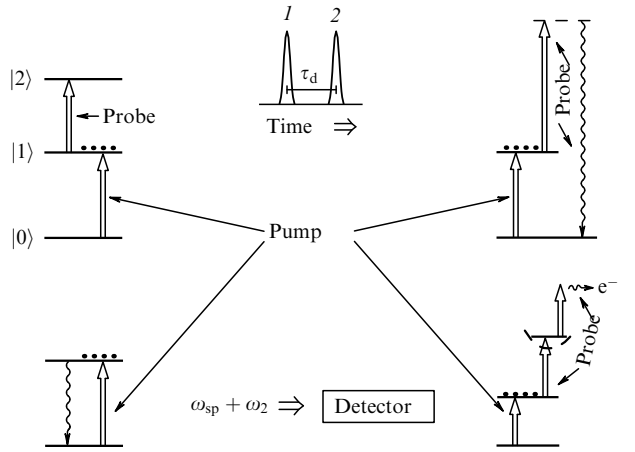

Figure 14. Schematics of different experiments for real-time studies of the IVR process. The signal is proportional to the population of the $|v = 1\rangle$ level. The IVR dynamics is diagnosed by the dependence of the signal on the delay time τ_d of probe laser pulse *2* with respect to pulse *1* exciting the $|v = 0\rangle \rightarrow |v = 1\rangle$ transition.

[29] In the English-language literature, as a rule, the 'pump–probe' term is involved; however, the probing of absorption is more often assumed. We avoid here the use of any translation of jargon into Russian and prefer to denote directly, although more lengthily, the probing method applied.

(ii) More direct are methods in which a signal is proportional to the energy in a mode and, therefore, can be interpreted unambiguously, independently of how strong the intramode anharmonicity is. One of these methods is anti-Stokes Raman scattering integrated over the excited mode band (see the top right part of Fig. 14), i.e. in our case, the $|1\rangle \to |0\rangle$ band. The necessary condition implies that the mode under study should be active with respect to IR absorption and Raman scattering. A drawback of the method resides in its limited sensitivity. Nevertheless, a number of results have recently been obtained for propyne and its derivatives, which considerably supplemented the pictures presented in Section 3.3. These results are discussed in Section 4.2.4.

Raman probing can theoretically provide the characterization of not only IVR from the initially excited mode, but also the energy supply to other modes that are active with respect to the Raman process. However, time-resolved experiments of this type have not been performed yet. At the same time, experiments with Raman methods proving the presence of energy in other modes *due to IVR* were performed back in the 1980s at the quantitative level and then interpreted (see review [210]; a brief discussion is presented at the beginning of Section 4.2.1).

(iii) Spontaneous IR radiation at the $|1\rangle \to |0\rangle$ transition is also promising from the point of view of interpreting results, but is probably more difficult to observe in experiments than Raman scattering: in this case (see the bottom left part of Fig. 14), the detection of spontaneous radiation with the required time resolution seems impossible at present.

The solution to this problem is known: spontaneous radiation should be mixed with a probe laser pulse in a nonlinear crystal, and the signal should be detected at the sum frequency (up-conversion).[30] Any results on the IVR dynamics are absent; however, a series of papers exist, beginning from Ref. [97], in which the *absence* or *presence* of IVR in various molecules was determined by measuring the absolute values of IR fluorescence signals. These papers are also briefly discussed at the beginning of Section 4.2.1.

(iv) Finally, IVR can, by and large, be detected by a particular method with additional excitation, for example, the fluorescence characterization of a final radical — a dissociation product or photoionization through an intermediate excited electronic state (see the bottom right part of Fig. 14), etc. The corresponding setups and results are discussed in Sections 4.2.1 and 4.2.2.

4.2 From probing intermode distributions to measuring IVR times

4.2.1 Vibrational chaos: experimental demonstrations. Let us return to the past, to experiments with laser pulses, which are certainly longer than the IVR time, but nevertheless gave answers to some questions of current interest. Thus, the IR MPE process was discussed in Section 1.3, and the most important issue at that time was formulated: where is the energy boundary E_{onset} of a passage from regular to chaotic vibrational motion located in one or other molecule? The IVR *dynamics* could not be studied by spectroscopy with so long pulses — it could give information only about the *result* of this dynamics, i.e. the distribution of molecules over the vibrational energy, the energy distribution over modes, etc.

The first experimental demonstration of the energy redistribution from a molecular mode pumped during IR MPE to all other modes at energies considerably lower than the dissociation limit was reported in papers [213, 214]. Under conditions when the energy of SF_6 and CF_3I molecules was approximately 7000 and 10,000 cm^{-1}, respectively, anti-Stokes Raman scattering was observed for *all* Raman-active vibrational modes.[31] A similar qualitative result for the SF_6 molecule was also obtained in papers [215, 216]. Later on, the direct Raman probing of mode distributions produced in the IR MPE process was performed simultaneously with the reconstruction of the total vibrational energy distribution function by various experimental methods. As a result, the values of E_{onset} were estimated for a number of molecules (see Table 4).

Figure 15 illustrates the idea of measuring E_{onset}. The method uses the property of partition of molecules during IR MPE into two ensembles: the lower ensemble, in which energy is concentrated in the mode being pumped, and the upper ensemble, where energy has the equilibrium distribution over modes (Fig. 15c). The problem reduces to finding the lower extreme energy of the upper ensemble as the laser pulse energy decreases. This energy is found by determining by different methods the dependence of the fraction of molecules in the upper ensemble on the laser pulse energy.

A most cardinal method should be specially mentioned here. Anti-Stokes Raman signals are measured not only at mode frequencies ν_i, which gives their mean occupation numbers $\langle v_i \rangle$ (i.e. energies), but also, if possible, at the frequencies of first overtones $2\nu_i$ and combination vibrations $\nu_i + \nu_j$, which gives the *second moments* of the distribution $\langle v_i^2 \rangle$ and $\langle v_i v_j \rangle$, respectively, which, due to nonlinearity, characterize quantitatively the separation of molecules into two ensembles. Details are presented in papers [222, 223, 229].[32]

Note that *none* of the papers on Raman probing cited above revealed any deviations of the mode distribution above the energy E_{onset} from the statistically equilibrium distribution in the terms of the effective temperature T_{eff} (see expression (2.13) and the corresponding explanation in Section 2.3). The only exception is paper [238] in which the observation of the nonequilibrium distribution during IR MPE of the CF_2Cl_2 molecule was reported. However, more accurate measurements performed later in Ref. [239] proved that this was not the case, and the statistically equilibrium mode distribution takes place for this molecule as well.

Experiments on the Raman probing of distributions produced in the IR MPE process proved to be the only experiments aspiring to *determine* the value of E_{onset}. Papers [230, 231], in which attempts were made to estimate E_{onset} by comparing the IR fluorescence spectrum of molecules in the IR MPE process with equilibrium hot spectra, gave rough estimates (see the middle part of Table 4) based on the 'model' difference of the spectra in the region of lower energy levels and above the assumed stochastization boundary.

[30] A similar idea, but applied to biomolecules in a condensed phase, was realized in papers [211, 212], where the IR absorption of radiation from a cw probe diode laser was detected by up-conversion with a high time resolution.

[31] Of course, experiments were performed at relatively low gas pressures to completely exclude the influence of collisions.

[32] The utility of signals in overtone and combination bands for diagnosing mode distributions was also demonstrated in paper [237], but in IR fluorescence experiments rather than in Raman scattering ones.

Table 4. Lower energy boundaries of the vibrational chaos region for a number of molecules.

Method[1*]	Molecule	E_{onset}, cm^{-1}	References
RS (MPE)	CF_3I	$\lesssim 6000$	[219, 220][2*]
	CF_3Br	7500 ± 300	[222, 223]
	CF_2HCl	4500 ± 500	[224]
	CF_2Cl_2	$\lesssim 7800$	[225]
	SF_6	5000 ± 500[3*]	[229]
IR (MPE)	C_2F_5Cl	$(2-3) \times 982$	[230]
	SF_6	> 3000	[231]
IR (IR)	CH_4, C_2H_6, C_6H_6, C_6H_5F[4*]	> 3000	[97]
	$O=C(CH_3)_2$[5*], C_3H_8, C_5H_8[6*], C_5H_{10}, C_6H_{12}[7*] etc.	< 3000	[97]
	$H_3C-O-CHO$	< 3000	[232]
	$H_3C-O-CH_3$	< 2800	[233]
	$C_4H_8O_2$[8*]	< 2800	[234]
	C_7H_8[9*]	< 3000	[235]
	CH_3CHO	< 2800	[236]

[1*] The method for diagnosing mode distributions (Raman scattering or IR fluorescence) is indicated. In parentheses, the excitation method is indicated (IR MPE or one-photon IR).
[2*] See also paper [221], where the theoretical estimate consistent with experiments was obtained.
[3*] The author of theoretical paper [120], in order to explain experiment [226] also used this value, which is the refinement of the value 3900 ± 500 cm^{-1} measured in Refs [219, 220]. The authors of Refs [227, 228] utilized close values by comparing the results of CARS spectroscopy of SF_6 molecules in the IR MPE process with the model calculation.
[4*] Of the various isomeric forms, only benzene and fluorobenzene were studied.
[5*] The acetone molecule has many isomeric forms. Two more forms were also studied: one (propylene oxide) falls into the same category. The other (oxetone), which has a considerably lower density of vibrational levels, does not reveal any traces of IVR at the energy of 3000 cm^{-1}.
[6*] Cyclopentene.
[7*] Cyclopentane and cyclohexane.
[8*] Of the different isomeric forms, only dioxane (a ring of C and O atoms) with the symmetric arrangement of oxygen atoms was studied.
[9*] Of the different isomeric forms, norbornadiene, a molecule with the unique three-ring nonplanar structure, was explored.

In papers with one-step excitation, only the position of the excited state above or below E_{onset} was determined. Thus, the results obtained for 23 molecules with CH vibrations in the 3000-cm^{-1} region were systematized in Ref. [97]. The researchers used a molecular beam and a laser emitting 14-ns pulses, their duration certainly exceeding the IVR time. The $|v=1\rangle$ state of the ν_{CH} mode was excited (when IVR was absent) or, correspondingly, a group of resonance states mixed with $|v_{CH}=1\rangle$ in the presence of IVR. Then, the IR fluorescence signal integrated over some time interval was measured in the same frequency region. The conclusion about the presence of IVR was based on the smallness of the signal compared to the calculated value expected in the absence of IVR. The conclusions made in Ref. [97] are partially presented in the bottom part of Table 4. The list was later supplemented in papers [232–236] reflected in the table (see also Ref. [240]).

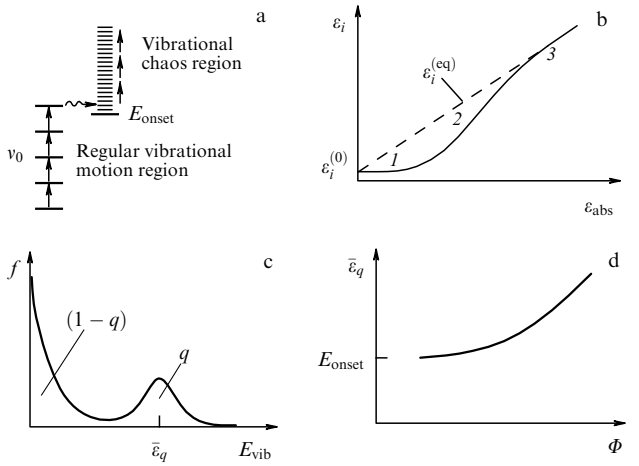

Figure 15. Determination of the lower energy boundary E_{onset} of the vibrational chaos region in a molecule by using IR MPE [210, 217, 218]. (a) Diagram of the process: the time of energy redistribution from the pumped mode above E_{onset} is much shorter than the excitation time. (b) The qualitative dependence of the Raman signal in a nonresonance mode on the total absorbed energy: (1) equilibrium energy at room temperature; (2) intermediate region with the energy excess in the mode being pumped, and (3) equilibrium region at high excitation energy. (c) Distribution function $f(E_{vib})$ for the total vibrational energy formed during IR MPE. (d) Dependence of the mean energy of the upper ensemble on the IR laser pulse fluence.

The presence of IVR in the region of the fourth overtone of the ν_{OH} mode in the $HONO_2$ molecule was elegantly demonstrated in paper [241]. This overtone was excited in the one-quantum process. Then, because the fifth overtone lies above the dissociation limit, an original probing method was applied, namely, the one-photon IR dissociation, followed by the detection of the dissociation product, the OH radical in the given case, by laser-induced fluorescence. The analysis was based on the fact that the ν_{OH} mode is strongly anharmonic. The spectrum (the dependence of the dissociation yield on the probe laser pulse frequency) in the paper was concentrated near the fundamental transition frequency, which suggests that IVR from the ν_{OH} mode proceeded during the pump pulse, whose duration was ~ 10 ns. This gives the estimate $E_{onset} < 13{,}300$ cm^{-1} (the pump laser frequency). This estimate was refined in paper [242], in which the first overtone of the ν_{OH} mode was excited by a short 100-fs pulse, and then a second, delayed 266-nm laser pulse was applied, resulting in the dissociation of the molecule with the formation of the excited NO_2 radical. The dissociation yield increased upon increasing the delay time, the characteristic time being 12 ps. The authors explained this effect as IVR from the ν_{OH} mode to other modes 'active' with respect to photodissociation at the second-pulse wavelength.[33] If this interpretation is correct, the estimate $E_{onset} < 7000$ cm^{-1} should be valid for the $HONO_2$ molecule.

[33] The setup of experiments in paper [242] principally differs from these presented in Fig. 14; it assumes that the $|ZOBS\rangle$ state excited by the first pulse is a 'dark' state with respect to the probing process. As far as we know, similar setups were not implemented later.

Table 5. IVR times for high-frequency valence vibrations of benzene derivatives, obtained by the time-resolved double IR–UV resonance method.

Molecule	v_{exc} [1*]	IVR time, ps	References
C_6H_5OH	v_{OH}	14	[243, 244]
	v_{CH}	< 5 [2*]	
C_6D_5OH	v_{OH}	80	[244]
C_6H_5OD	v_{OD}	~ 50 [3*]	[245]
C_6D_5OD	v_{OD}	~ 15 [4*]	[245]
$C_6H_5NH_2$	$v_{NH(s)}$ [5*]	18	[246]
	$v_{NH(a)}$ [5*]	34	
	$v_{CH(3047)}$ [6*]	$\lesssim 5$	
	$v_{CH(3105)}$	10	

[1*] Mode excited by a short IR laser pulse.
[2*] The finite duration ($\sim$ 14 ps) of laser pulses did not allow us to obtain a more accurate estimate.
[3*] Beats were observed, which were interpreted as the presence of two $|\mathcal{DWS}\rangle$ (see Fig. 11 and explanations in the text) separated from the $|\mathcal{Z}_0\rangle$ state by a distance smaller than 1 cm^{-1}.
[4*] The same effect as in the previous note, but involving only one $|\mathcal{DWS}\rangle$.
[5*] Subscript in parentheses indicates the mode symmetry.
[6*] The CH mode frequency is indicated in parentheses. The same estimate was made for the CH mode with frequency 3087 cm^{-1}.

4.2.2 IVR dynamics: photoionization detection. By considering the scheme presented in the bottom right part of Fig. 14, we can principally propose a few spectroscopic methods. In reality, the choice is determined by the properties of the molecule under study, and so far only one diagnostic method has been applied — laser photoionization detection using a resonance at the intermediate UV transition to the excited electronic–vibrational state [resonance enhanced multiphoton ionization (REMPI)]. The method of cooled beams was utilized to study molecules with the cyclic structure: C_6H_5OH (phenol) [243–245], and $C_6H_5NH_2$ (aniline) [246], including some isotope-substituted modifications. Such molecules possess a convenient electronic transition in the near UV region.

The estimates of IVR times reported by the authors are summarized in Table 5. They are based on the time evolution of REMPI spectra, although the interpretation of this evolution is not completely unambiguous, because bath states to which energy is redistributed from the excited state *are not principally dark* with respect to the probing method at any frequency. Therefore, it is necessary to include in the model, first, REMPI signals at different frequencies and, second, a spectrum measured for time delays τ_d of the probe laser pulse with respect to the pump pulse, which are certainly larger than τ_{IVR}. Nevertheless, this method is quite promising, being a step forward compared to earlier attempts (see, for example, paper [247]) to characterize mode vibrational distributions by nonresonance photoionization signals. Due to the high sensitivity of photoionization detection, the method successfully operates in conjunction with a cold molecular beam, and so it can also be used for studying IVR in small clusters. Such a possibility was recently demonstrated in paper [248] by the example of benzene dimers and trimers.

4.2.3 IVR dynamics: IR absorption diagnostics. A schematic of diagnosing the IRV process by absorption from the upper level of the excited transition shown in the top left part of Fig. 14 works in the pure form if and only if the anharmonic shift of the $|1\rangle \rightarrow |2\rangle$ (see Fig. 14) transition frequency is high enough. The sufficient criterion is represented by the inequality

$$2|x_{aa}| > \Delta v_a + \left|2x_{aa}\langle v_a\rangle_{v_a} + \sum_{b\neq a} x_{ab}\langle v_b\rangle_{v_a}\right|, \qquad (4.1)$$

where the notation corresponds to that adopted in Section 2 [formula (2.10)], i.e. the subscript a is related to the mode being excited, and b to all other modes. In addition, Δv_a is the spectral width of a band at a given temperature, including rotational branches and hot bands, and angle brackets denote equilibrium occupation numbers of modes (in the given case, for the total energy of the molecule equal to one quantum in the v_a mode) In this situation, it is best to perform integral probing over the entire band.

Otherwise, when inequality (4.1) is not fulfilled, we encounter the same problem as in the method considered in Section 4.2.2: the bath states to which energy from the excited state is redistributed *are not principally dark* with respect to absorption at any frequency. Therefore, it is necessary to perform frequency-selective probing and to reconstruct the picture from the evolution of the spectrum upon changing the time delay τ_d. In particular, it is reasonable to monitor the absorption recovery dynamics by using one narrowband source tuned to the center of the Q branch for pumping and probing. Experiments with a spherical top type $W(CO)_6$ molecule [137] were performed by this method.

The spectrum of a degenerate mode corresponding to the collective vibration of C–O bonds and allowed with respect to IR absorption is displayed in Fig. 16. This figure also presents the spectrum of an optical parametric oscillator (OPO) used for pumping and probing. The pulse duration was 40 ps. The authors described the absorption recovery dynamics by three exponentials. They correctly interpreted the fastest of the observed processes with a characteristic time of 140 ps as the 'spectral diffusion'. In the context of our Section 2, this term means the following. Molecules at the temperature of the experiment are mainly found in the stochastic region above E_{onset}, and therefore their $|0\rangle \rightarrow |1\rangle$ transition spectrum is

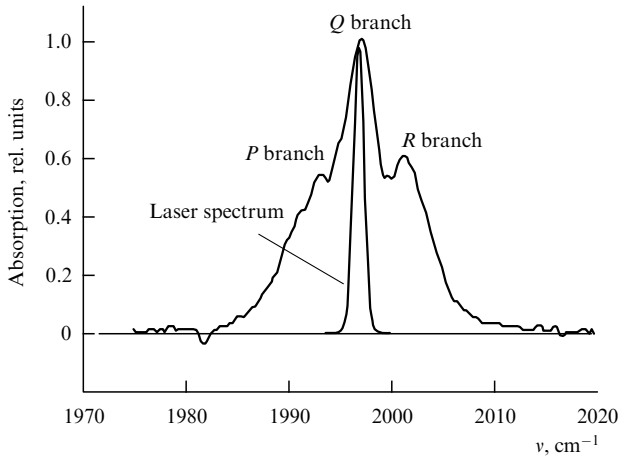

Figure 16. Vibrational–rotational spectrum of the triply degenerate asymmetric mode of the $W(CO)_6$ molecule corresponding to the collective vibration of valence C – O bonds in the gas phase. For comparison, the laser line at 1997 cm^{-1} is shown. (Taken from Ref. [249].)

subject to the SIB effect. A laser pulse burns a hole in the SIB spectrum, and then IVR between bath modes recovers the SIB spectrum.

The next process in duration, with a characteristic time of 1.3 ns, was interpreted by the authors as IVR from the excited mode.[34] In this case, absorption is not recovered completely because the increase in energy in bath modes due to intermode anharmonicity shifts the absorption band. Finally, the third process (*a fortiori* longer than 100 ns) can probably be related only to collisional relaxation (the gas-kinetic collision time under these experimental conditions was estimated by the authors as 1 μs).

Experiments with $(CF_3)_2C=C=O$ molecules [252, 253] were performed in a different way. Molecules were excited by focused 100–300-fs pulses from an OPO providing the energy density ~ 80 mJ cm^{-2} in the caustic region. The emission spectrum of the OPO was rather broad (FWHM ≈ 240 cm^{-1}) and certainly covered the absorption band of the ν_1 mode corresponding to the asymmetric vibration of the C = C = O group. Probing was performed by a small portion of a pulse from the same source, and then the probe and reference beams passed through a monochromator. The spectral resolution ranged 3–5 cm^{-1}, which, with the intramode anharmonicity constant $x_{11} \approx 12.6$ cm^{-1} at room temperature, even despite the bandwidth $\Delta\nu_1 \approx 18$ cm^{-1}, allowed the adequate observation of IVR dynamics, notably, at the $|1\rangle \rightarrow |2\rangle$ transition as well. The picture proved to be even richer because the broadband pumping radiation excited not only the first but also a few next levels. Results are illustrated in Fig. 17.

The characteristic time of IVR from the ν_1 mode was ~ 5 ps. In addition, an attempt was made to determine energy migration paths in the IVR process. For this purpose, the second information channel was invoked — a parametric generator emitting in frequency regions corresponding to other modes. The idea of these measurements was as follows. The appearance of energy in the ν_1 mode is reflected in a change in the spectrum of other ν_b modes due to intermode anharmonicity constants x_{1b}. If the spectrum of some mode is recovered more slowly than in ν_1, we can assume that the initial accumulation of energy in this part occurs faster than the establishment of the statistical equilibrium over the entire molecule. In any case, such an effect was distinctly observed during the probing of the ν_3 mode — one of the modes corresponding to collective vibrations of C – F bonds, where the characteristic time of transition to equilibrium was above 20 ps. In Section 4.1, we emphasized the principal advantage of anti-Stokes Raman scattering and IR fluorescence allowing one to monitor energies in all modes during IVR. However, the example presented above shows that absorption probing can also be, albeit partially, informative.

Another example is offered in paper [254], where absorption probing was also utilized. The object was qualitatively different — a small HONO molecule embedded into a low-temperature matrix. The IVR in such a system, even if it mainly occurs between molecular modes, inevitably involves

[34] They presented an additional strong argument that a close time characterizes the IVR of the same molecules at low concentrations in solvents under supercritical conditions [250]. Note that the result obtained on slow IVR from the pumped mode gave impetus to paper [251] on the IR MPD of $W(CO)_2$ molecules and some other metallocarbonyls by high-power 100-fs laser pulses. The results of this paper indicated to the nonstatistical nature of dissociation.

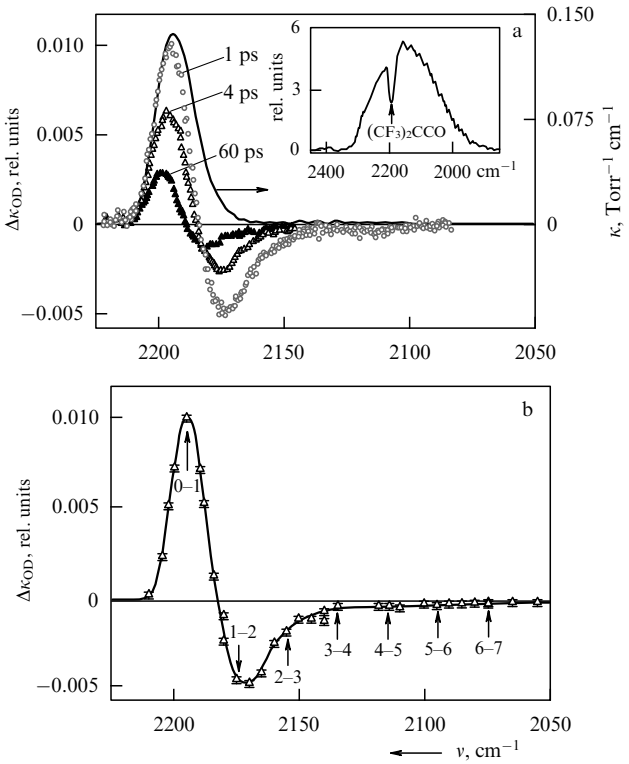

Figure 17. Spectral dependences of the change $\Delta\kappa_{OD}$ in the optical density of a cell with $(CF_3)_2C=C=O$ gas in the region of the ν_1 mode caused by its pumping with a pulse from a parametric generator. (a) $\Delta\kappa_{OD}(\nu)$ for different delay times τ_d (left scale). For comparison, the linear absorption spectrum is displayed (right scale, where κ is the absorption coefficient); the inset shows the spectrum of the laser pulse transmitted by the cell. (b) $\Delta\kappa_{OD}(\nu)$ at $\tau_d = 1$ ps. The arrows mark the positions of the maxima of corresponding transitions in the ν_1 mode. (Taken from Ref. [253].)

the interaction with a phonon subsystem. The authors pointed out that anti-Stokes Raman scattering potentially provides a complete set of data about energies and modes and concluded that "The present study shows that comparable information can also be obtained with IR pump–IR-probe spectroscopy avoiding the very weak Raman scattering process, provided that the molecule is small so that various hot hands are spectrally resolved, and provided that a reliable set of anharmonic constants is known from either theory or experiment."

Finally, we return to the initial formulation of the problem — the employment of IR absorption exclusively in accordance with the diagram presented in the top left part of Fig. 14. This scheme was realized only in one paper [255], where only one ν_{HC} mode of propyne and its $H - C \equiv C - R$ derivatives was investigated. The duration and spectral width of OPO pulses were 1.4 ps and 25 cm^{-1}, respectively, whereas the frequency shift of the $|1\rangle \rightarrow |2\rangle$ transition from the $|0\rangle \rightarrow |1\rangle$ transition frequency for these molecules was considerably greater, approximately 110 cm^{-1}. Ten molecules were studied. Because experiments were performed at room temperature, the results differed, of course, from those discussed in Section 3.3. The differences, one of them quantitative and another qualitative, were:

(i) the IVR times in most cases were considerably shorter in gas at room temperature than in a cooled molecular beam;

(ii) in some cases, when IVR was not observed in a cooled molecular beam, it was manifested in gas at room temperature.

We will discuss these results in detail in the next section, because the same subject was investigated in experiments where probing was performed by utilizing spontaneous anti-Stokes Raman scattering. All the more this is appropriate because the authors of paper [255] failed (for unknown reasons) to measure a quantity of great interest, namely, the dilution factor containing information on the density of bath states efficiently involved in the process of IVR from the $|\mathcal{ZOBS}\rangle$ state [see expression (2.8), Figs 4 and 5, and the relevant discussion in Section 2.2). In our case, the $|\mathcal{ZOBS}\rangle$ states belong to an *ensemble* of many vibrational–rotational states occupied at room temperature, and it is natural to attempt to find out the degrees of freedom whose population plays the key role in new, averaged properties of IVR.

4.2.4 IVR dynamics: Raman probing. We discussed in Section 4.2.1 experiments on a time scale of ~ 100 ns with spontaneous anti-Stokes Raman probing of the mode distribution of vibrational energy stored during the IR MPE process. The first step to time-resolved spectroscopy with this probing method was made in paper [256], where the time scale was reduced to 5 ns. The subject of studies was the collisional relaxation of molecules excited *a fortiori below* the boundary E_{onset}. Experiments were mainly performed with CF_3H and CF_2HCl molecules, and the rapid (at least during gas-kinetic collisions) redistribution of excitation from the $|v_{CH} = 1\rangle$ state to other vibrational states was unexpectedly found.

This effect was later interpreted [257] as collision-induced IVR (CIIVR): in other words, IVR occurring, during a collision, in a complex of two molecules, one of which is excited. This observation proved to be very important because it dictated the necessity of working with low gas pressures (on the order of 10 Torr) in further IVR experiments on time scales down to 1 ns, which produced additional difficulties for measuring extremely weak spontaneous Raman signals.

IVR dynamics experiments involving Raman diagnostics were performed with longer pulses (~ 20 ps) than in paper [255]. As a whole, the same properties as in Section 4.2.3 were found, but with one important addition. Consider first papers [116, 182, 183] wherein those molecules were studied that did not reveal IVR in cooled beams (see discussion in Section 3.3.1), The results are presented in Fig. 18. They are similar to the curves in Fig. 4, where the behavior of the ensembles of systems was calculated, in which the initially populated $|\mathcal{ZOBS}\rangle$ state (or $|\mathcal{Z}_0\rangle$ state in the notation of Section 2.2) interacts with the bath $|\mathcal{B}_s\rangle$ states, the statistics of distances between adjacent $|\mathcal{B}_s\rangle$ levels and the statistics of matrix elements of their interaction with the $|\mathcal{Z}_0\rangle$ state obeying distributions (1.1) and (2.9), respectively, which are inherent in dynamic chaos. Recall that the behavior of dependences $\mathcal{P}(t)$ in Fig. 4 is specified by the product $\varkappa = \hbar W\rho$. The density of states ρ is a parameter which can be calculated for a given molecule if vibrational frequencies and rotational constants of the molecule are known for any energy. Only a physically substantiated assumption is needed about quantum numbers that are conserved during the IVR process.

Curves A and B in Fig. 18 correspond to the two most natural assumptions. Scenario A assumes that the effective density of states ρ_{eff} coincides with the density of *vibrational* states ρ_{vib} for the energy of a given initial vibrational level with the same vibrational symmetry, i.e. rotational quantum numbers are conserved. The second scenario B assumes that, except for the rotational quantum number J, only total *vibrational–rotational* symmetry is conserved, while another rotational quantum number K (for $HC \equiv CCH_3$ and $HC \equiv CCF_3$ molecules) or K_a (for the $HC \equiv CCH_2Cl$ molecule) is not conserved, i.e. $\rho_{\text{eff}} = \rho_{\text{vib-rot}}$. Because the maximum of the rotational distribution for given molecules at room temperature lies at $J \sim 30$–45, it is clear that the majority of initially excited levels (populated states with one vibrational quantum added to the ν_{HC} mode) interact with the bath in which $\rho_{\text{vib}} \ll \rho_{\text{vib-rot}}$ (results from papers [116, 182, 183] illustrating this fact are presented in the third and fifth columns of Table 6). As a consequence, it is seen from Fig. 18 that experimental data can be fitted well with calculated curve B by varying the IVR rate W, whereas curve A is located far away from them. We will return to discussing the role of vibrational–rotational interactions in Section 4.3.

The IVR times presented in the second column of Table 6 for three molecules greatly differ. The probable explanation of this difference was given in paper [183]. It coincides as a whole with the initial assumption made in paper [1] (see Section 3.3.1) that the dominant $|\mathcal{DWS}\rangle$ state during IVR from the $|\mathcal{ZOBS}\rangle$ to the bath states (see Fig. 11) is the combination $\nu_{C\equiv C} + 2\nu_{H-C\equiv C}$. Indeed, the IVR time increases from $HC \equiv CCH_3$ to $HC \equiv CCF_3$ simultaneously with the Fermi resonance defect ΔE (see the next to the last column in Table 6). The last column in Table 6 also presents the IVR times from the $|\mathcal{DWS}\rangle$ state estimated from formula (3.1). It is quite reasonable that these times, on the contrary,

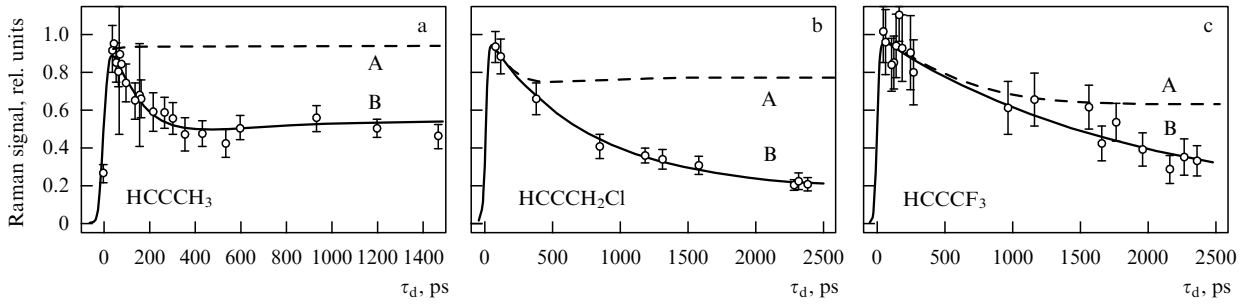

Figure 18. Anti-Stokes Raman signal in the ν_1 band as a function of the time delay τ_d of the probe pulse with respect to the pump pulse (in the units of I_0 defined as a signal for $\tau_d = 0$ and ultimately short pulses). Results are presented for propyne (at a pressure of 15 Torr) (a), propargyl chloride (10 Torr) (b), and trifluoropropyne (6 Torr) (c). These gas pressures were chosen to exclude the noticeable influence of collisions for the longest time delays τ_d used. (The CIIVR rates were measured to be 8.5 μs^{-1} $Torr^{-1}$ for $HC \equiv CCH_2Cl$ [182], and 10.1 μs^{-1} $Torr^{-1}$ for $HC \equiv CCF_3$ [183].) The FWHM lengths of the 3330-cm^{-1} laser pump and 1.06-μm probe pulses were 20 and 37 ps, respectively. The measurement error is determined by the statistics of photocounts. The solid curves correspond to the best fit of experimental results in accordance with scenario B. The dashed curves show what should be for the same IVR rate and scenario A [116, 182, 183].

Table 6. Experimental and calculated data for propyne, propargyl chloride, and trifuoropropyne. The IVR times (reciprocal to the corresponding W_{Z_0} and W_{DWS} rates) are given in picoseconds. The densities of bath states (in levels per wavenumber) and dilution factors are presented for two scenarios of IVR from the ν_{HC} mode. (Compilation of data from papers [116, 182, 183].)

Molecule	$W_{Z_0}^{-1}$	Scenario A		Scenario B		DWS	ΔE, cm^{-1}	W_{DWS}^{-1}
		$\langle \rho_{vib} \rangle^{1*}$	σ	$\langle \rho_{vib-rot} \rangle^{1*}$	σ			
$HC \equiv CCH_3$	350	0.25	0.93	18.2	0.54	$\nu_3 + 2\nu_9$	-47^{2*}	7.8
$HC \equiv CCH_2Cl$	1050	3.6	0.78	486	0.25	$\nu_3 + 2\nu_8$ $\nu_3 + 2\nu_{14}$	-112^{3*} -86^{3*}	5.5
$HC \equiv CCF_3$	2300	60	0.67	5800	0.12	$\nu_2 + 2\nu_7$	-170^{4*}	3.9

[1*] Angle brackets denote averaging over the Boltzmann distribution.
[2*] From paper [181] on the spectroscopy of the 3381-cm^{-1} $\nu_3 + 2\nu_9$ band.
[3*] Harmonic position.
[4*] Estimate.

Table 7. IVR times for the first excited state of the ν_{HC} mode in $H - C \equiv C - R$ type molecules at room temperature, measured by two time-resolved spectroscopy methods.

Molecule	Method	IVR time, ps	References
$HC \equiv CCH_2F$	IR	89	[255][1*]
$HC \equiv CCH_2OH$	RS	170	[116, 258][2*]
$HC \equiv CCH_2NH_2$	RS	130	[116, 258][2*]
$HC \equiv CCH_2CH_3$	IR	44 (8.3)[3*]	[255]
$HC \equiv CC(CH_3) = CH_2$	IR	23 (4.0)[3*]	[255]
$HC \equiv CCH(CH_3)_2$	IR	25 (5.6)[3*]	[255]
$HC \equiv CCHFCH_3$	IR	52 (22)[3*]	[255]
$HC \equiv CCH_2CH_2F$	IR	140 (34)[3*]	[255]
$HC \equiv CC(CH_3)_3$	IR	39 (5.9)[3*]	[255]
$HC \equiv CSi(CH_3)_3$	IR	96	[255]
	RS	128	[259]

[1*] In this case, the authors observed in fact the zero dilution factor, whereas we estimated it as at least 0.15. Probably, the influence of collisions is stronger than was assumed by the authors.

[2*] It was pointed out that the 'intermediate' scenario was realized: mainly B, but with the exclusion of the low-frequency torsion mode. The experiment is in good agreement with a model assuming a considerably slower involvement in IVR of this mode.

[3*] The authors observed a two-exponential decay, as in paper [249], discussed in Section 4.2.3. However, they assume that this evidence is better explained by the two-tier IVR model (see details in Ref. [255]) than by spectral diffusion.

decrease from $HC \equiv CCH_3$ to $HC \equiv CCF_3$, in accordance with the accompanying increase in the density of resonances due to an increase in the number of low-frequency modes.

The IVR times for other propyne derivatives are collated in Table 7, which includes the results obtained by both probing methods: Raman spectroscopy, and IR absorption spectroscopy. One can see that these times are considerably shorter than those obtained from high-resolution spectra of molecular beams (see Table 1). This fact also indicates the indirect role of vibrational–rotational mixing, although the effects of thermal population of low-frequency modes cannot be excluded, especially for large molecules, namely, the enhancement of anharmonic interaction for Fermi resonances involving modes with nonzero occupation numbers.

4.3 Manifestations of vibrational–rotational interactions: a summary

We pointed out in Section 3.6 that data obtained from high-resolution spectra give evidence that the effect of strong vibrational–rotational interaction occurs, as follows from the observed density of spectral lines, i.e. the density of states with essentially a nonzero projection onto the $|\mathcal{ZOBS}\rangle$ state. As shown in Section 4.2.4, the existence of this effect can also by proved by at least one of the methods of time-resolved spectroscopy — anti-Stokes Raman probing. These two experimental approaches have only a few intersection points because their subjects of study are quite different. In the case of high-resolution spectroscopy, this is a cooled molecular beam, while in the case of time-resolved Raman spectroscopy, this is gas at room temperature. Correspondingly, the spectrum of transitions from states with small J is measured in the first case, while in the second case it is the IVR dynamics mainly from states with large J. Therefore, of special interest are molecules in which vibrational–rotational mixing is absent for small J and takes place for large J.

The results presented in Section 3.6 imply that only a few molecules demonstrated the presence of the effect for small J. Because of this, it was assumed that a critical value J_{cr} exists for mixing. Moreover, the quantity J_{cr} acquires fundamental meaning for molecules in which IVR is completely absent at small J, and is distinctly present for large J. Examples of this type are the three molecules that were discussed in Section 4.2.4 (see Fig. 18 and the accompanying text). In these cases, the statement is valid that vibrational–rotational interactions play a key role in the appearance of IVR, i.e. the Chirikov criterion, which was discussed in Section 1.3 (see also Fig. 2), should include both anharmonic and Coriolis resonances in the concept of the 'overlap of resonances'.

The question of J_{cr} or, in a more general form, of the dependence $\sigma(J)$ should be addressed first of all to high-resolution IR spectroscopy. In the dynamic aspect, approaches based on laser excitation, which is selective over rotational quantum numbers, can be useful for solving the problem. This idea was partially realized in some papers cited in the bottom part of Table 4. Recall that the authors of these papers used a cooled molecular beam and a parametric generator emitting 14-ns pulses with a linewidth of ~ 1 cm^{-1}

to excite the IR fluorescence of molecules, from which the dilution factor σ was estimated.

A further idea was to excite molecules in different parts of rotational branches, which, in principle, gave the approximate dependence $\sigma(J)$ (because of the relatively broad line of the OPO). Such data were obtained, for example, in paper [260], which was specially devoted to this problem. Then, a logical step was made in paper [261] where the development of a single-mode parametric generator emitting a narrow line of width 0.001 cm^{-1} was briefly reported, and the first demonstration experiment with the $H_3C-O-CHO$ molecule was described.[35]

Note, however, that these papers had no relation to time-resolved spectroscopy itself, and it is difficult to directly apply this idea to real-time studies of the intramolecular dynamics because of the large width of the spectrum of short laser pulses. Instead of this, the double resonance and four-wave mixing methods can be applied, in which selective excitation is performed by a laser at the first stage emitting relatively long pulses with a narrow spectrum, while the dynamics is measured at other stages. Such schemes are, in principle, not restricted by the conditions of a cooled molecular beam, i.e. the range of J can be considerably expanded.

One of the capabilities of time-resolved J-selective spectroscopy is based on a scheme [184, 262] in which, along with two stages (excitation and Raman probing), a selective stage is involved: the quasistationary, quasiresonance excitation of an individual $J \to J+1$ rotational transition. In this case, coherent directional radiation at the frequency $\omega_{AS} + \omega_{J+1}$ (where ω_{AS} is the anti-Stokes Raman frequency) serves as a signal, which corresponds to one of the four-wave mixing schemes.

However, the most selective over J in its essence and direct purpose is the MW spectroscopy of rotational transitions in its pure form. Therefore, it is interesting to discuss its potential for solving the problem of determining J_{cr}. Rotational spectral lines in the vibrational chaos region can be, despite a scatter of rotational constants in an ensemble, extremely narrow [92, 263, 264], provided the IVR rate considerably exceeds the inhomogeneous width expected in the case of regular vibrational motion. Such an effect was observed in papers [265, 266]. It is similar to the collapse of the SIB spectrum considered in Section 2.3 (motional narrowing) and takes place in the absence of energy exchange between vibrational and rotational degrees of freedom (the exchange rate is $\tau_{vib-rot}^{-1} = 0$). However, a change in K should result in broadening (the finite time $\tau_{vib-rot}$). Consequently, the MW spectroscopy of ensembles of molecules in excited vibrational states can give information on the time $\tau_{vib-rot}$, which is difficult to reliably obtain by other methods.

5. Brief supplements

Many aspects of intramolecular dynamics and related investigation techniques were discussed in our review only partially or were not touched on at all. Of course, the scope of actual topics is considerably wider than the framework within which we tried to restrict ourselves to retain the logical development of the subject in the way (possibly subjective) we see it. Because of this, we will mention only briefly other issues concerning IVR, focusing either on objects or processes under study or on the investigation technique.

5.1 Theory

The case in point is a search for more specific regularities of the generation mechanisms of vibrational chaos than those mentioned in Sections 1.2 and 2.

We cite here quite interesting papers [267–271] and references therein. These papers were not considered in the main text because the results presented in them are not yet directly related to experiments and cannot be used for their explanation or any predictions. Nevertheless, the future development of ideas contained in them is promising.

Of interest is a hypothesis about the key role of high-order anharmonic resonances in the generation of vibrational chaos [120, 272, 273], which was also earlier discussed [223] in the interpretation of experiments on Raman probing mode distributions produced upon IR MPE (Section 4.2.1).

Great attention was devoted to numerical simulations of the intramolecular dynamics within the framework of both classical and quantum mechanics. An additional step here was an *ab initio* calculation of the potential-energy surface. Papers [274, 275] are representative examples (see also references cited therein and in review [130]).

5.2 IVR in excited electronic states

The first publications on this topic are papers [276, 277], where large aromatic molecules (anthracene, *trans*-stilbene, etc.) were mainly studied in cooled jets. All these molecules have electronic transitions convenient for laser excitation. The dynamics of fluorescence was investigated by the excitation of different vibrational levels in the upper electronic term by picosecond laser pulses. As an example, we refer to two series of studies focusing on different molecules; papers [278] and [279] are concluding investigations in these two series.[36]

We did not consider these experiments in the main text because their interpretation requires a serious analysis of the vibronic structure of electronic transitions, which is beyond the scope of our main topic. Let us simply note that the authors of these papers analyzed the role of rotational degrees of freedom in IVR in anthracene type molecules [281]. This problem was also considered in reviews [207, 282].

5.3 Stimulated emission pumping

In this method, the spectroscopy of highly excited vibrational–rotational levels in the ground electronic state $\mathcal{X}$ of simple molecules is performed via an auxiliary excited electronic term $\mathcal{E}$. The first laser excites selectively a certain vibrational–rotational level in $\mathcal{E}$, whereas the second, tunable laser effects transitions from $\mathcal{E}$ to high states in $\mathcal{X}$. Transition resonances to these states are recorded by a decrease in the fluorescence intensity from $\mathcal{E}$. This method is called stimulated emission pumping (SEP). The first study [283] was performed with an iodine molecule. Then, acetylene molecules were also studied [284, 285].

Also, formaldehyde [286], SO_2 [287], and other molecules were investigated, including small clusters (using the technique of cooled molecular jets), such as C_3 [288]. The vibrational ergodicity [289], chaos [284, 290], and vibrational–rotational mixing [285, 286] were central topics in these studies. A part of the results was described in review [87]. This method was also described in collective monograph [291] with an extensive theoretical section containing papers on simulations of SEP spectra. Because the objects were

[35] We have failed to find any further traces of this activity in the literature.

[36] See also review [280].

molecules with three to four atoms, these theoretical simulations were more detailed and active than those in the case of more complex molecules touched upon in our discussion. In this connection, we point out papers [292–294] and also review [295], demonstrating methods that are especially useful for the interpretation of complex spectra with 'mixed' properties with respect to the stability/chaos dilemma.

5.4 High-sensitive-detection spectroscopy of overtone states

In considering the first papers on the spectroscopy of benzene overtones in Section 3.1, we mentioned some original method for measuring spectra in a molecular beam used in papers [147, 148]. In fact, this method was similar to the REMPI method discussed in Section 4.2.2, but with the original difference that in the former case the signal was produced due to vibrational excitation, while in the latter case it was due to the escape of molecules from the ground vibrational state, i.e. the resonance at the $0 \rightarrow 0$ transition to an excited electronic term was utilized. Although this method for measuring spectra is convenient because it uses a strong transition at a well-known frequency, its application is limited by a low excitation efficiency, which decreases upon increasing the overtone order. For this reason, a more popular approach is one in which the spectroscopy of direct one-photon transitions from the ground vibrational state to a high $\mathcal{V}$ state, most often an overtone state, is performed by selective excitation of the previously excited molecule, resulting in its dissociation. This group of methods was recently called 'action spectroscopy'.

The first of these methods is a combination of IR MPD and laser-induced fluorescence (LIF) of one of the dissociation fragments. It was called 'infrared laser-assisted photofragment spectroscopy' (IRLAPS). The method was applied to CH_3OH [296–300] and CF_3H [301, 302] molecules. The fluorescence yield was measured as a function of the frequency of a tunable first-stage laser exciting the transition to the $\mathcal{V}$ state by tuning the laser frequency along the line profile. Because the cooled molecular beam technique is used, the recovery of the IVR time from the linewidth seems quite reliable.

Another method is based on the employment of single-stage photodissociation, but with the LIF detection of one of the fragments, as in the previous case. The potential of this method was illustrated in studies of hydrogen peroxide (HOOH) molecules [303, 304] (see also review [305]), where the third and fourth overtones of the asymmetric ν_{OH} mode were excited and OH radicals produced in photodissociation were detected.

Instead of LIF detection, photoionization of a fragment is also possible. This variant of the method was first tried out in Ref. [306] on several molecules, and then applied for a detailed study of the third overtone of the ν_{CH} mode in different isotopic modifications of the CCl_3H molecule [307]. Recent photoionization detection studies were applied to different vibrational overtones of propyne [308, 309] and butyne [310, 311] molecules.

5.5 Spectroscopy of transitions between highly excited vibrational states

When both initial and final states of the transition lie in the ergodicity region, it follows from the discussion in Section 2.3 that the ideal statement of experiments (from the point of view of a possible theoretical interpretation) is the measurement of the spectrum for a narrow enough distribution over the total vibrational energy. Otherwise, conditions should be produced at least to control this distribution. The simplest approach consists in using IR MPE (see Section 1.3) and measuring the spectrum after a time delay ensuring the establishment of the Boltzmann distribution. This method was used for measuring the absorption spectrum in one of the bands of the C_6F_{12} molecule [312], the ν_3 IR MPE spectrum of the SF_6 molecule [313], the ν_1 Raman spectrum of the same molecule [314, 315], and the ν_1 Raman spectrum of the UF_6 molecule [316]. However, in some papers spectra were measured for narrow vibrational distributions. Thus, the method was applied in Refs [317, 318], in which high vibrational states were efficiently populated due to a laser-induced transition to the excited electronic term, which was accompanied by the radiationless transition to the ground electronic term[37] (the CrO_2Cl_2 molecule; ν_6-mode absorption was probed).

A rather original method of one-photon dissociation was implemented in studies of $(CF_3)_3CI$ [320] and CF_3I [321] molecules. This method is conceptually close to action spectroscopy, at least concerning the detection (multiphoton ionization of a detached iodine atom). Infrared MPE produces a distribution near and above the dissociation threshold, and then, by adding a weak probe pulse delayed with respect to the excitation pulse, we can relate the addition to the photoion signal to the absorption spectrum of molecules in excited vibrational states, because the decay rate rapidly increases with the energy excess over the molecular dissociation threshold. A review devoted to the substantiation of this method and a detailed description of the results is presented in Ref. [322].

The spectra of transitions between highly excited vibrational states, which were measured and interpreted in the papers cited above, are described, as a rule, by one of the dominating mechanisms: either by broadening due to IVR from a mode under study [312, 318, 320] or by the SIB effect [314–316, 321]. It is interesting that different in form vibrational bands of the same CF_3I molecule demonstrate different effects: the ν_1 band (totally symmetric vibration of C – F bonds) revealed traces of a structure related to the three-frequency $\nu_1 \leftrightarrow 2\nu_5$ Fermi resonance (see Fig. 2), and the width was mainly determined by IVR from this mode, while in the ν_4 band (doubly degenerate vibration of the same C – F bonds), the SIB effect dominated.

We also add here that the authors of papers [313, 323] interpreted a mixed situation: a small homogeneous broadening against the background of dominating SIB. Here, due to the multiplicity of the IR MPE process, the authors have managed to estimate the homogeneous component of the spectrum making the main contribution to the wings of the band profile.

5.6 Reactions of molecules in excited vibrational states

The hypothetic possibilities of laser-induced initiation of chemical reactions excited selectively via molecular bonds have been widely discussed in the literature (see also our discussion in Section 1.3). As for the highly lying states, the ideas of laser-induced controling of the so-called transition state[38] to direct the reaction along the required path are still

[37] This effect of reverse electronic relaxation is described, for example, in review [319].

[38] In the Russian literature, the term 'activated complex' is more often adopted.

rather popular. This research field is associated with the term 'femtochemistry' [324], assuming that the time scale of initiated directional processes should be shorter than the characteristic IVR time. Topical reviews discussing key ideas and, in particular, problems of controling dissociation products (vibrationally mediated photochemistry) are presented in Refs [305, 325, 326] and in a collection of papers [327], including the Nobel lecture by Ahmed H Zewail. Note that the subject of such studies can also be a weakly coupled complex (see, for example, Ref. [328]). A field related to the laser initiation of selective bimolecular reactions [329–331] should also be mentioned.

5.7 Molecules in solutions and helium droplets

The questions of what amounts of matter a condensed state and statistical physics begin from have always been of great interest, and they seem especially attractive at the present 'time of nanoprojects'. These questions are related to some extent to our topic as well: we hope that the universal description of the mechanisms of chaos in simple, say, 5–7-atomic compact molecules will help to solve a similar problem for the condensed media which, in principle, consist of such blocks. Therefore, it is interesting, in particular, to compare the dynamics of isolated vibrationally excited molecules with the dynamics of the same molecules in some environment.

We mentioned above the results related to CIIVR — the efficient redistribution of vibrational energy in collisions in methane [256, 257] and propyne [182, 183] halogen derivatives. By extrapolating gas concentrations to liquids, we obtain times of $\lesssim 100$ fs. The IVR rates for molecules in gas and solution were compared for propyne derivatives in papers [255, 332], and CH_3I molecules in paper [333]. The times proved to be considerably longer than could be expected from the CIIVR extrapolation — up to tens of picoseconds.

An interesting solvent is liquid helium, which can be exploited in the form of nanodroplets propagating like a molecular beam. Principally, the situation can be achieved where a droplet contains only one molecule. Thus, the advantages of the matrix isolation and a cooled molecular beam are combined, i.e. we can study unstable clusters, complexes, etc. in the absence of inhomogeneous broadening.[39] The spectroscopy of such systems has been performed in different wavelength regions (see, for example, review [335]). We refer first of all to papers [336, 337] in which fundamental transitions and first overtones were investigated, including the ν_{HC} mode of propyne and its derivatives, to which the greatest part of the review was devoted. It should be noted, however, that the main area here is the spectroscopy of clusters and complexes [338–340] and molecules with well-studied spectra used as probes for studying the properties of droplets themselves [341–344]. Therefore, here the same tendency as with solid solutions is observed, namely, the study of the properties of a matrix by applying single-molecule spectroscopy [345].

5.8 Two-dimensional spectroscopy

Currently, methods of 2D (two-dimensional) spectroscopy have found wide applications for studying the dynamics of condensed states [346]. Various experimental setups are utilized — from pump–probe and double resonance methods to a three-pulse echo with additional signal heterodyning [347] allowing the separation of contributions from different relaxation processes. It may appear at first glance to a reader familiar with the history of the development of nuclear magnetic resonance and laser spectroscopy that this 'mainstream' field contains nothing fundamentally new. This is, however, not the case. It is not the setups themselves that are fundamentally new, but the methods for data processing. The reference to the corresponding program product can be found in book [346].

Papers with titles containing the terms 3D spectroscopy, 4D spectroscopy, and multidimensional spectroscopy are also encountered. The general concept is discussed in paper [348], which is an introduction written by the 'fathers' of the method to a special thematic issue of *Chemical Physics*. However, useful information concerning IVR in an isolated molecule that can be found from this concept is quite trivial. Various pump–probe schemes are an indispensable attribute of *all* approaches to the real-time studies of the IVR dynamics, which we discussed in Section 4. Double resonance methods are used in high-resolution spectral experiments, notably, in many papers discussed in Section 3.

6. Conclusions

A chief aim of our review was to describe the results of numerous papers on the study of IVR in free molecules in the ground electronic state, performed by spectroscopic or dynamic methods. A qualitative jump in these studies occurred in the early 1990s with the application of high-resolution spectroscopy. Various derivatives of the propyne series have been studied in great detail. The first papers in this area are considered in reviews [87, 169]. In our review, this picture is supplemented with recent results. As for papers on observing real-time IVR dynamics, they were started much later,[40] and our review is the first attempt to systematize them.

In principle, both these approaches can duplicate each other; however, at present they are often applied to different subjects: high-resolution spectroscopy has been used so far only in conjunction with a cooled molecular beam, while time-resolved spectroscopy has been applied to date (with only one exception) only to gases at room temperature. As a result of this difference, spectral transitions are studied in the former case for states with small rotational quantum numbers, whereas in the latter case they are studied for states with large rotational quantum numbers. But it is in this part that experiments of these two types mutually supplement each other. So far, such a supplement has been implemented only for propyne and its derivatives, albeit, quite efficiently, by revealing the important role of vibrational–rotational interactions in the IVR process (see Sections 3.6 and 4.3).

Experiments in these two fields were described in Sections 3.2–3.5 and 4.2. All the experiments mentioned in our review have been performed only at a few laboratories. High-resolution spectroscopy is represented by the work of research teams at the Universities of Colorado and Virginia, Princeton and Akron Universities, and NIST (National Institute of Standards and Technologies, USA), their joint publications demonstrating the important role of their

[39] However, one source of the inhomogeneous broadening caused by the dependence of the transition frequency on the droplet size is still present [334].

[40] For example, it is mentioned in comparatively recent monograph [349] that "almost all measurements were performed with pure liquids or concentrated solutions."

collaboration. Time-resolved spectroscopy is also represented by the work of groups at Stanford University,[41] Tohoku University (Japan), and the Institute of Spectroscopy, RAS. The limited scope of laboratories engaged in these studies can only be explained by the complexity of these investigations, whereas the topic itself is far from being exhausted. Thus, most recent papers [350, 351] present a rather advanced variant of spectroscopy combining the concepts of MW–IR double resonance and MW Fourier transform spectroscopy (FTMW–IR).[42] Then, very interesting first results were obtained for the methanol molecule in the region where the stretching vibrations of C – H bonds form, together with the first overtones of C – H and O – H bending vibrations, an islet on the energy scale with a relatively large number of closely spaced levels.[43] It seems that new impressive results with earlier uninvestigated subjects should be expected, however, we emphasize that we are dealing here again with an absolutely unique setup.

Nevertheless, we hope that more universal and accessible methods for studying IVR will be found in the future than those existing at present, resulting in the expansion of the scope of studies, as, for example, has been already demonstrated by the development of 2D spectroscopy (see Section 5.8) in the condense-state studies involving many tens of laboratories. It seems that a breakthrough can be expected in the field of time-resolved spectroscopy, because femtosecond IR laser pulses are already available in many laboratories. The application of coherent methods can become an actual step in their employment for analyzing the IVR process. For example, a three-pulse echo, similarly to one of the variants of 2D spectroscopy, can become useful in studies of transitions between ergodic states, where competition between different contributions to the spectral broadening is possible.

The real-time dynamics of IVR from the initially prepared state, when the lower state of the transition is the ground state, can be studied by utilizing simpler setups. For example, different variants of a two-pulse photon echo, four-wave mixing schemes that show promise for studying vibrational–rotational mixing (see Section 4.3), etc., can be applied. Although to date no experimental results have been obtained in this field (experiments with molecular gases and, moreover, with molecular beams impose much more stringent requirements on the sensitivity than, for example, experiments with liquids), the wide development and applications of methods of coherent laser spectroscopy for studying IVR in isolated molecules seems quite real in the near future.

Acknowledgments. The authors thank their colleague G N Makarov for fruitful discussions. Our recent work cited in the review was supported by the Russian Foundation for Basic Research (grant Nos 96-02-17278-a, 02-02-16687-a, 06-02-16663-a, 08-02-00581-a, and 09-02-00495-a).

References

1. Mcllroy A, Nesbitt D J *J. Chem. Phys.* **92** 2229 (1990)
2. Mcllroy A, Nesbitt D J *J. Chem. Phys.* **91** 104 (1989)
3. Herzberg G *Infrared and Raman Spectra of Polyatomic Molecules* (New York: Van Nostrand, 1945) [Translated into Russian (Moscow: IL, 1949)]
4. Haake F *Quantum Signatures of Chaos* (Berlin: Springer, 1992)
5. Steiner F, in *Schlaglichter der Forschung: zum 75. Jahrestag der Universität Hamburg 1994* (Ed. R Ansorge) (Hamburg: D. Reimer, 1994) p. 543 [Translated into Russian (Moscow – Izhevsk: RKhD, 2008) p. 102]
6. Cornfeld I P, Sinai Ya G, Fomin S V *Ergodicheskaya Teoriya* (Ergodic Theory) (Moscow: Nauka, 1980) [Translated into English: Cornfeld I P, Fomin S V, Sinai Ya G *Ergodic Theory* (New York: Springer-Verlag, 1982)]
7. Einstein A *Verhandl. Deutsch. Phys. Ges.* **19** 82 (1917) [Translated into English: *The Collected Papers of Albert Einstein* Vol. 6 (Transl. A Engel) (Princeton: Princeton Univ. Press, 1997) p. 434; Translated into Russian: *Albert Einstein. Sobranie Nauchnykh Trudov* (Collected Scientific Works) Vol. 3 (Moscow: Nauka, 1966) p. 407]
8. Landau L D *Phys. Z. Sowjetunion* **10** 67 (1936) [Translated into Russian: *Sobranie Trudov* (Collected Works) Vol. 1 (Moscow: Nauka, 1969) p. 189]
9. Rice O K, Ramsperger H C *J. Am. Chem. Soc.* **49** 1617 (1927)
10. Rice O K, Ramsperger H C *J. Am. Chem. Soc.* **50** 617 (1928)
11. Kassel L S *J. Phys. Chem.* **32** 225 (1928)
12. Kassel L S *J. Phys. Chem.* **32** 1065 (1928)
13. Markus R A *J. Chem. Phys.* **20** 359 (1952)
14. Markus R A *J. Chem. Phys.* **43** 2658 (1965)
15. Nikitin E E *Teoriya Elementarnykh Atomno-Molekulyarnykh Protsessov v Gazakh* (Theory of Elementary Atomic and Molecular Processes in Gases) (Moscow: Khimiya, 1970) [Translated into English (Oxford: Oxford Univ. Press, 1974)]
16. Robinson P J, Holbrook K A *Unimolecular Reactions* (New York: Wiley-Intersci., 1972) [Translated into Russian (Moscow: Mir, 1975)]
17. Forst W *Theory of Unimolecular Reactions* (New York: Academic Press, 1973)
18. Kondrat'ev V N, Nikitin E E *Kinetika i Mekhanizm Gazofaznykh Reaktsii* (Kinetics and Mechanism of Gas-Phase Reactions) (Moscow: Nauka, 1974)
19. Eyring H, Lin S H, Lin S M *Basic Chemical Kinetics* (New York: Wiley, 1980)
20. Artamonova N D, Platonenko V T, Khokhlov R V *Zh. Eksp. Teor. Fiz.* **58** 2195 (1970) [*Sov. Phys. JETP* **31** 1185 (1970)]
21. Basov N G et al. *Pis'ma Zh. Eksp. Teor. Fiz.* **14** 251 (1971) [*JETP Lett.* **14** 165 (1971)]
22. Letokhov V S, Ryabov E A, Tumanov O A *Zh. Eksp. Teor. Fiz.* **63** 2025 (1972) [*Sov. Phys. JETP* **36** 1069 (1973)]
23. Isenor N R et al. *Can. J. Phys.* **51** 1281 (1973)
24. Ambartzumian R V et al. *Chem. Phys. Lett.* **25** 515 (1974)
25. Ambartzumian R V, Letokhov V S, in *Chemical and Biochemical Applications of Lasers*, Vol. 3 (Ed. C B Moore) (New York: Academic Press, 1977) p. 167
26. Bloembergen N, Yablonovitch E *Phys. Today* **31** (5) 23 (1978)
27. Schulz P A et al. *Annu. Rev. Phys. Chem.* **30** 379 (1979)
28. Bagratashvili V N et al. *Mnogofotonnye Protsessy v Molekulakh v Infrakrasnom Lazernom Pole* (Multiphoton Processes in Molecules in an IR Laser Field) (Summary of Science and Technology, Ser. Physics of Atoms and Molecules, Optics, Magnetic Resonance, Vol. 2, Pt. 1) (Moscow: VINITI, 1980)
29. Letokhov V S, Makarov A A *Usp. Fiz. Nauk* **134** 45 (1981) [*Sov. Phys. Usp.* **24** 366 (1981)]
30. King D S, in *Dynamics of the Excited State* (Ed. K P Lawley) (New York: Wiley, 1982) p. 105
31. Bagratashvili V N et al. *Multiple Photon Infrared Laser Photophysics and Photochemistry* (Chur: Harwood Acad. Publ., 1985)
32. Cantrell C D (Ed.) *Multiple-Photon Excitation and Dissociation of Polyatomic Molecules* (Berlin: Springer-Verlag, 1986)
33. Lyman J L, in *Laser Spectroscopy and Its Applications* (Eds L J Radziemski, R W Solarz, J A Paisner) (New York: M. Dekker, 1987) p. 417
34. Lupo D W, Quack M *Chem. Rev.* **87** 181 (1987)
35. Makarov G N *Usp. Fiz. Nauk* **175** 41 (2005) [*Phys. Usp.* **48** 37 (2005)]
36. Ambartzumyan R V et al. *Pis'ma Zh. Eksp. Teor. Fiz.* **20** 597 (1974) [*JETP Lett.* **20** 273 (1974)]

[41] At present, this group is completely engaged in condensed state studies.
[42] The fundamentals of MW Fourier transform spectroscopy are considered, for example, in review [352].
[43] This case with complex, branched energy migration paths is rather exotic for our topic. In our opinion, an unambiguous interpretation in this case is premature.

37. Ambartzumyan R V et al. *Pis'ma Zh. Eksp. Teor. Fiz.* **21** 375 (1975) [*JETP Lett.* **21** 171 (1975)]
38. Letokhov V S, Moore C B *Kvantovaya Elektron.* **3** 485 (1976) [*Sov. J. Quantum Electron.* **6** 259 (1976)]
39. Karlov N V, Prokhorov A M *Usp. Fiz. Nauk* **118** 583 (1976) [*Sov. Phys. Usp.* **19** 285 (1976)]
40. Basov N G et al. *Usp. Fiz. Nauk* **121** 427 (1977) [*Sov. Phys. Usp.* **20** 209 (1977)]
41. Ryabov E A *Usp. Fiz. Nauk* **174** 684 (2004) [*Phys. Usp.* **47** 627 (2004)]
42. Zewail A H *Phys. Today* **33** (11) 27 (1980) [Translated into Russian: *Fizika za Rubezhom, 82. Lazernaya Khimiya. Sverkhprovodimost. Fizika Tverdogo Tela* (Physics Abroad, 82. Laser Chemistry, Superconductivity. Solid State Physics) (Moscow: Mir, 1982) p. 63]
43. Bloembergen N, Zewail A H *J. Phys. Chem.* **88** 5459 (1984)
44. Shuryak E V *Zh. Eksp. Teor. Fiz.* **71** 2039 (1976) [*Sov. Phys. JETP* **44** 1070 (1976)]
45. Zaslavskii G M, Chirikov B V *Usp. Fiz. Nauk* **105** 3 (1971) [*Sov. Phys. Usp.* **14** 549 (1972)]
46. Fermi E *Mem. Accad. d'Italia Fis.* **3** (1) 239 (1932) [Translated into Russian *Enrico Fermi. Nauchnye Trudy* (Enrico Fermi. Scientific Works) Vol. 1 (Exec. Ed. B Pontecorvo) (Moscow: Nauka, 1971) p. 440]
47. Krylov N S *Raboty po Obosnovaniyu Statisticheskoi Fiziki* (Works on the Foundations of Statistical Physics) (Moscow – Leningrad: Izd. AN SSSR, 1950) [Translated into English (Princeton, N.J.: Princeton Univ. Press, 1979)]
48. Balescu R "Appendix: The Ergodic Problem", in *Equilibrium and Nonequilibrium Statistical Mechanics* (New York: Wiley, 1975) p. 495 [Translated into Russian, Vol. 2 (Moscow: Mir, 1978) p. 354]
49. Fermi E, Pasta J, Ulam S, Los Alamos Report LA-1940 (1955); in *The Collected Papers of Enrico Fermi* Vol. 2 (Chicago: The Univ. of Chicago Press, 1955) p. 978 [Translated into Russian: *Enrico Fermi. Nauchnye Trudy* (Enrico Fermi. Scientific Works) Vol. 1 (Exec. Ed. B Pontecorvo) (Moscow: Nauka, 1972) p. 647]
50. Izrailev F M, Chirikov B V *Dokl. Akad. Nauk SSSR* **166** 57 (1966) [*Sov. Phys. Dokl.* **11** 30 (1966)]
51. Toda M *Theory of Nonlinear Lattices* (Berlin: Springer-Verlag, 1981) [Translated into Russian (Moscow: Mir, 1984)]
52. Poincaré H *Les Méthodes Nouvelles de la Mécanique Céleste* (Paris: Gauthier-Villars, 1892 – 1899) [Translated into Russian (Moscow: Nauka, 1971, 1972)
53. Moser J *Stable and Random Motions in Dynamical Systems: with Special Emphasis on Celestial Mechanics* (Princeton, N.J.: Princeton Univ. Press, 2001)
54. Celletti A *Stability and Chaos in Celestial Mechanics* (Berlin: Springer, 2010)
55. Berman G P, Zaslavskii G M *Zh. Eksp. Teor. Fiz.* **58** 1453 (1970) [*Sov. Phys. JETP* **31** 778 (1970)
56. Gaponov-Grekhov A V, Rabinovich M I *Usp. Fiz. Nauk* **128** 579 (1979) [*Sov. Phys. Usp.* **22** 590 (1979)
57. Chirikov B V *Phys. Rep.* **52** 263 (1979)
58. Casati G, Ford J (Eds) *Stochastic Behavior in Classical and Quantum Hamiltonian Systems: Volta Memorial Conf., Como, Italy, 1977* (Berlin: Springer-Verlag, 1979)
59. Lichtenberg A J, Lieberman M A *Regular and Stochastic Motion* (New York: Springer-Verlag, 1983) [Translated into Russian (Moscow: Mir, 1984)]
60. Zaslavsky G M *Stokhastichnost' Dinamicheskikh Sistem* (Chaos in Dynamic Systems) (Moscow: Nauka, 1984) [Translated into English (Chur: Harwood Acad. Publ., 1985)]
61. Gutzwiller M C *Chaos in Classical and Quantum Mechanics* (New York: Springer-Verlag, 1990)
62. Ott E *Chaos in Dynamical Systems* (Cambridge: Cambridge Univ. Press, 1993)
63. Nakamura K *Quantum Chaos: A New Paradigm of Nonlinear Dynamics* (New York: Cambridge Univ. Press, 1993)
64. Casati G, Chirikov B (Comp.) *Quantum Chaos: Between Order and Disorder* (New York: Cambridge Univ. Press, 1995)
65. Stöckmann H-J *Quantum Chaos: An Introduction* (Cambridge: Cambridge Univ. Press, 1999) [Translated into Russian (Moscow: Fizmatlit, 2004)]
66. Kuznetsov S P *Dinamicheskii Khaos* (Dynamical Chaos) (Moscow: Fizmatlit, 2001)
67. Schuster H G, Just W *Deterministic Chaos: An Introduction* (Weinheim: Wiley-VCH, 2005)
68. Toda M et al. (Eds) *Geometric Structures of Phase Space in Multidimensional Chaos* (Hoboken, N.J.: Wiley, 2005)
69. Bolotin Yu, Tur A, Yanovsky V *Konstruktivnyi Khaos* (Constructive Chaos) (Khar'kov: Inst. Monokristallov, 2005) [Translated into English: *Chaos: Concepts, Control and Constructive Use* (New York: Springer, 2009)]
70. Scheck F *Mechanics: from Newton's Laws to Deterministic Chaos* (Berlin: Springer, 2010)
71. Kolmogorov A N *Dokl. Akad. Nauk SSSR* **98** 527 (1954)
72. Arnold V I *Matematicheskie Metody Klassicheskoi Mekhaniki* (Mathematical Methods of Classical Mechanics) (Moscow: Nauka, 1974) [Translated into English (New York: Springer-Verlag, 1978)]
73. Moser J *Lectures on Hamiltonian Systems* (New York: Courant Inst. of Math. Sci., 1968) [Translated into Russian (Moscow: Mir, 1973)]
74. Sinai Ya G (Ed.), Shafarevich A I (Sci. Ed.) *Kvantovyi Khaos* (Quantum Chaos) (Moscow – Izhevsk: RKhD, 2008)
75. Akulin V M et al. *Zh. Eksp Teor. Fiz.* **69** 836 (1975) [*Sov. Phys. JETP* **42** 427 (1975)]
76. Bloembergen N *Opt. Commun.* **15** 416 (1975)
77. Letokhov V S, Makarov A A *Opt. Commun.* **17** 250 (1976)
78. Coggiola M J et al. *Phys. Rev. Lett.* **38** 17 (1977)
79. Windhorn L et al. *J. Chem. Phys.* **119** 641 (2003)
80. Quick C R, Wittig C *J. Chem. Phys.* **72** 1694 (1980)
81. Bagratashvili V N et al. *Chem. Phys. Lett.* **120** 211 (1985)
82. Hénon M, Heiles C *Astron. J.* **69** 73 (1964)
83. Toda M *Phys. Rep.* **18** 1 (1975)
84. Noid D W et al. *J. Chem. Phys.* **72** 6169 (1980)
85. Rice S A, in *Photoselective Chemistry* Vol. 1 (Eds J Jortner, R D Levine, S A Rice) (New York: Wiley, 1981) p. 117
86. Brumer P, in *Photoselective Chemistry* Vol. 1 (Eds J Jortner, R D Levine, S A Rice) (New York: Wiley, 1981) p. 201
87. Nesbitt D J, Field R W *J. Phys. Chem.* **100** 12735 (1996)
88. Bixon M, Jortner J *J. Chem. Phys.* **48** 715 (1968)
89. Weisskopf V, Wigner E *Z. Phys.* **63** 54 (1930)
90. Fano U *Phys. Rev.* **124** 1866 (1961)
91. Makarov A A, Platonenko V T, Tyakht V V *Zh. Eksp. Teor. Fiz.* **75** 2075 (1978) [*Sov. Phys. JETP* **48** 1044 (1978)
92. Makarov A A, in *Laser Spectroscopy of Highly Vibrationally Excited Molecules* (Ed. V S Letokhov) (Bristol: A. Hilger, 1989) p. 106 [Translated into Russian (Moscow: Nauka, 1990) p. 77]
93. Cohen-Tannoudji C, Dupont-Roc J, Grynberg G *Atom – Photon Interactions: Basic Processes and Applications* (New York: Wiley, 1992) p. 64
94. Stey G C, Gibberd R W *Physica* **60** 1 (1972)
95. Lefebvre R, Savolainen J *J. Chem. Phys.* **60** 2509 (1974)
96. Medvedev E S, Osherov V I *Teoriya Bezyzluchatel'nykh Perekhodov v Mnogoatomnykh Molekulakh* (Theory of Radiationless Transitions in Polyatomic Molecules) (Moscow: Nauka, 1983) [Translated into English: *Radiationless Transitions in Polyatomic Molecules* (Berlin: Springer-Verlag, 1995)]
97. Stewart G M, McDonald J D *J. Chem. Phys.* **78** 3907 (1983)
98. Dyson F J, Mehta M L *J. Math. Phys.* **4** 701 (1963)
99. Wigner E P *SIAM Rev.* **9** 1 (1967)
100. Porter C (Ed.) *Statistical Theory of Spectra: Fluctuations* (New York: Academic Press, 1965)
101. Brody T A et al. *Rev. Mod. Phys.* **53** 385 (1981)
102. Mehta M L *Random Matrices* 3rd ed. (Amsterdam: Academic Press, 2004)
103. Bohr A, Mottelson B R *Nuclear Structure* Vol. 1 (New York: W. A. Benjamin, 1969) [Translated into Russian (Moscow: Mir, 1971) p. 287]
104. Haq R U, Pandey A, Bohigas O *Phys. Rev. Lett.* **48** 1086 (1982)
105. Papenbrock T, Weidenmüller H A *Rev. Mod. Phys.* **79** 997 (2007)
106. Haller E, Köppel H, Cederbaum L S *Chem. Phys. Lett.* **101** 215 (1983)
107. Mukamel S, Sue J, Pandey A *Chem. Phys. Lett.* **105** 134 (1984)
108. Zimmermann Th et al. *Phys. Rev. Lett.* **61** 3 (1988)
109. Camarda H S, Georgopulos P D *Phys. Rev. Lett.* **50** 482 (1983)

110. Held H et al. *Europhys. Lett* **43** 392 (1998)
111. Bohigas O, Giannoni M J, Schmit C *Phys. Rev. Lett*. **52** 1 (1984)
112. Sinai Ya G *Usp. Mat. Nauk* **25** (2) 141 (1970) [*Russ. Math. Surv*. **25** (2) 137 (1970)]
113. Stöckmann H-J, Stein J *Phys. Rev. Lett*. **64** 2215 (1990)
114. Porter C E, Thomas R G *Phys. Rev*. **104** 483 (1956)
115. Alhassid Y, Levine R D *Phys. Rev. Lett*. **57** 2879 (1986)
116. Malinovsky A L, Makarov A A, Ryabov E A *Zh. Eksp. Teor. Fiz*. **133** 45 (2008) [*JETP* **106** 34 (2008)]
117. Srednicki M *Phys. Rev. E* **50** 888 (1994)
118. Stuchebrukhov A A, Ionov S I, Letokhov V S *J. Phys. Chem*. **93** 5357 (1989)
119. Makarov A A et al. *J. Phys. Chem. A* **102** 1438 (1998)
120. Angelié C *J. Chem. Phys*. **98** 2541 (1993)
121. Kubo R, in *Fluctuation, Relaxation, and Resonance in Magnetic Systems* (Ed. D Ter Haar) (Edinburgh: Oliver and Boyd, 1962) p. 23
122. Dicke R H *Phys. Rev*. **89** 472 (1953)
123. Bazhulin P A *Usp. Fiz. Nauk* **77** 639 (1962) [*Sov . Phys. Usp*. **5** 661 (1963)]
124. Rautian S G, Sobel'man I I *Usp. Fiz. Nauk* **90** 209 (1966) [*Sov. Phys. Usp*. **9** 701 (1967)]
125. Alekseev V A, Sobel'man I I *Zh. Eksp. Teor. Fiz*. **55** 1874 (1969) [*Sov. Phys. JETP* **28** 991 (1969)]
126. Alekseev V A, Malyugin A V *Zh. Eksp. Teor. Fiz*. **80** 897 (1981) [*Sov. Phys. JETP* **53** 456 (1981)]
127. Bagratashvili V N et al. *Chem. Phys*. **97** 13 (1985)
128. Kuz'min M V, Letokhov V S, Stuchebryukhov A A *Zh. Eksp. Teor. Fiz*. **90** 458 (1986) [*Sov. Phys. JETP* **63** 264 (1986)]
129. Kuzmin M V, Stuchebrukhov A A, in *Laser Spectroscopy of Highly Vibrationally Excited Molecules* (Ed. V S Letokhov) (Bristol: A. Hilger, 1989) p. 178 [Translated into Russian (Moscow: Nauka, 1990) p. 129]
130. Uzer T, Miller W H *Phys. Rep*. **199** 73 (1991)
131. Nitzan A, Persson B N J *J. Chem. Phys*. **83** 5610 (1985)
132. Makarov A A, Tyakht V V *Zh. Eksp. Teor. Fiz*. **93** 17 (1987) [*Sov. Phys. JETP* **66** 9 (1987)]
133. Personov R I, in *Shpol'skii Spectroscopy and Other Site Selection Methods: Applications in Environmental Analysis, Bioanalytical Chemistry, and Chemical Physics* (Eds C Gooijer, F Ariese, J W Hofstraat) (New York: Wiley-Intersci., 2000) p. 1
134. Zel'dovich B Ya, Perelomov A M, Popov V S *Zh. Eksp. Teor. Fiz*. **55** 589 (1968) [*Sov. Phys. JETP* **28** 308 (1969)]
135. Dykman M I, Krivoglaz M A *Zh. Eksp. Teor. Fiz*. **64** 993 (1973) [*Sov. Phys. JETP* **37** 506 (1973)]
136. Dykman M I *Fiz. Tverd. Tela* **15** 1075 (1973) [*Sov. Phys. Solid State* **15** 735 (1973)]
137. Myers D J et al. *Chem. Phys. Lett*. **312** 399 (1999)
138. Dübal H-R, Quack M *Chem. Phys. Lett*. **72** 342 (1980)
139. Ovchinnikov A A, Érikhman N S *Usp. Fiz. Nauk* **138** 289 (1989) [*Sov. Phys. Usp*. **25** 738 (1982)]
140. Baggott J E et al. *J. Chem. Phys*. **82** 1186 (1985)
141. Bray R G, Berry M J *J. Chem. Phys*. **71** 4909 (1979)
142. Reddy K V, Heller D F, Berry M J *J. Chem. Phys*. **76** 2814 (1982)
143. Tam A S, in *Ultrasensitive Laser Spectroscopy* (Ed. D S Kliger) (New York: Academic Press, 1983) p. 1 [Translated into Russian (Moscow: Mir, 1986) p. 13]
144. Zharov V P, Letokhov V S *Lazernaya Optiko-Akusticheskaya Spektroskopiya* (Laser Optoacoustic Spectroscopy) (Moscow: Nauka, 1984) [Translated into English (Berlin: Springer-Verlag, 1986)]
145. Levy D H, Wharton L, Smalley R E, in *Chemical and Biochemical Applications of Lasers* Vol. 2 (Ed. C B Moore) (New York: Academic Press, 1977) p. 1
146. Levy D H *Annu. Rev. Phys. Chem*. **31** 197 (1980)
147. Page R H, Shen Y R, Lee Y T *Phys. Rev. Lett*. **59** 1293 (1987)
148. Page R H, Shen Y R, Lee Y T *J. Chem. Phys*. **88** 4621 (1988)
149. Shen Y R *The Principles of Nonlinear Optics* (New York: J. Wiley, 1984) p. 227 [Translated into Russian (Moscow: Nauka, 1989) p. 219]
150. Heller D F, Mukamel S *J. Chem. Phys*. **70** 463 (1979)
151. Sibert E L, Reinhardt W P, Hynes J T *J. Chem. Phys*. **81** 1115 (1984)
152. De Souza A M, Kaur D, Perry D S *J. Chem. Phys*. **88** 4569 (1988)
153. Bunker Ph R *Molecular Symmetry and Spectroscopy* (New York: Academic Press, 1979) Ch. 10 [Translated into Russian (Moscow: Mir, 1981) Ch. 10]
154. Kerstel E R T et al. *J. Phys. Chem*. **95** 8282 (1991)
155. Fraser G T, Pine A S *J. Chem. Phys*. **91** 637 (1989)
156. Fraser G T et al. *Chem. Phys*. **175** 223 (1993)
157. Green D et al. *J. Chem. Phys*. **110** 1979 (1999)
158. Steinfeld J I, Houston P L, in *Laser and Coherence Spectroscopy* (Ed. J I Steinfeld) (New York: Plenum Press, 1978) p. 1 [Translated into Russian (Moscow: Mir, 1982) p. 11]
159. Lee C Y, Pate B H *J. Chem. Phys*. **107** 10430 (1997)
160. Lee C Y, Pate B H *Chem. Phys. Lett*. **284** 369 (1998)
161. Lawrance W D, Knight A E W *J. Phys. Chem*. **89** 917 (1985)
162. Coy S L, Lehmann K K *Phys. Rev. A* **36** 404 (1987)
163. Coy S L, Hernandez R, Lehmann K K *Phys. Rev. A* **40** 5935 (1989)
164. Lehmann K K *J. Phys. Chem*. **95** 7556 (1991)
165. Lawrence W D, Knight A E W *J. Phys. Chem*. **95** 7557 (1991)
166. Davis M J *J. Chem. Phys*. **98** 2614 (1993)
167. Perry D S *J. Chem. Phys*. **98** 6665 (1993)
168. Davis M J, Bethardy G A, Lehmann K K *J. Chem. Phys*. **101** 2642 (1994)
169. Lehmann K K, Scoles G, Pate B H *Annu. Rev. Phys. Chem*. **45** 241 (1994)
170. Boyall D, Reid K L *Chem. Soc. Rev*. **26** 223 (1997)
171. Kerstel E R Th et al. *J. Chem. Phys*. **100** 2588 (1994)
172. Yoo H S, McWhorter D A, Pate B H *J. Phys. Chem. A* **108** 1380 (2004)
173. Pate B H, Lehmann K K, Scoles G *J. Chem. Phys*. **95** 3891 (1991)
174. Hudspeth E, McWhorter D A, Pate B H *J. Chem. Phys*. **109** 4316 (1998)
175. Andrews A M, Fraser G T, Pate B H *J. Chem. Phys*. **109** 4290 (1998)
176. Keske J C et al. *Phys. Chem. Chem. Phys*. **5** 1599 (2003)
177. Lehmann K K, Pate B H, Scoles G *J. Chem. Phys*. **93** 2152 (1990)
178. Gambogi J E et al. *J. Chem. Phys*. **98** 1116 (1993)
179. Gambogi J E et al. *J. Chem. Phys*. **98** 1748 (1993)
180. Go J, Bethardy G A, Perry D S *J. Phys. Chem*. **94** 6153 (1990)
181. Kerstel E R Th et al. *J. Chem. Phys*. **100** 2588 (1994)
182. Malinovsky A L et al. *Chem. Phys. Lett*. **419** 511 (2006)
183. Malinovsky A L, Makarov A A, Ryabov E A *Pis'ma Zh. Eksp. Teor. Fiz*. **93** 139 (2011) [*JETP Lett*. **93** 124 (2011)]
184. Malinovsky A L, Makarov A A, Ryabov E A *Phys. Scr*. **85** 058102 (2012)
185. Stuchebrukhov A A, Marcus R A *J. Chem. Phys*. **98** 6044 (1993)
186. Marshall K T, Hutchinson J S *J. Chem. Phys*. **95** 3232 (1991)
187. Zhang Y, Marcus R A *J. Chem. Phys*. **96** 6065 (1992)
188. Stuchebrukhov A A, Mehta A, Marcus R A *J. Phys. Chem*. **97** 12491 (1993)
189. Engelhardt C et al. *J. Phys. Chem. A* **105** 6800 (2001)
190. Go J, Perry D S *J. Chem. Phys*. **97** 6994 (1992)
191. Go J, Cronin T J, Perry D S *Chem. Phys*. **175** 127 (1993)
192. Mcllroy A et al. *J. Chem. Phys*. **100** 2596 (1994)
193. Gambogi J E et al. *J. Chem. Phys*. **100** 2612 (1994)
194. Mehta A, Stuchebrukhov A A, Marcus R A *J. Phys. Chem*. **99** 2677 (1995)
195. Lehmann K K, Pate B H, Scoles G *Laser Chem*. **11** 237 (1991)
196. Bethardy G A, Perry D S *J. Chem. Phys*. **98** 6651 (1993)
197. Bethardy G A, Perry D S *J. Chem. Phys*. **99** 9400 (1993)
198. McWhorter D A, Pate B H *J. Phys. Chem. A* **102** 8786 (1998)
199. McWhorter D A, Pate B H *J. Mol. Spectrosc*. **193** 159 (1999)
200. Cupp S et al. *J. Chem. Phys*. **109** 4302 (1998)
201. Bethardy G A, Wang X, Perry D S *Can. J. Chem*. **72** 652 (1994)
202. McWhorter D A, Hudspeth E, Pate B H *J. Chem. Phys*. **110** 2000 (1999)
203. Halonen M et al. *J. Phys. Chem. A* **102** 9124 (1998)
204. Callegari A et al. *J. Chem. Phys*. **106** 432 (1997)
205. Wilson E B *J. Chem. Phys*. **4** 313 (1936)
206. Papoušek D, Aliev M R *Molecular Vibrational/Rotational Spectra* (Prague: Academia, 1982) Ch. III; *Molecular Vibrational–Rotational Spectra*: *Theory and Applications of High Resolution Infrared, Microwave, and Raman Spectroscopy of Polyatomic Molecules* (Amsterdam: Elsevier, 1982)
207. Knight A E W, in *Excited States* Vol. 7 (Eds E C Lim, K K Innes) (San Diego: Academic Press, 1988) p. 1
208. Kaiser W, Laubereau A, in *Nonlinear Spectroscopy* (Ed. N Bloembergen) (Amsterdam: North-Holland, 1977) Ch. 17 [Translated into Russian (Moscow: Mir, 1979) p. 528]

209. Laubereau A, Kaiser W *Rev. Mod. Phys.* **50** 607 (1978)
210. Ryabov E A, in *Laser Spectroscopy of Highly Vibrationally Excited Molecules* (Ed. V S Letokhov) (Bristol: A. Hilger, 1989) p. 55 [Translated into Russian (Moscow: Nauka, 1990) p. 42]
211. Moore J N, Hansen P A, Hochstrasser R M *Chem. Phys. Lett.* **138** 110 (1987)
212. Locke B, Lian T, Hochstrasser R M *Chem. Phys.* **158** 409 (1991)
213. Bagratashvili V N et al. *Pis'ma Zh. Eksp. Teor. Fiz.* **30** 502 (1979) [*JETP Lett.* **30** 471 (1979)
214. Bagratashvili V N et al. *Appl. Phys.* **22** 101 (1980)
215. Mazur E, Burak I, Bloembergen N *Chem. Phys. Lett.* **105** 258 (1984)
216. Wang J, Chen K-H, Mazur E *Phys. Rev. A* **34** 3892 (1986)
217. Makarov A A, in *Primenenie Lazerov v Atomnoi, Molekulyarnoi i Yadernoi Fizike*: *Trudy II Vsesoyuz. Shkoly, Vil'nyus, 29 Iyunya — 7 Iyulya 1981 g.* (Applications of Lasers in Atomic, Molecular, and Nuclear Physics: Proc. of the II All-Union School, Vilnius, 29 June – 7 July 1981) (Moscow: Nauka, 1983) p. 67 [Makarov A A *J. Russ. Laser Res.* **6** 334 (1985)]
218. Makarov A A, Ryabov E A, in *Lasers in Atomic, Molecular, and Nuclear Physics* (Ed. V S Letokhov) (Singapore: World Scientific, 1989) p. 150
219. Bagratashvili V N et al. *Zh. Eksp. Teor. Fiz.* **80** 1008 (1981) [*Sov. Phys. JETP* **53** 512 (1981)]
220. Bagratashvili V N et al. *Opt. Commun.* **38** 31 (1981)
221. Angelie C *J. Chem. Phys.* **98** 9284 (1993)
222. Doljikov Yu S et al. *Chem. Phys. Lett.* **124** 304 (1986)
223. Dolzhikov Yu S et al. *Zh. Eksp. Teor. Fiz.* **90** 1982 (1986) [*Sov. Phys. JETP* **63** 1161 (1986)]
224. Doljikov V S et al. *Chem. Phys.* **102** 155 (1986)
225. Doljikov Yu S, Malinovsky A L, Ryabov E A *Laser Chem.* **8** 81 (1988)
226. Angelie C *J. Chem. Phys.* **96** 8072 (1992)
227. Ambartsumyan R V et al. *Pis'ma Zh. Eksp. Teor. Fiz.* **35** 170 (1982) [*JETP Lett.* **35** 210 (1982)]
228. Alimpiev S S et al. *Pis'ma Zh. Eksp. Teor. Fiz.* **35** 291 (1982) [*JETP Lett.* **35** 210 (1982)]
229. Dolzhikov Yu S et al. *Izv. Akad. Nauk SSSR, Ser. Fiz.* **53** 1055 (1989)
230. Hudgens J W, McDonald J D *J. Chem. Phys.* **74** 1510 (1981)
231. Hudgens J W, McDonald J D *J. Chem. Phys.* **76** 173 (1982)
232. Stewart G M et al. *J. Chem. Phys.* **79** 3190 (1983)
233. Stewart G et al. *J. Chem. Phys.* **80** 5353 (1984)
234. Kulp T et al. *J. Chem. Phys.* **80** 5359 (1984)
235. Minton T K, Kim H L, McDonald J D *J. Chem. Phys.* **88** 1539 (1988)
236. Kim H L et al. *J. Chem. Phys.* **89** 3955 (1988)
237. Gordienko V M et al. *Khim. Vys. Energ.* **21** 83 (1987) [*High Energy Chem.* **21** 65 (1987)]
238. Chen K-H, Wang J, Mazur E *Phys. Rev. Lett.* **59** 2728 (1987)
239. Malinovsky A L, Ryabov E A *Phys. Rev. Lett.* **63** 1533 (1989)
240. Kim H L, Kulp T J, McDonald J D *J. Chem. Phys.* **87** 4376 (1987)
241. Fleming P R, Li M, Rizzo T R *J. Chem. Phys.* **94** 2425 (1991)
242. Bingemann D et al. *J. Chem. Phys.* **107** 661 (1997)
243. Ebata T et al. *J. Phys. Chem. A* **105** 8623 (2001)
244. Yamada Y et al. *J. Chem. Phys.* **120** 7400 (2004)
245. Yamada Y, Mikami N, Ebata T *J. Chem. Phys.* **121** 11530 (2004)
246. Yamada Y et al. *J. Chem. Phys.* **123** 124316 (2005)
247. Akulin V M et al. *Pis'ma Zh. Eksp. Teor. Fiz.* **41** 239 (1985) [*JETP Lett.* **41** 291 (1985)]
248. Kusaka R, Inokuchi Y, Ebata T *J. Chem. Phys.* **136** 044304 (2012)
249. Stromberg C, Myers D J, Fayer M D *J. Chem. Phys.* **116** 3540 (2002)
250. Myers D J et al. *Chem. Phys. Lett.* **313** 592 (1999)
251. Windhorn L et al. *Chem. Phys. Lett.* **357** 85 (2002)
252. Kompanets V O et al. *Pis'ma Zh. Eksp. Teor. Fiz.* **92** 157 (2010) [*JETP Lett.* **92** 135 (2010)]
253. Chekalin S V et al. *Chem. Phys. Lett.* **512** 178 (2011)
254. Botan V, Hamm P *J. Chem. Phys.* **129** 164506 (2008)
255. Yoo H S, DeWitt M J, Pate B H *J. Phys. Chem. A* **108** 1348 (2004)
256. Kosterev A A, Malinovskii A L, Ryabov E A *Pis'ma Zh. Eksp. Teor. Fiz.* **54** 16 (1991) [*JETP Lett.* **54** 14 (1991)]
257. Kosterev A A et al. *Chem. Phys.* **219** 305 (1997)
258. Makarov A A, Malinovsky A L, Ryabov E A *J. Chem. Phys.* **129** 116102 (2008)
259. Malinovsky A L, Makarov A A, Ryabov E A *Pis'ma Zh. Eksp. Teor. Fiz.* **80** 605 (2004) [*JETP Lett.* **80** 532 (2004)]
260. Kulp T J, Kim H L, McDonald J D *J. Chem. Phys.* **85** 211 (1986)
261. Minton T K et al. *J. Chem. Phys.* **89** 6550 (1988)
262. Makarov A A, Malinovsky A L, Ryabov E A *Izv. Ross. Akad. Nauk, Ser. Fiz.* **72** 737 (2008) [*Bull. Russ. Acad. Sci. Phys.* **72** 698 (2008)]
263. Makarov A A *Opt. Spektrosk.* **62** 1183 (1987) [*Opt. Spectrosc.* **62** 697 (1987)]
264. Pate B H *J. Chem. Phys.* **109** 4396 (1998)
265. Green D et al. *J. Chem. Phys.* **109** 4407 (1998)
266. Douglass K O et al. *J. Chem. Phys.* **121** 6845 (2004)
267. Logan D E, Wolynes P G *J. Chem. Phys.* **93** 4994 (1990)
268. Bigwood R, Gruebele M *Chem. Phys. Lett.* **235** 604 (1995)
269. Schofield S A, Wolynes P G, Wyatt R E *Phys. Rev. Lett.* **74** 3720 (1995)
270. Schofield S A, Wyatt R E, Wolynes P G *J. Chem. Phys.* **105** 940 (1996)
271. Gruebele M, in *Advances in Chemical Physics* Vol. 114 (Eds I Prigogine, S A Rice) (New York: Wiley, 2000) p. 193
272. Leitner D M, Wolynes P G *Phys. Rev. Lett.* **76** 216 (1996)
273. Leitner D M, Wolynes P G *J. Chem. Phys.* **105** 11226 (1996)
274. Minehardt T J, Adcock J D, Wyatt R E *J. Chem. Phys.* **110** 3326 (1999)
275. Quack M, Willeke M *J. Chem. Phys.* **110** 11958 (1999)
276. Lambert W R, Felker P M, Zewail A H *J. Chem. Phys.* **75** 5958 (1981)
277. Felker P M, Zewail A H *Chem. Phys. Lett.* **102** 113 (1983)
278. Syage J A et al. *J. Chem. Phys.* **82** 2896 (1985)
279. Felker P M, Lambert W R, Zewail A H *J. Chem. Phys.* **82** 3003 (1985)
280. Felker P M, Zewail A H in *Jet Spectroscopy and Molecular Dynamics* (Eds J M Hollas, D Phillips) (London: Blackie Acad. & Professional, 1995) p. 222
281. Felker P M, Zewail A H *J. Chem. Phys.* **82** 2994 (1985)
282. Medvedev E S *Usp. Fiz. Nauk* **161** (1) 31 (1991) [*Sov. Phys. Usp.* **34** 16 (1991)]
283. Kittrell C et al. *J. Chem. Phys.* **75** 2056 (1981)
284. Abramson E et al. *J. Chem. Phys.* **80** 2298 (1984)
285. Abramson E et al. *J. Chem. Phys.* **83** 453 (1985)
286. Dai H L et al. *J. Chem. Phys.* **82** 1688 (1985)
287. Yamanouchi K, Takeuchi S, Tsuchiya S *J. Chem. Phys.* **92** 4044 (1990)
288. Rohlfing E A, Goldsmith J E M *J. Opt. Soc. Am. B* **7** 1915 (1990)
289. Sundberg R L et al. *J. Chem. Phys.* **83** 466 (1985)
290. Pique J P et al. *Phys. Rev. Lett.* **58** 475 (1987)
291. Dai H-L, Field R W (Eds) *Molecular Dynamics and Spectroscopy by Stimulated Emission Pumping* (Singapore: World Scientific, 1995)
292. Farantos S C et al. *J. Chem. Phys.* **93** 76 (1990)
293. Jacobson M P et al. *J. Chem. Phys.* **111** 600 (1999)
294. Jung C, Taylor H S *J. Chem. Phys.* **132** 234303 (2010)
295. Taylor H S, in *Molecular Dynamics and Spectroscopy by Stimulated Emission Pumping* (Eds H-L Dai, R W Field) (Singapore: World Scientific, 1995) p. 1073
296. Settle R D F, Rizzo T R *J. Chem. Phys.* **97** 2823 (1992)
297. Boyarkin O V et al. *J. Chem. Phys.* **107** 8409 (1997)
298. Boyarkin O V, Rizzo T R, Perry D S *J. Chem. Phys.* **110** 11346 (1999)
299. Boyarkin O V, Rizzo T R, Perry D S *J. Chem. Phys.* **110** 11359 (1999)
300. Maksyutenko P et al. *J. Chem. Phys.* **126** 044311 (2007)
301. Boyarkin O V, Rizzo T R *J. Chem. Phys.* **103** 1985 (1995)
302. Boyarkin O V, Rizzo T R *J. Chem. Phys.* **105** 6285 (1996)
303. Butler L J et al. *J. Chem. Phys.* **85** 2331 (1986)
304. Ticich T M et al. *J. Chem. Phys.* **87** 5820 (1987)
305. Crim F F *Annu. Rev. Phys. Chem.* **44** 397 (1993)
306. Hippler M, Quack M *Chem. Phys. Lett.* **231** 75 (1994)
307. Hippler M, Quack M *J. Chem. Phys.* **104** 7426 (1996)
308. Portnov A et al. *J. Chem. Phys.* **122** 224316 (2005)
309. Ganot Y, Rosenwaks S, Bar I *J. Chem. Phys.* **122** 244318 (2005)
310. Portnov A, Rosenwaks S, Bar I *J. Chem. Phys.* **121** 5860 (2004)
311. Portnov A et al. *J. Chem. Phys.* **123** 084316 (2005)
312. Bagratashvili V N et al. *Chem. Phys. Lett.* **137** 45 (1987)
313. Lokhman V N et al. *J. Phys. Chem. A* **103** 11293 (1999)

314. Malinovsky A L et al. *J. Phys. Chem. A* **102** 9353 (1998)
315. Malinovskii A L et al. *Khim. Fiz.* **18** (9) 9 (1999) [*Chem. Phys. Rep.* **18** 1597 (1999)
316. Kosterev A A et al. *J. Phys. Chem. A* **104** 10259 (2000)
317. Evseev A V et al. *Zh. Eksp. Teor. Fiz.* **87** 111 (1984) [*Sov. Phys. JETP* **60** 64 (1984)
318. Evseev A V et al. *Chem. Phys.* **106** 131 (1986)
319. Puretzky A A, Tyakht V V, in *Laser Spectroscopy of Highly Vibrationally Excited Molecules* (Ed. V S Letokhov) (Bristol: A. Hilger, 1989) p. 329 [Translated into Russian (Moscow: Nauka, 1990) p. 235]
320. Bagratashvili V N et al. *Pis'ma Zh. Eksp. Teor. Fiz.* **44** 450 (1986) [*JETP Lett.* **44** 580 (1986)]
321. Boyarkin O V, Ionov S I, Bagratashvili V N *Chem. Phys. Lett.* **146** 106 (1988)
322. Bagratashvili V N, Ionov S S, Makarov G N, in *Laser Spectroscopy of Highly Vibrationally Excited Molecules* (Ed. V S Letokhov) (Bristol: A. Hilger, 1989) p. 265 [Translated into Russian (Moscow: Nauka, 1990) p. 192]
323. Lokhman V N et al. *J. Phys. Chem. A* **103** 11299 (1999)
324. Zewail A H (Ed.) *Femtochemistry: Ultrafast Dynamics of the Chemical Bond* (Singapore: World Scientific, 1994)
325. Zewail A H *J. Phys. Chem.* **100** 12701 (1996)
326. Zewail A H *Angew. Chem. Int. Ed.* **39** 2586 (2000)
327. De Schryver F C, De Feyter S, Schweitzer G (Eds) *Femtochemistry* (Weinheim: Wiley-VCH, 2001)
328. Ionov S I et al. *J. Chem. Phys.* **99** 6553 (1993)
329. Panfilov V N, Molin Yu N *Usp. Khim.* **47** 967 (1978) [*Russ. Chem. Rev.* **47** 503 (1978)]
330. Molin Yu N, Panfilov V N, Petrov A K *Infrakrasnaya Fotokhimiya* (Infrared Photochemistry) (Novosibirsk: Nauka, 1985)
331. Crim F F *J. Phys. Chem.* **100** 12725 (1996)
332. Yoo H S, DeWitt M J, Pate B H *J. Phys. Chem. A* **108** 1365 (2004)
333. Elles C G, Cox M J, Crim F F *J. Chem. Phys.* **120** 6973 (2004)
334. Lehmann K K *J. Chem. Phys.* **126** 024108 (2007)
335. Makarov G N *Usp. Fiz. Nauk* **174** 225 (2004) [*Phys. Usp.* **47** 217 (2004)]
336. Nauta K, Moore D T, Miller R E *Faraday Discuss. Chem. Soc.* **113** 261 (1999)
337. Callegari C et al. *J. Chem. Phys.* **113** 10535 (2000)
338. Metzelthin A et al. *J. Chem. Phys.* **129** 114307 (2008)
339. Stiles P L, Douberly G E, Miller R E *J. Chem. Phys.* **130** 184313 (2009)
340. Gutberlet A, Schwaab G, Havenith M *J. Chem. Phys.* **133** 154313 (2010)
341. Rudolph S et al. *J. Chem. Phys.* **126** 124318 (2007)
342. Lehnig R, Blinov N V, Jäger W *J. Chem. Phys.* **127** 241101 (2007)
343. Grebenev S et al. *J. Chem. Phys.* **132** 064501 (2010)
344. Hoshina H et al. *J. Chem. Phys.* **132** 074302 (2010)
345. Moerner W E *J. Phys. Chem. B* **106** 910 (2002)
346. Hamm P, Zanni M T *Concepts and Methods of 2D Infrared Spectroscopy* (Cambridge: Cambridge Univ. Press, 2011)
347. Park S, Kwak K, Fayer M D *Laser Phys. Lett.* **4** 704 (2007)
348. Mukamel S, Hochstrasser R M *Chem. Phys.* **266** 135 (2001)
349. Tramer A, Jungen Ch, Lahmani F *Energy Dissipation in Molecular Systems* (Berlin: Springer, 2005) p. 56
350. Twagirayezu S et al. *J. Phys. Chem. A* **114** 6818 (2010)
351. Twagirayezu S et al. *J. Phys. Chem. A* **115** 9748 (2011)
352. Schmalz T G, Flygare W H, in *Laser and Coherence Spectroscopy* (Ed. J I Steinfeld) (New York: Plenum Press, 1978) p. 125 [Translated into Russian (Moscow: Mir, 1982) p. 160]